

Abradable Seal Test Rig Development and Material Analysis

By
Jason Fong
Andrew Pease
Trevor Plaine

Project Advisor: John Fabijanic

Instructor's Comments:

Instructor's Grade: _____

Date: _____

Abradable Seal Test Rig Development and Material Analysis

By
Jason Fong
Andrew Pease
Trevor Plaine

Mechanical Engineering Department
California Polytechnic State University
San Luis Obispo

2010

Statement of Disclaimer

Since this project is a result of a class assignment, it has been graded and accepted as fulfillment of the course requirements. Acceptance does not imply technical accuracy or reliability. Any use of information in this report is done at the risk of the user. These risks may include catastrophic failure of the device or infringement of patent or copyright laws. California Polytechnic State University at San Luis Obispo and its staff cannot be held liable for any use or misuse of the project.

Table of Contents

Executive Summary	4-5
List of Tables	6
List of Figures.....	7
Executive Summary	8
Chapter 1: Introduction	9-10
Sponsor Background and Needs	9
Problem Definition	9
Method of Approach	9-10
Project Management	10
Chapter 2: Background research	11-16
Test Rig Research	12
Materials Research.....	14-15
Materials Research Path.....	15-16
Chapter 3: Design Development – Test Rig	17-22
Test Rig Requirements.....	17
Concepts Generated	17-19
Concept Selection	20-22
Chapter 4: Detailed Analysis of the Final Design	23-35
Overall Description	23
Motor selection	23-24
Belt Design	24-25
Motor Mount.....	25
Rotor Design	25-26
Shaft and Bearing selection	26-27
Vibrations Analysis	27-29
Frame Design	29-30
Linear Actuator Selection.....	30-31
Linear Assembly Design	31-32
Strain Gauge Set-Up	32-33
Instrumentation	33-34
Cost/Bill of Materials Estimation	35
Chapter 5: Product Realization	36-38
Welding	36

Lathe and Mill.....	36
Drilling	36
Rotor Build	37
Changes made in Construction	38
Recommendation for Future Manufacturing	38
Chapter 6: Design Verification and Testing	39-42
Test Descriptions	39
Fluorosint 207 Testing	39
Fluorosint 500 Testing	40
Lead Babbitt Testing	41
Verification Check List	42
Chapter 7: Conclusion and Recommendations.....	43
Appendix A: Bibliography	44
Appendix B: Detailed Drawings.....	45-53
Appendix C: List of Vendors	54
Appendix D: Gantt Chart.....	55
Appendix E: CES Materials Charts	56-57
Appendix F: Original Horizontal Test Rig Modification	58
Appendix G: Operation Procedure	59
Appendix H: Vendor supplied Component Specifications and Data Sheets	60-71
F58S Hall Effect Cut Sheet	60-62
SCB-68 (Manual for Connect Block)	63-70
Strain Gauges selection	71
Appendix I: Detailed Supporting Analysis	72-82
Strain Gauge Analysis	72-74
Belt Design	75-76
Shaft Analysis	77-80
Bearing Analysis	81
Strain Gauge Calibration	82
Appendix J: Testing Data (Material Test Sheets and Graphs)	83-91
Appendix K: LabView Program.....	92-93
Appendix L: Fluorosint 500 and 207 MSDS	94-107

List of Tables

Table 1: Material table of requirements	16
Table 2: Table of Requirements for the Test Rig.....	17
Table 3: Decision Matrix Used to Select the Best Concept	20
Table 4: Table of Linear Actuator Requirements	30
Table 5: Make, Model, and Descriptions for Various Manufactures of Linear Actuators	31
Table 6: Bill of Materials and Cost.....	35
Table 7: Summary of Test Results	41

List of Figures

Figure 1: Single swing pendulum test.....	12
Figure 2: Current Solar Turbines Test rig	13
Figure 3: Example of an existing test rig.....	13
Figure 4: Current Seal for Solar Turbines.....	14
Figure 5: R2D2 design concept	18
Figure 6: Horizontal Ring Test Rig	18
Figure 7: Horizontal Plate Rig	19
Figure 8: Reciprocating Motor concept	19
Figure 9: Horizontal test rig concept	21
Figure 10: Horizontal test rig concept	23
Figure 11: Torque required getting the motor up to speed for different time intervals	24
Figure 12: Power required getting the rotor up to speed for different time intervals	24
Figure 13: Motor Mount Assembly	25
Figure 14: 3-D model of the stainless steel rotor	26
Figure 15: Shaft and Rotor assembly (exploded)	27
Figure 16: The 1st natural frequency showing the whirl effect	27
Figure 17: The 1st natural frequency showing bending	28
Figure 18: The 1st natural frequency of the frame	28
Figure 19: Final balance of the rotor assembly.....	29
Figure 20: 3-D model of the Frame.....	30
Figure 21: 3-D model of Linear Actuator assembly	32
Figure 22: Strain gauge placement on Dummy Shaft	32
Figure 23: A) Wheatstone bridge configuration for measuring bending strain	33
Figure 23: B) Wheatstone bridge configuration for measuring axial strain	33
Figure 24: A) and B) Photos showing the welding process	36
Figure 25: Lathing process for the stainless steel rotor	37
Figure 26: Graph showing the bending strain of the dummy shaft with respect to time for test 1 of the Fluorosint 207	39
Figure 27: Graph showing the bending strain of the dummy shaft with respect to time for test 1 of the Fluorosint 500	40
Figure 28: Graph showing the bending strain of the dummy shaft with respect to time for test 2 of the Lead Babbitt.....	41
Figure 29: Frequency comparison of the Hall Effect sensor vs. VFD controller	42

Executive Summary:

This project deals with the analysis of abradable seal materials in centrifugal compressors and the development and design of a test rig able to test the seals performance. The project was sponsored by Solar Turbines to determine a suitable future material that could be used for their compressor seals. The project can be broken down into four goals, first to understand the mechanics of how the seals work and identify ideal material properties, second develop a list of materials that meet our material requirements for abradable seals, third to produce a test rig to evaluate the abradability of various materials, and finally test the list of materials developed with the test rig and make recommendations for the best material to use for abradable seal.

Material requirements were researched to determine what material properties are recommended for abradable seals. If the material was too hard the seal could damage the labyrinth teeth, if too soft there might not be tight enough clearances causing the compressor to leak in-between stages. Temperature also was a major concern when selecting a material due to the fact that the service temperature had to be greater than 325 °F. Cambridge Education Services (CES) was the program used to set up material requirements and filter out materials that don't meet the specified requirements. The final list of materials consisted of Fluorosint 500 & 207, Aluminum 6061, and a variety of Lead Babbitts specified by our sponsor.

The function of the test rig is to simulate the dynamic forces that the seal goes through in a compressor. The main variable to consider was the tip speed required for the labyrinth teeth when they would abrade the test material. Solar's centrifugal compressors are broken in at around 5000 rpm which correlates to around 260 ft/s. Our test rig required a 5 HP motor to achieve the proper speed of our rotor. The other driving design factor was being able to measure the force required to abrade the 0.01 in incursion into the test samples. Strain gauges were applied to a shaft that connected the material mount to a linear actuator which would record the strain needed to abrade the different samples. A data acquisition system was required to analyze the strain, linear movement, and speed of rotor making sure the experiment was repeatable.

We tested three of the four recommended materials, (6 runs) of the Fluorosint 207, (3 runs) of the Fluorosint 500 three times, and (1 run) of the Lead Babbitt. The testing procedure consisted of moving each test sample into the rotor at 0.01", then pausing for 5 seconds, and abrading another 0.01", before backing out. The material that abraded the best was determined to be the Lead Babbitt which required a force of 5lbs. However, Solar wishes to increase the operating temperature of their compressors making the service temperature an important variable. With this in mind, the material that abraded the best with the highest rated service temperature was the Fluorosint 207. Our recommendation to Solar is to continue testing with the Fluorosint 207.

CHAPTER 1: Introduction

Sponsor Background and Needs

Solar Turbines is one of the leading manufacturers of natural gas centrifugal compressors. A very significant component of their machines is the abradable seal that separates the rotor from the stator. The purpose of an abradable seal is to create a sealing system that will allow the relative movement of rotor parts with respect to stationary parts while ensuring inter-stage and end sealing. The Abradable seal must not cause any damage to the surrounding material, hence the name Abradable. These seals are very important because they affect a significant number of critical factors including: efficiency, performance, available flow, and axial load. Solar Turbines is interested in looking to replace the current Lead Babbitt seals with a material that abrades just as well but has a higher service temperature. With a seal having a higher service temperature it would allow Solar Turbines to run their compressors at higher temperatures leading to higher efficiency.

Problem Definition

The goal for this project is to find a material to use for the seal that will provide the performance requirements; in other words, “what material is best suited for an Abradable seal?” The goal is to understand the mechanics of how the seal works and to produce a test rig to evaluate various materials. Producing a test rig that can accurately measure the difference in abradable materials repeatedly is crucial for evaluating the different test materials. Having tested a variety of materials, we can analyze each material considering its positive and negative features, and recommend the most suitable material to Solar Turbines.

Method of Approach

To design a successful test rig and determine which material is best suited for the application the project was organized into two separate parts: Material Selection and Design/Construction of the test rig.

For Materials Selection, we have specified a set of Material Requirements that our desired material must meet or exceed. With the help of a materials engineering student, Patrick Hyland, we were able to use a Program called Cambridge Education Services (CES). This program allowed us to narrow down thousands of existing materials within a database by applying our specified material requirements. We were then able to graph a relationship between Hardness and Max Service Temperature shown in Appendix C. The two limiting materials included Solar’s current sealing material, and the material that makes up Solar’s rotors in their compressors (Stainless Steel). The materials that fell in-between our limits were theoretically the materials that would work for our application. After removing the materials that we and our sponsor’s decided wouldn’t work, we were left with a set of suitable materials. With this list, and the help of our sponsor’s suppliers, we are now able to find out when and where we are getting our test samples.

The test rig design and analysis was the next step in completing the project. Once Solar Turbines approved of the design and all the components we ordered the parts required from vendors. Fabrication commenced immediately once the parts arrived. After finishing the construction of the test rig we began work on the data acquisition system. This step consisted of gathering the hardware and software necessary to monitor the speed of the rotor, strain, and temperature. Once the data

acquisition system was working testing commenced immediately. After all the data was collected analysis began to determine the best abradable material.

Project Management

Jason Fong was the main point of contact between Solar Turbines and PPF engineering. His primary responsibilities included documentation of project progress, creating agendas, and tracking the project with a Gantt chart. His main design responsibilities consisted of the linear actuator design and he was also in charge of the data acquisition system. Andrew Pease was in charge of research and testing plans. His design responsibilities consisted of designing the drive system for the test rig. Trevor Plaine was responsible for manufacturing considerations and prototype fabrications. His design responsibilities included structural analysis and the rotor assembly design.

CHAPTER 2: Background Research

Depending on the application, an abradable seal may be composed of a variety of materials. However, abradable seals are required to prevent or control the flow of fluids such as gases or liquids. In our application, a set of teeth -called the labyrinth- contracts the gas as it flows through the clearance between the seal and the tooth expanding when the fluid flows between the teeth. This repeated contraction and expansion reduces the flow of the gas and lowers its flow rate. This is why abradable seals are so critical; as the rotating labyrinth cuts into the seal the sealing material begins to abrade away making room for the labyrinth. The contact between the two materials cause a rubbing tolerance that makes the seals control or prevent fluid flow. Seals used for this purpose have a tendency to fail for the following reasons; the material of the seals expand and contract under temperature change and friction cause's parts to seize, wear rapidly, distort, fracture, melt, or otherwise fail to function and require premature removal and replacement.

For this project we will be focusing on many material properties and characteristics that contribute to the functionality of an abradable seal. In order to select the correct material all the desirable characteristics of a seal must be reviewed. A Lead Babbitt is the current material used by Solar Turbines for their abradable seals. Lead alloys have the lowest stiffness in the metal category with a modulus of elasticity around 4.14Mpsi. If a material is too stiff or too brittle it will shatter when the high contact stress from the labyrinth is applied during break in. Therefore one very desirable characteristic of abradable seals is a relatively low stiffness which is important in order to prevent shattering. Lead also has one of the lowest yield strengths in the metal group at 1.45kpsi. Having a lower yield strength allows for deformation long before the Labyrinth's steel teeth deform which helps to maintain proper clearance. Thus, another required characteristic of the abradable seal is lower yield strength when compared to steel to prevent deformation or wear on the steel teeth which could change the groove depth.

Thermal properties are also a very important consideration when designing an abradable seal. A major goal in terms of material selection is to increase the service temperature of the seal making it well above the highest temperatures achieved by Solar Turbine's compressor at 400°F. The lead alloy currently used by Solar Turbines begins to lose its material characteristics around 325°F. Lead also has a relatively low thermal conductivity for metals at 20.39 Btu/hr-ft-°F. Both these properties are important in finding a new seal that can withstand temperatures above 400°F, and will have a low thermal conductivity in order to have a favorable heat transfer to the other components. One of the last properties to be analyzed in regard to thermal design is the coefficient of thermal expansion. If significant growth or shrinkage occurs for high or low temperature exposure these variables must be accounted for in the design.

Durability and erosion are two other very important considerations when selecting a material. In many cases these seals are exposed to extremely sour natural gases and chlorine which can erode the seal. Not only does the material have to be soft enough in order to be easily abraded away, the material also needs to be hard enough to resist erosion by the high speed gas flow and solid particles that may be mixed in with the natural gas. In order to achieve the goal of finding a material that will increase the lifespan of a seal, we must find a good balance between abrasability and erosion resistance. Erosion can mainly be attributed to the impact speed and impact angle of the particles when they hit the material. These effects may need to be tested in order to find the correct material. One major characteristic of abradable materials that we may want to consider is the porosity, the measure of void space in a material. Porosity goes hand in hand with weak adhesion between the grain structures of the

material. This being said the impact of particles and debris have the ability to weaken the grain structure causing grains to break off resulting in a loss of mass. The resulting loss of mass causes a gap between the labyrinth and seal thus resulting in lower efficiency and eventually failure all together. We will be looking to find the ideal hardness in our material choices to make sure erosion can be avoided thus increasing the lifespan of the seal.

Test Rig Research

There are many different testing methods that can be used to gather information on material characteristics. For determining the strain inflicted on the seal, strain gages can be attached to the different test samples that will be placed in the test rig. To evaluate the thermal properties, thermo couples can be used to determine the temperature of the seals throughout testing and how the heat spreads. A scratch test is a common to obtain the Progressive Abradability Hardness (PAH). The PAH is a characteristic of a material that measures the ease at which a material can be scratched, or abraded. In order to determine the PAH, Equation (1) must be referenced where H_a is the PAH coefficient, W is the energy consumed during the scratching process, and V is the volume of the indentation made.

$$\text{Equation (1)} \quad H_a = \frac{W}{V}$$

The equation above measures the amount of energy required to abrade different materials; the more energy needed the less abradable the material is. For this project it is most likely a low PAH will be beneficial meaning that the material is easy to abrade while meeting other material characteristic requirements. A common experiment used to carry out this test is a single pass pendulum apparatus seen in Figure 1. The potential energy of pendulums are easy to determine by measuring the initial swing angle vs. the final swing angle, and the groove damage of the material. Once these values are measured the PAH can be determined. This test can be performed in order to determine which material is most likely to abrade well.

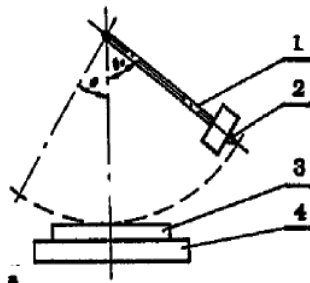


Figure 1: Single swing pendulum test

The current test rig that Solar Turbines have used, seen in Figure 2, was built specifically to test these abradable seals. However, the problem with this test rig is the complexity of the machine. There were too many parts when it came to installing new seals and calibrating existing equipment. It was also noted that new instrumentation may need to be added in order to improve the accuracy or the type of information coming out of the machine. In our design we are seeking to simplify the test process as much as possible while still achieving accurate results. Another focus will be cutting the run time involved in order to be able to test many different materials in a time efficient matter.

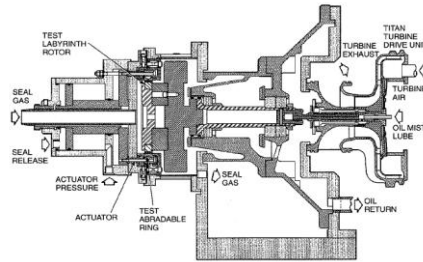


Figure 2: Current Solar Turbines Test rig

There are many different ways to test an abradable seal; however the point of the rig is to mimic the heat transfer and the surface contact of the seal in the actual compressor assembly. When considering the pendulum test rig seen in Figure 1 it is important to realize that this current set-up is only able to test how easy it is for the material to be worn away. This presents a problem with analyzing other characteristics and properties of a material, therefore to examine these other properties a different test rig will need to be built.

Another test rig concept found uses a disk on an electric motor and flat plates of abradable materials. The rig pushes the abradable material into the disk as it is spinning. This test simulates the actual process in that the disk rim can be shaped like the labyrinth and made out of the same material. Thus, if the process of moving the abradable material into the disk deforms the labyrinth teeth in any way it is apparent that the material will not perform according to requirements. This device will also come close to simulating the same heat from friction on startup that the actual compressor produces. There are still some drawbacks with using this testing concept. This test rig would be better if the abradable material covered the entire perimeter of the disk, the same as the seal does in the compressor. This test rig seen in Figure 3 allows the debris that is abraded to go into the air when in reality the abradable material covers the entire perimeter of the disk and the material that gets rubbed off has to work its way out of the labyrinth. The problem with wrapping the material all the way around the disk is that it will make the test rig more complex and each material that gets tested will have to be cast into rings which will involve more time and cost. When designing our test rig we will rate the pros and cons of both testing apparatuses to create a design that is as simple as possible while still providing the most accurate testing conditions.

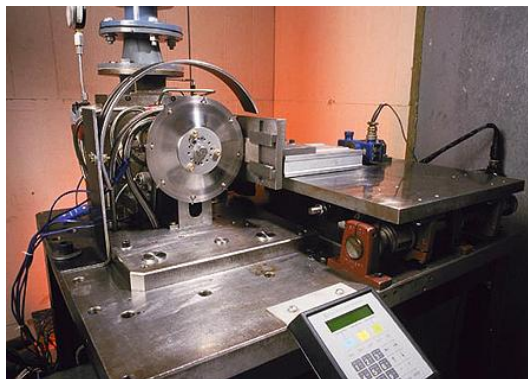


Figure 3: Example of an existing test rig

Materials Research

There are two main materials that are currently used for sealing the labyrinths of the centrifugal compressors at Solar Turbines; the use of a Lead (Pb) and Tin (Sn) Babbitts with a stainless steel backing. Figure 4 shows a cross sectional view of the actual seal used by Solar Turbines. In each compartment throughout the compressor there are seats in which individual seals are placed. These seals are first frozen with liquid nitrogen to contract them in order to be placed in the seat. As the material defrosts in the seat it will expand and thus creating an interference fit. The current break-in method involves starting and stopping the machine in various intervals of time so that the labyrinth may cut into the seals properly. As the labyrinth cuts into the seal, fine strands of hair like mesh make their way through the compressor. This method of breaking-in the seals is undesirable for the following reasons; the break-in process is time consuming, residue from the break-in process may ball-up creating unwanted objects floating around in the compressor, and after a factory overhaul where a systematic break-in process is not preformed, clients tend to put seals into full use thus not allowing seals to properly break in. If the break-in process is not properly followed the life-cycle of the seal, durability, and other properties of the seal may be compromised.

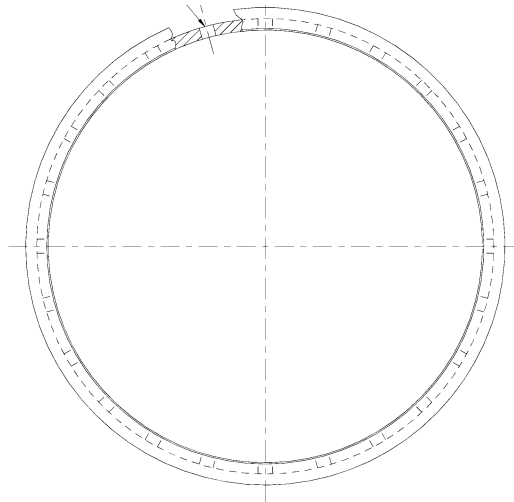


Figure 4: Current Seal for Solar Turbines

There are numerous Patents and articles on materials which are applicable to abradable seals. The following are examples of Patents and articles that are intended for our application.

- I. Patent 3,701,536 refers to alternate method and material of creating an abradable seal. This invention requires flame-spraying a metallic fiber (called FELTMETAL) on to a support material, at an acute angle (15 to 45 degrees) causing a desired porosity and grain structure. This combination of material and structure is said to allow the material to displace rather than abrade. This method allows the material not to tear, abrade, or ball up when engaged with a moving part. If achievable, this characteristic is highly desirable in terms of start up, and life-cycle. For our application, it means that the machine may be turned on without the current process of start-up. This also increases the life cycle of these seals because the sealing material is being moved to either side rather than being cut away. It is also said that the material being used is a heat resisting material with a service temperature exceeding 1200°F. This invention was intended for the use on turbine engines, the indicated service temperature is a desirable

feature, but for our application we would need to alter the material composition to obtain a service temperature of around 600°F.

- II. Patent 3,831,258 refers to a reinforced porous metal structure secured to a backing sheet. The composition of the porous metal contains metals such as nickel, chromium, iron, magnesium, silicon, carbon, and copper with metal particles of 1 to 100 microns. The objective of this invention is to provide a sheet of reinforced porous metal structure that is easy to fabricate and admirably suited for an abradable seal.
- III. Patent 3,053,694 refers to an abradable material composed of Silver, Boron, and Sodium Silicate. The purpose of this invention is to come up with an abradable composite and honeycomb backing that would be capable of functioning at temperatures of the order of 1300° F and to be capable of being easily repaired or patched. This composite was specifically composed of the following materials; Silver powdered, Boron nitride, Sodium silicate, Vermiculite, and Mica. From the Patent it was found that this specific composite exhibited excellent resistance to thermal shock, erosion, extreme variations of environment, shrinkage, deflection, and remain stable over a temperature range of -100° F to +1300°F. The honeycomb structure was composed in a variation of Chrome, Titanium, Iron, Nickel, and Cobalt. With these two composites, a heat treatment procedure was comprised of heating and cooling at different lengths of time so that the two would bond together without losing the abradable characteristics. For our application the characteristics mentioned above are highly desirable in terms of environmental resistance, temperature range, and ease of overhaul.
- IV. An article by Sealing Technology labeled, “Development of abradable and rub-tolerant seal materials for application in centrifugal compressors and steam turbines” refers to a new silicon rubber intended for sealing liquids and gases between rotating and non-rotating components. The article contains a series of tests on rub-tolerant polymers such as carbon-filled polyetheretherketone (PEEK) and Polyamideimide (PAI). This characteristic of being rub-tolerant is highly desirable because residue will not be created, meaning the seals will not have to worry about start-up conditions. It was concluded that PAI will not function at higher temperatures than 150°F, and noted that polymers such as PEEK will. However, there is no indication of the temperature limit for PEEK. It would be undesirable if the temperature limit is less than 600°F, the temperature limit of the current sealing material.

These materials and methods all have properties that look promising and have also been used by other companies in similar situations. Material research must be conducted in order to find the sweet spot of all the material characteristics we are looking to tie together. The way we started our research was by looking at materials being used by other companies, like the ones listed above, and determining why those materials are used in industry so frequently for abradable seals.

Material Research Path

One of the main objectives of this project was one of two paths; either prove that the existing material, Lead-Tin Babbitt, is the most economic material that will satisfy most of the specifications, or come up with a new and improved material that will meet or exceed all the requirements that have been specified. Since there are thousands of materials to choose from, we specified a method to narrow down this list of materials and to gain an understanding of where our optimal material characteristics lay. The following table explains the material requirements that the abradable material needed to meet:

Table 1: Material table of requirements

Material Table of requirements					
Spec. #	Parameter	Requirement or Target (units)	Tolerance	Risk	Compliance
1	Production Cost	-		L	A
2	Service Temperature	400°F	± 50°F	H	A, T
3	Hardness	<110 Vickers	-	H	A, T
4	Durability	8 years	± 2 years	H	S
5	Flammable	Material must not be flammable	-	H	S
6	Material Ductility	Brittle material is unacceptable	-	H	A, T
7	Yield Strength	1-10ksi	-	H	S
9	Modulus of Elasticity	Current material is rated 4.21 Msi	-	H	S
10	Size	Flat Test sample is sufficient (2" x2")	-	H	S

Table 1 presents the characteristics that an abradable material are a function of. Furthermore the abradable material must be softer than the labyrinth teeth, needs to be able to reach a service temperature of around 400°F, and to be able to last around 8 years before failing in operation. To further refine the number of materials, we referenced the material database program called "*Cambridge Engineering Selector*" to aid us in focusing on ideal characteristics of an abradable material. With this program we applied guidelines with our known characteristics thus siphoning out materials that do not meet the specified requirements.

Appendix C shows the results from CES where we were able to plot the desired characteristics from Table 3 to CES's database of materials. The program enabled us to see where the current Lead Babbitt material sits compared to our limiting material, Stainless Steel. With this knowledge we were able to generate a list of materials that fall in between the Lead Babbitt and the Stainless Steel. As for the material selection we now have a set of materials and material characteristics that we can gather and test from individual data sheets of each material (See Appendix C for list of materials that was generated). Please keep in mind that CES was just a tool for us to gain a starting point on what materials we were dealing with.

The final selection of materials consisted of Fluorosint 207, Fluorosint 502, Aluminum 6061, and a series of Lead Babbitt materials specified by our sponsor. All samples were tested and compared to determine which meets the material requirement the material requirement the best.

CHAPTER 3: Design Development - Test Rig

Test Rig Requirements

When considering the development of the test rig it was very important to know what requirements the test rig must be able to accomplish. The basic motive that ties together all the concepts for the test rig was the idea that the device will rub different materials against a part shaped like a labyrinth. To narrow down such a broad definition we have developed a list of requirements that the test rig must meet as presented in Table 1. The simplicity parameter in the table of requirements was added in order to meet Solar Turbines request to simplify the test process. For us simplicity is measured by how many steps the concept will require for setting up the test sample and the number of operations involved in running the actual rig. Setup time was another requirement directly related to simplicity. When testing a variety of different samples the time it takes to load each material can be significant. Therefore a main consideration in our design was to minimize the time required to load the test sample into the rig. All the requirements specified in Table 1 were the driving force behind all concepts generated below.

Table 2: List of requirements that the test rig must meet

Test Rig Table of requirements					
Spec. #	Parameter	Requirement or Target (units)	Tolerance	Risk	Compliance
1	Tip Speed	600 ft/s	± 100 ft/s	H	A,S
2	Weight	200 lb	± 50 lb	M	A, T, S
3	Production Cost	\$5,000	max	L	A
4	Power	TBD	-	H	A, T
5	Simplicity	5 steps	± 1 step	H	A
6	Durability	Infinite life	-	M	S
7	Size	Must be Table Mounted	-		
8	Set Up Time	5 minutes	± 1 min	L	

Concepts Generated

Five concepts were evaluated in detail. The first design considered was called R2D2 seen in Figure 5. The basics of this design were to have a motor attached to the vertical shaft that would spin the rotor with the labyrinth teeth on it. The idea was to make it so the seal could be simply dropped in and clamped before running the machine. Then a protective shield would cover the device protecting users from any shrapnel if the test seal were to shatter.

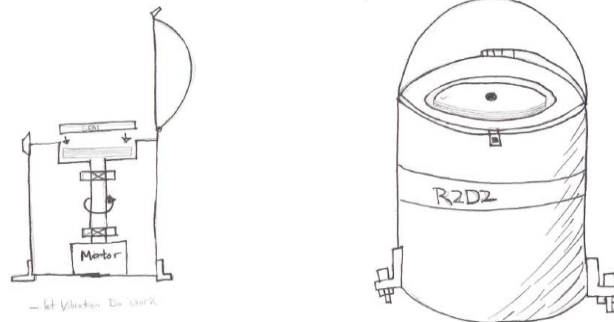


Figure 5: R2D2 design concept

The second design concept considered was given the name Horizontal Ring Test Rig shown in Figure 6. The main idea for this rig was to deviate from the vertical rotating shaft design seen in R2D2 and make the rotating shaft horizontal. A motor will be mounted on a table and connected to a shaft using a belt in order to help achieve the required tip speed of the rotor. The rotor with the labyrinth teeth around the circumference will be placed on the spinning shaft and will go through a circular frame which holds the test seals.

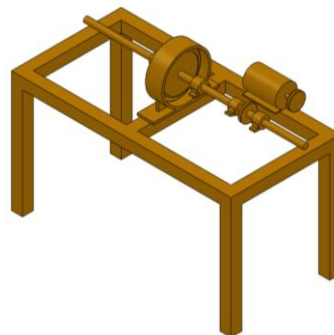


Figure 6: Horizontal Ring Test Rig

Our third concept, the Horizontal Plate Rig (Figure 7), is the exact same design as the horizontal ring test rig except the circular frame is removed and a platform with a sliding vice grip is added. This feature allows us to grip a flat piece of test material for the seal and move it into the rotating labyrinth.

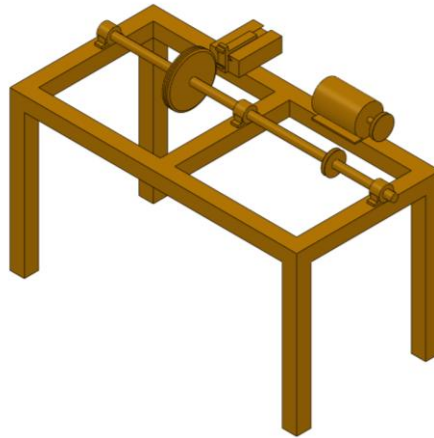


Figure 7: Horizontal Plate Rig

The last concept under consideration was called the reciprocating motor method seen in Figure 8. This concept's goal was to simulate the interaction between the labyrinth and seal by clamping down a semicircular piece of the test material and run a section shaped like labyrinth teeth with a pendulum moving back and forth. To move the pendulum back and forth a reciprocating motor would be hooked up to the pendulum causing it to rotate about a fixed point along the shaft connecting to the labyrinth teeth.

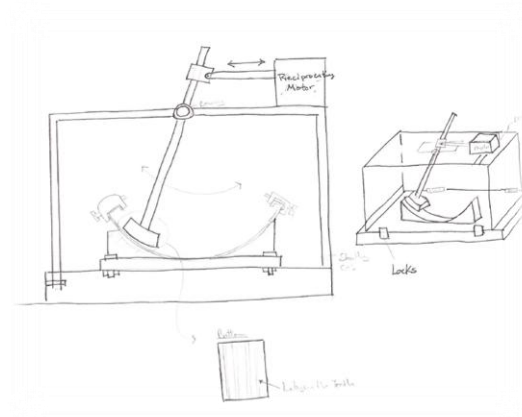


Figure 8: Reciprocating Motor concept

Concept Selection

In order to select our top choices a decision matrix was used to see which one of our proposed concepts fulfilled the most desired characteristics. The decision matrix shown in Table 2 indicates how each concept compares to the original test rig. Solar turbines existing test rig was given a score of zero all across the board, and then if the desired characteristic was better than the existing solar rig then the concept would receive a plus one, if it was worse it would receive a minus one. The concept with the highest score in the end was the idea we will pursue.

Table 3: Decision matrix used to select the best concept

Desired Characteristics	R2D2	Reciprocating Motor	Pendulum	Horz. Ring Rig	Horz. Plate Rig	Solar Turbines
Cost	+1	+1	+1	+1	+1	0
Safety	+1	+1	+1	+1	+1	0
Simplicity	0	0	-1	0	+1	0
Durability	0	-1	+1	+1	+1	0
Repeatability	0	0	+1	0	0	0
Size	+1	+1	+1	+1	+1	0
Weight	+1	+1	+1	+1	+1	0
Contact speed	0	0	0	0	0	0
Dynamic Simulation	0	-1	-1	0	0	0
Debris Analysis	+1	-1	0	+1	0	0
Set up time	0	-1	+1	0	+1	0
Sum of +1	5	4	7	6	7	0
Sum of -1	0	-4	-2	0	0	0
Total	5	0	5	6	7	0

The four top scores coincide with the design concepts presented previously. The pendulum test was a major consideration in this project. After further investigation, we found that the Pendulum Rig was not feasible for us to build. It was discovered that the most critical aspect of this test rig is the measurement of the divot created from the scratch element. According to Y.N. Liang's article on "Effects of fiber Orientation on a Graphite Fiber Composite in Single Pendulum Scratching" the volume of the divot needs to be accurate to the nearest micron. To achieve this type of tolerance a profilometer and a measurement microscope would need to be used. To obtain access to these devices it would require supervision of a MATE Engineering faculty member and a lot of time to obtain results that would not benefit us significantly. The original reasoning for using the Pendulum test was because of its simplicity, however it was determined that it is much more difficult than we anticipated making it unnecessary for this project. It became apparent that the pendulum test may be a project within itself. With this in mind, we decided to not pursue the Pendulum Test Rig and concentrate our efforts on design the Horizontal Plate Rig. When analyzing the decision matrix each of our top four designs were better in terms of cost than the Solar Turbines existing test rig. However none of the top concepts were able to better the existing rig in terms of contact speed and dynamic simulation. At best our design will match the

accuracy of Solar's previous test rig by simulating the proper tip speed and dynamic simulation, which includes forces due to friction and stresses experienced at full speed. The reciprocating motor concept received the lowest score out of our top choices. The design's downfall, illustrated in the decision matrix, was due to the fact that the design seemed less robust and therefore less durable. The remaining concerns for the reciprocating motor concept was that it wouldn't produce debris that could be analyzed to see what possible effects it could have on the labyrinth, and also the fact that it would take a long time to set up each test piece. R2D2 was the third best design concept, but the simplicity of building the device seemed to be an issue. Due to the fact that the rotor and bearing would be vertical we felt that this would add complexity to the design in terms of making sure the components don't slide down the shaft due to gravity as well as having to select different bearings.

The horizontal ring rig and horizontal plate rig had the two highest point totals in the decision matrix. They are very similar both having a spinning rotor allowing for best possible accuracy in terms of contact speed and required dynamic simulation. Both have all the desirable characteristics we are looking for with respect to size, cost, durability, weight, and safety. What sets them apart however is simplicity and set up time. The horizontal ring rig falls short due to the fact that tolerances would have to be much higher to design a frame that could hold a whole circular seal without slip. It is also difficult and more expensive to obtain test samples that are formed in a ring shape. The loading process would also be much more difficult with the ring because in order to make sure the ring doesn't slip an interference fit might need to be applied by cooling the ring and inserting it and then waiting for it to expand. The only characteristic where the ring rig overtakes the plate rig is debris analysis. With the ring design the material abraded away has to work its way out of the labyrinth because it is completely enclosed in a circle. This makes it possible to analyze the damage done to the labyrinth or seal by the debris. With the plate rig the material abraded away will just fall off the flat plate being pushed into the rotor making analysis of the debris effect on the seal more difficult.

In the end the horizontal plate rig had the highest score in the decision matrix and is the concept decided to pursue. We were confident that this design had the ability to test the seals with an accurate contact speed and dynamic simulation while maintaining the simplicity needed to keep the project feasible.

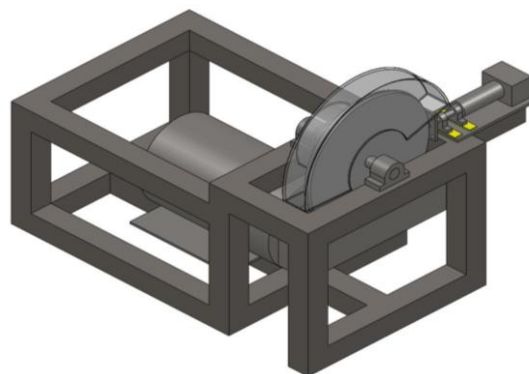


Figure 9: Horizontal test rig concept

A final addition to the requirements that was determined later in the design process was to make the test rig a table mounted machine. The horizontal plate rig was redesigned using the exact same concepts of dynamic simulation but was designed to fit to smaller frame instead of a whole frame. The

rough design of the horizontal plate test rig consisted of the following components: 1) A rigid frame, 2) two support bearings, 3) a rotor, 4) a horizontal pushing mechanism, 5) an electric motor, 6) a gear/pulley system, 7) a shaft and measuring devices (strain gages and thermocouples). Please refer to Figure 9 for a representation. The rig fits on a table that is 2.5' wide, 1.5' long, and 2' tall. As for material selection, we know that the rotor needed to be made out of Stainless Steel 15-5 as specified in our customer requirements. We expected the frame, bearing, and shaft to be made out of a carbon steel alloy to ensure stiffness and durability. A dynamic analysis was required to size the electric motor, shaft size, bearings, and gear/pulley system.

CHAPTER 4: Detailed Analysis of Final Design

Overall Description

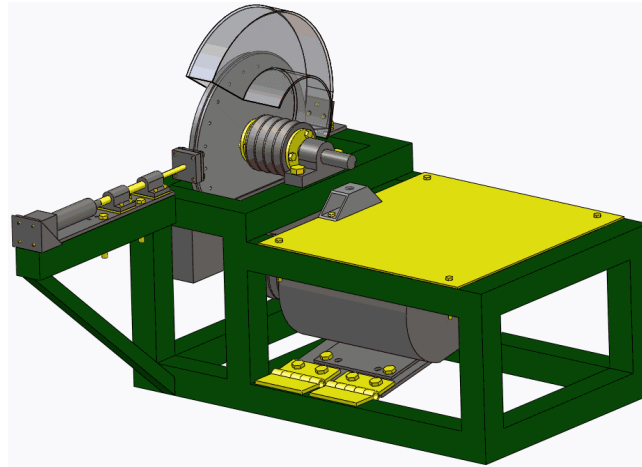


Figure 10: Horizontal test rig concept

Our final design consists of many components. The main component of the test rig is the 1' diameter, 5/8" thick 15-5 Stainless Steel rotor that is designed to reach a tip speed of 260 ft/s. In order to fix the rotor and pulley onto the shaft metal bushings were used. To fix the shaft assembly onto the frame two pillow block bearings were used. The shaft is driven by v-belts connected to a 5 HP 3 Phase induction motor. The belts are tensioned by a hinged assembly motor mount that will allow vertical movement of the motor along an ACME screw. An Ultra Motion Digit linear actuator was chosen to accurately move the test samples into the rotor. A dummy shaft connects the linear actuator to the material mount which is held by two linear bearings. Strain gauges are applied onto a necked down portion of the dummy shaft which will measure the force required to abrade each material. A safety shield and collection bucket was installed to redirect and collect the shavings abraded by the rotor. All the components were mounted on a table mounted frame made of 2"x2" box tubing. A data acquisition system was used to monitor the strain generated, speed of the rotor, and the motion of the linear actuator. Figure 10 shows a 3-D model of the actual test rig.

Motor Selections

When sizing the motor the main variable considered was how long it will take for the rotor to accelerate up to a speed of 5000 rpm or 524 rad/s. Many samples were tested and if it took a long time to accelerate the rotor to the required testing speed then the time spent testing would have been increased significantly. The longer the rotor takes to get up to speed is also more strenuous on the motor. The torque and horse power required to get the rotor up to speed was determined for different time intervals seen in Figure 11 and Figure 12. . The angular momentum is equal to the mass moment of inertia for the 12 inch steel rotor, which is $360 \text{ (lb}_m\text{-in}^2\text{)}$, multiplied by the angular velocity which was 524 rad/s. By assuming the torque from the motor is the only moment acting on the rotor and varying the time interval the horse power required was generated. When the relationship between power and time was developed it was up to us to determine the size and type of motor based on the torque requirement, the speed the motor runs at, the cost, and minimal time required to accelerate the rotor

to 5000 rpm. The rpm the motor runs at is significant because it will lead the design of the belt ratio to make sure the rotor reaches it proper design speed of 5000 rpm.

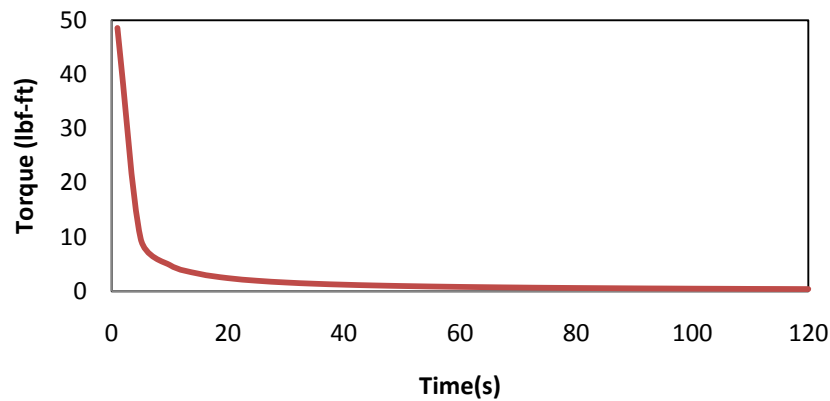


Figure 11: Torque required getting the motor up to speed for different time intervals

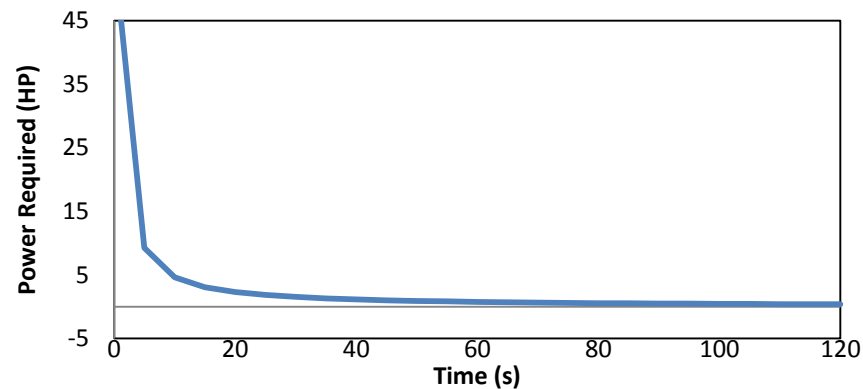


Figure 12: Power required getting the rotor up to speed for different time intervals

A Dayton 5 HP three phase induction motor was selected which will take around 9 seconds to get up to speed. This will require a 4.9 ft-lb torque that will need to be applied to the rotor the whole 9 seconds to get the rotor up to 5000 rpm. A variable frequency controller was also selected so the motor could be ramped up to speed gradually and so the samples could be tested at different speeds. The generalized motor selected runs at 3430 rpm which was the fastest motor found helping to minimize the required belt ratio. The motor is wired for low voltage at 230v volts so the design runs off a 240 volts, 30 amp, three phase outlet. In order to use the outlets that are provided by the school, the terminal plug required a 30 amp, 240 volt, model# L15 plug.

Belt Design

For selecting a belt to drive the shaft, a V-belt was considered due to the low cost of V-belts and availability. The motor runs at 3430 rpm and to achieve a shaft rpm of 5000 a belt reduction ratio is required. The minimum sheave diameter that can be used for a V-belt is 2.6 inches. A sheave with a pitch diameter of 3.8 inches is connected to the shaft and a sheave with a pitch diameter of 5.6 inches is

connected on the motor in order to ensure the shaft speed is 5000 rpm. The diameters of the sheaves and the center distance between them, which is 9 in, was used to calculate the pitch length. A pitch length of 37 inches was calculated which lead to the selection of a standard size A36 belt. An allowable power per belt of 1.91 was calculated and with a 5 HP motor the design HP was calculated at 7 HP. Four section A36 inch belts were needed for a proper safety factor.

Motor Mount

To tension the belts a motor mount was designed that would allow for the relative movement of the motor with respect to the frame. This feature makes it easy to attach the belts and tension them using the weight of the motor with an ACME screw. The ACME screw was used to support the mount with two nuts that would screw onto the shaft locking the motor mount in place. The motor mount is attached to the frame with two 4 inch steal hinges to allow for rotation. The ACME screw is attached to frame by pivoting on a 0.25 inch bolt between two brackets. The estimated load from tensioning the belts was estimated to be 175 lbs causing a moment on the mount. The ACME screw was placed as close to the belts as possible to minimize the moment. Figure 13 shows the model representation of the actual mount.

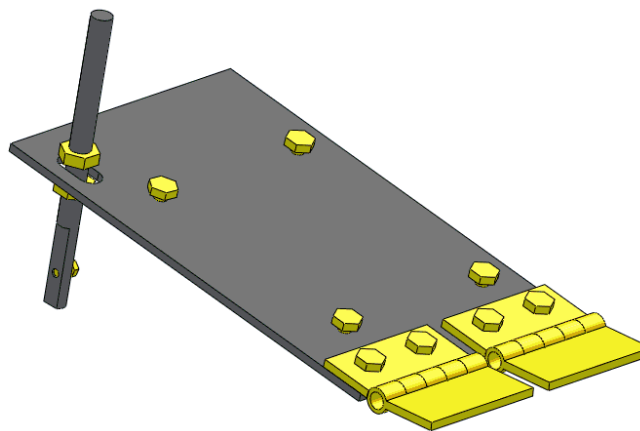


Figure 13: Motor Mount Assembly

Rotor Design

To simulate the actual rotor used by Solar Turbines a nominal diameter of 12inches was chosen. This diameter was large enough to generate the required tip speed while minimizing the sheave ratio required between the shaft and rotor. The geometry of the labyrinth tooth and balance holes was given by Solar seen in Figure 12. 15-5 Stainless steel is the material used to machine rotor; this is the same material that their compressors rotors are made out of. Figure 14 shows a 3-D model representing the actual rotor.

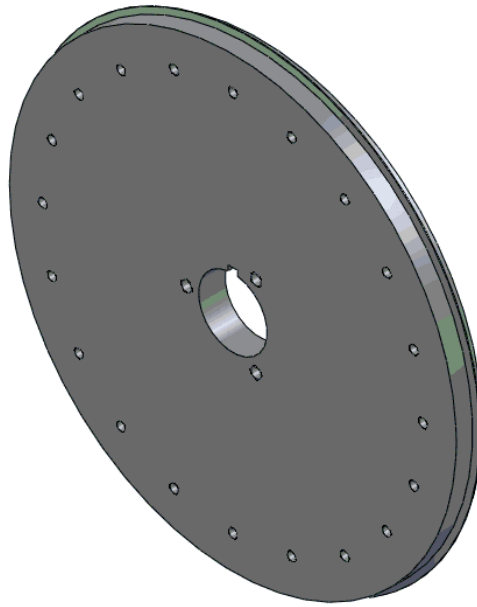


Figure 14: 3-D model of the stainless steel rotor

Shaft and Bearing design

Several factors were considered in designing the overall dimensions of the shaft for the test rig. The shaft is simply supported by two pillow block bearings and incorporates the rotor disk with the labyrinth tooth on the outer edge. A drive pulley connects the motor to the shaft by two belts. The first factor to consider was fatigue analysis to ensure the shaft has an infinite life. The loads on the shaft from the belt drive due to tension in the belts was calculated to be 300 lbs, which is considerably greater than the force expected on the rotor by the test material. If the force on the rotor becomes too large then it will over power the motor and the rotor will slow down. This is a situation that we will avoid by controlling the feed rate of the seal material into the labyrinth. The max moment on the shaft is 36.7 ft-lbs at the pulley. The max combined stress in the shaft is 24089 psi. The yield strength of AISI 1030 which is a mild steel is 94ksi and the infinite fatigue strength is one half of the yield strength to make S_e equal to 47ksi which gave us a safety factor of 3.3 for a one inch diameter shaft.

The deflection at the pulley is 0.0013 inches and the deflection at the rotor is 0.00052 inches. The deflection at the rotor was the main concern because that is where the deflection can cause the most problems. The last component to shaft analysis is the bearings. The maximum load on the bearings is 155 lbs which is a lot lower than the maximum load of any one inch inner diameter bearing can handle. Having determined the appropriate size of the shaft, the bearings had to be properly sized. The first bearings that were considered were Browning pillow block ball bearings with a one inch bore. Using the recommended calculations and values from Browning, the life span of the bearings under the projected use conditions will be 42 thousand hours. This computes to about 20 years of useful life assuming a usage of 8 hours a day, 5 days a week. This means under this usage the bearings would have to be changed every 20 years. Figure 15 shows an exploded view of our Shaft assembly.

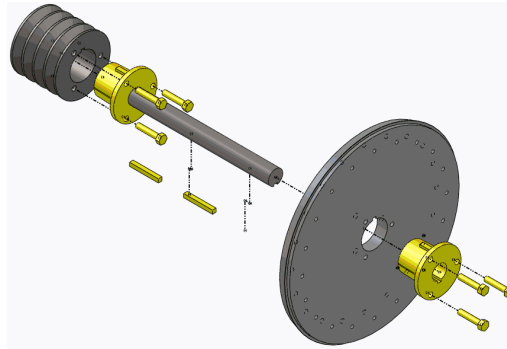


Figure 15: Shaft and Rotor assembly (exploded)

Our initial plan to attach the rotor onto the shaft involved heat shrinking the rotor onto the shaft. After realizing that the bushings that came with the pulleys allowed the user to change and move the pulley as they wanted, we applied the same concept onto the rotor and shaft. The bushings are split tapered bushing used on sprockets, pulleys, and drives. Although the rotor had to be machined to adapt for the bushing, the design of the rotor and shaft did not require a high tolerance as specified by shrink fitting.

Vibrations Analysis

With the rotor and shaft rotating at 5000 rpm a main aspect of the design was avoiding natural frequencies. With a 1 inch steel shaft the deflection was small enough to not hinder the design. The two types of deflection considered with the vibration analysis were the whirl of the rotor and then the bending of the beam. The first natural frequency found in the hand calculations done treating the beam as a spring and the rotor as a lumped mass on the spring was 11900 rpm. Using Abaqus an FEA model consisting of the rotor and shaft was developed yielding the first nodal frequency to be 13140 rpm (Figure 17). This gave us a discrepancy of 9%, an acceptable value for the FEA model.

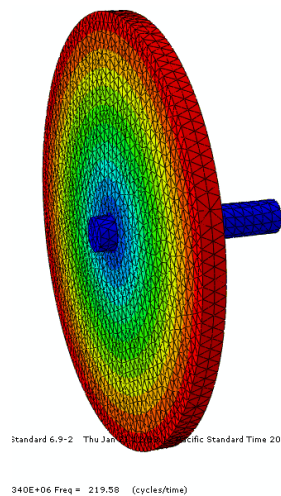


Figure 16: The 1st natural frequency showing the whirl effect

The mode shown in figure 17 appeared to be the natural frequency pertaining to whirl so next we found the bending mode. Using Abaqus the first bending mode of the shaft occurred 107520 rpm much higher than the speeds we are running at (Figure 18). A good goal when designing for natural frequency is to

have the first natural frequency at least twice as large as the operating speed. Our operating speed of 5000 rpm is much lower than both frequencies making the design sound when considering vibrations.

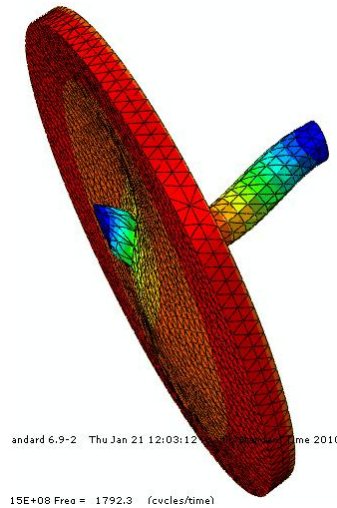


Figure 17: The 1st natural frequency showing bending

The vibration in the frame was another major concern. Using Abaqus an FEA model of the frame was constructed to determine the natural frequencies. If the frame has significant vibration the accuracy of the strain gauges and movement of the linear actuator may be affected. Over time continuous vibration of the frame may also break down the controllers that are mounted on the frame. To dampen the vibration on these components a rubber liner is placed between the controller and the frame.

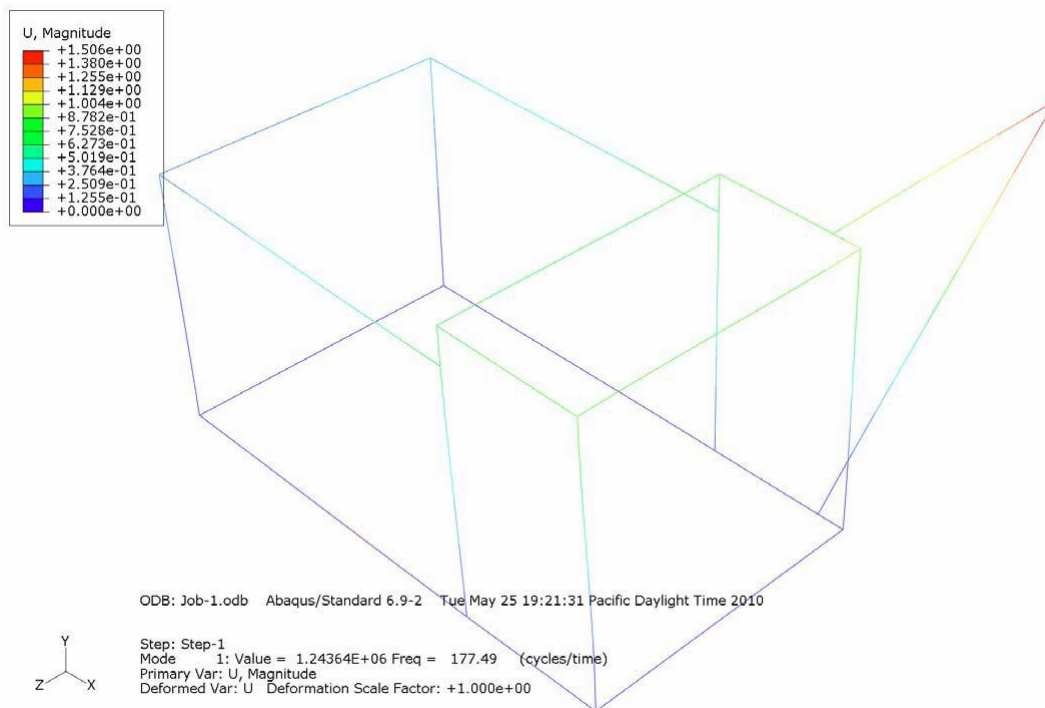


Figure 18: The 1st natural frequency of the frame

The frame of our test rig is consisted of 2" x 2" box beams at 1/8" thick, and the support leg for the linear actuator is made of 1" x 1" square tube at 1/8" thick. Both are made out of general purpose carbon steel 1008-1026. Using Abaqus the first natural frequency is estimated to be at 10,649 rpm, since this value is more than twice the operating speed we believe that the frame will not be anywhere near the 1st natural frequency. Figure 19 shows the FEA model used to predict the 1st natural frequency of the frame.

Rotor Balance

After assembling the shaft and rotor the unit was transported to Solar Turbines in order to balance the assembly. A representative from Solar placed the assembly on their balance machine and added/removed the required weights to balance the assembly. Figure 16 shows the results of balancing the rotor assembly on Solar's equipment. Both sides of the assembly achieved an eccentricity of 3-4 mils.



Figure 19: Final balance of the rotor assembly.

Frame Design

The frame has been designed to have minimal deflection under load and is made out of 2"x2" 1/8" thick box tubing carbon steel AISI 1029. Then frame analysis was done using an FEA program, and the deflection from normal loading was 0.6 thousands. This deflection is in the vertical direction at the pulley end, which is not very critical. The deflection at the rotor is in the vertical direction and is 0.12 thousands in the downward direction. This deflection is a result of the loads in the frame from the pulley and the force generated when the test material comes in contact with the rotor. The frame was also designed to be as stiff as possible to make sure vibration wouldn't be a big issue (see Vibrations section above). Figure 20 shows a model of the frame.

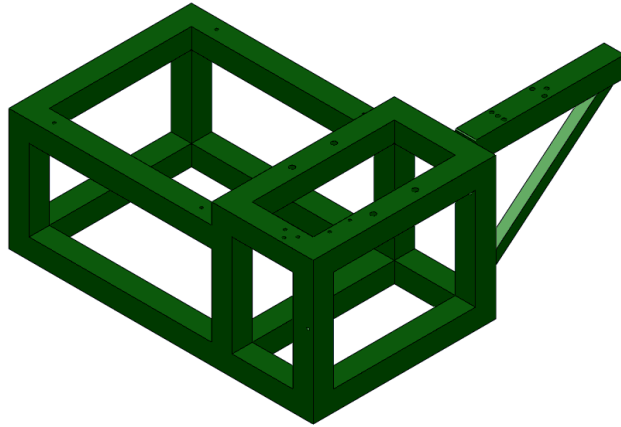


Figure 20: 3-D model of the Frame

Linear Actuator Selection

In order to test samples with our test rig, we were required to implement a device that would retract and extend in increments of a thousandth of an inch; in addition this device will need to be electronically controlled by the user. Table 4 tabulates the requirements that our linear actuator must meet:

Table 4: Linear Actuator Requirements

Requirements	Value
Accuracy	± 0.0005 inch
Controller	Must be electronically controlled
Travel	> 1.0 inch

Table 5 shows makes and models of various linear actuators that will meet or exceed our specifications.

Table 5: Make and Model descriptions for various manufactures.

Manufacture	Make and Model	Accuracy (thou)	Backlash (thou)	Travel (inches)	Max Force (lbf)	Minimum Speed (in/s)	Cost
Zaber	T-LA13A	± 0.472	< 0.1575	0.51	5.6	0.00004	\$782
Zaber	T-LA28A	± 0.472	< 0.1575	1.102	5.6	0.00004	\$852
Zaber	KT-NA08A25	± 0.315	< 0.1575	1.00	14.6	0.00001	\$1050
Zaber	KT-NA08A50	± 0.315	< 0.1575	2.00	14.6	0.00001	\$1200
Zaber	NA-08A16	± 0.315	< 0.0787	0.630	4.3	0.00002	\$532
Zaber	NA-08A30	± 0.315	< 0.0787	1.181	4.3	0.00002	\$556
Zaber	NA-08B16	± 0.315	< 0.0787	0.630	4.3	0.00004	\$532
Zaber	NA-08B30	± 0.315	< 0.0787	1.181	4.3	0.00004	\$556
Zaber	NA-11B16	± 0.315	< 0.0787	0.630	17.9	0.00004	\$389
Zaber	NA-11B30	± 0.315	< 0.0787	1.181	17.9	0.00004	\$433
UltraMotion	NEMA 17 with Controller	± 0.420	$<.5000$	2.00	75		\$1175

* Please note that Zaber T-Series have controllers incorporated in there linear actuators. Zaber NA-Series needs an additional controller that costs \$714.

Linear Actuator Assembly Design

Taking into consideration price, maximum applicable force, travel distance, and accuracy Ultra Motion's Digit Serial#: D-A.083-HT17-21NO-/4 was chosen. This unit exceeds all the requirements and allows the user to push the test material into the rotor with ample force. To protect the linear actuator from the rotor without sacrificing accuracy a dummy shaft attaches to the end of the linear actuator before attaching to the material mount. The dummy shaft is held in place by two linear bearings which will only allow for linear motion. These linear bearings will also nullify any moment created when the rotor hits the test sample thus protecting the linear actuator from any transverse force. The dummy shaft is designed to capture the bending and axial strain as the rotor hits the test sample. With an estimated force of 5 to 10 lbs (both bending and axial) for the rotor to abrade into the test material, strain gauges will be applied to a portion of the shaft that is necked down from 0.5in to .35in. With the estimated force and a lever arm of 3.5in we estimate a bending and axial strain of about 807 and 10 microstrain. Figure 21 shows a 3-D model of our Linear Actuator Assembly. Please refer to Appendix B – Detailed Drawings for full dimensions.

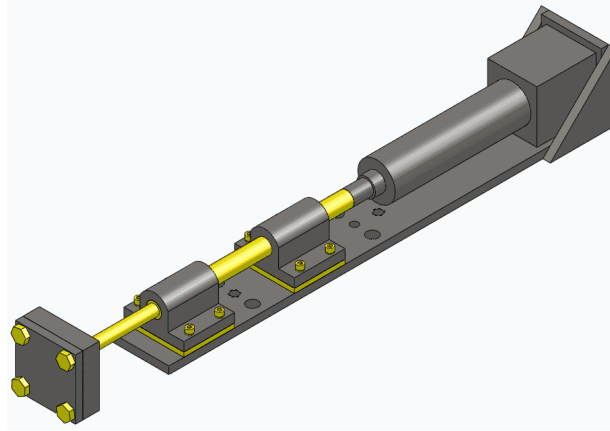


Figure 21: 3-D model of Linear Actuator assembly

Strain Gauge Set-Up

With such a low expectation of strain for both axial and bending a full Wheatstone bridge will be utilized for both cases to maximize the sensitivity. Figure 22 shows the current strain gauge setup on the dummy shaft. Please refer to Appendix I – Strain Gauge Analysis (ESS program) for detailed analysis.

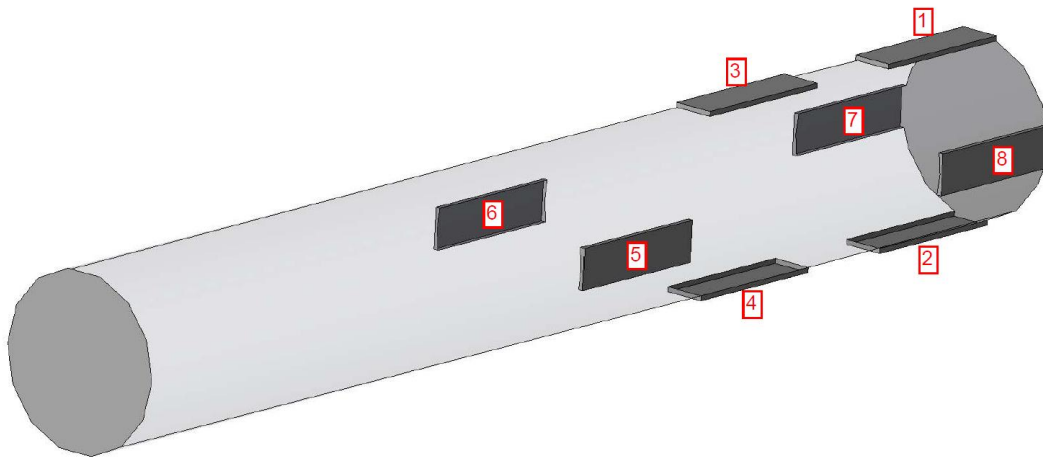


Figure 22: Strain gauge placement on Dummy Shaft

Figure 23 A and B shows the Wheatstone bridge configuration for measuring bending and axial load.

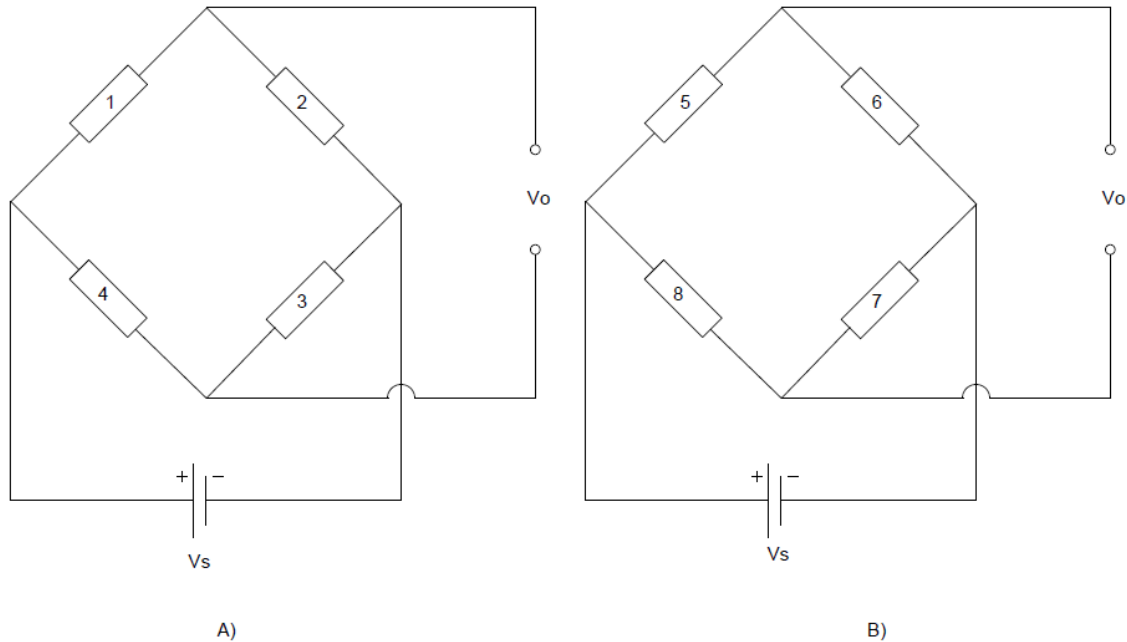


Figure 23: A) Wheatstone bridge configuration for measuring bending strain. B) Wheatstone bridge configuration for measuring axial strain.

Instrumentation:

The following data must be collected: Surface temperature of the test sample (metallic only), torque generated from the motor due to the applied force, rate at which the linear actuator moves, length of movement of the linear actuator, the rotational speed of the shaft, and the duration of operation. Please refer to Appendix D for Testing procedure and diagram.

Hardware and Software

Computer: Dell Desktop

Software: LabView 8.6 (Please refer to Appendix K – “Position VI” and “Temperature and Strain Monitor VI” for a description of the programming that was used)

Data acquisition card: National Instruments PCI-6220

I. Sample rate collection rate: 1000 samples at 1.5Khz

Interface Block: National Instruments SCB-68 (Please refer to Appendix H – SCB-68 for data sheet)

Strain gauges: Vishay’s general purpose strain gauges – SN: EA-13-120LZ-120/E

Strain Gauge Conditioners: (2) Vishay’s P3 box (Please refer to Appendix H –Vishay P3 Manual for data sheet)

Settings:

I. Bending – Full bridge, automatic balance, analog output - normal.

Calibration Equation: $Y=2560X-3200$

Calibration done within LabView refer to Appendix I - Strain gauge calibration

II. Axial – Full bridge, automatic balance, analog output - low.

Calibration Equation: $Y=217X-320$

Calibration done within LabView refer to Appendix I - Strain gauge calibration

Speed Sensor: Jaquet Hall Effect Sensor – Model# F58S (Please refer to Appendix H - F58S for data sheet)

Settings:

- I. Input: 8.6Volts DC, output 5.6Volts Square wave.

Position indicator: Applied Motion ST5-S Stepper motor controller (Please refer to Appendix H –ST5S for data sheet)

Speed Sensor: To verify the speed at which the rotor is spinning, a Hall Effect sensor will monitor the rotation of the shaft. A small magnet is attached on the keyway of the shaft and the sensor will be located right underneath. LabView is programmed to plot the square generated by the sensor in analog signal. A timing and measurement VI will count the number of square waves within a second and then display the frequency of the shaft.

Position Indicator: After testing the validity of the positioning of the linear actuator, the linear position will be tracked by the number of steps indicated by the stepper controller.

Temperature sensor: In order to record the surface temperature, thermocouples are attached onto the test samples themselves. Thermocouples will be read through the SCB-68 with the use of the Cold Junction Compensator.

Strain Indicator: Vishay's P3 boxes will provide the required conditioning and amplification of the strain gauges. These boxes will then output an analog signal into the interface block (SCB-68) at 480Hz. Within the DAQ system the strain gauges will be calibrated to output microstrain. Calibration included weighing know weights on the end of the shaft and calculating the calibration constant with that process.

Cost/Bill of Materials Estimation:

The set budget for this project is \$5000.00 Table 6 shows the breakdown of all the spending required for the completion of project. The majority of the spending is attributed to the cost of the linear actuation plus its controller, and the motor and the motor controller.

Table 6: Bill of Materials and Cost

Bill of Materials						
	Item	Cost	Quantity	Predicted Cost	Actual Cost	Shipping + Tax
1	Rotor Assembly			\$326.70	\$645.47	
	1-1/8" Shaft	26.7	1	\$26.70	\$25.28	\$9.89
	1" Shaft with key				\$36.00	
	1" Pillow Block Bearings	150	2	\$300.00	\$109.30	
	Rotor	-	1	-	\$340.00	
	Machining the Rotor CNC				\$125.00	
2	Linear Actuator Assembly			\$1,175.00	\$1,357.41	
	Steel - 1/2" Dummy Shaft				\$9.67	
	Aluminum - 1/2" Dummy Shaft				\$7.15	
	Linear Bearings		2		\$96.60	\$26.82
	Actuator with controller	389	1	\$1,175.00	\$1,175.00	\$40.00
	1/4" Flat Bar Stock				\$2.17	
3	Frame Assembly			\$338.74	\$226.58	
	2x2 box	48.06 per 6 ft	30 feet	\$240.30	\$112.00	
	1/8" Steel Plate	24.61	2 ft^2	\$98.44	\$76.57	\$25.00
	1/4" Plate				\$13.01	
4	Motor Assembly			\$1,183.42	\$1,686.44	
	5hp 3 phase motor	399.5	1	\$399.50	\$399.50	\$151.43
	Motor Controller	696	1	\$696.00	\$775.50	
	Section A V-Belts	6.69	4	\$26.76	\$43.88	\$18.46
	Pulley (Sheave 1")	30.58	1	\$61.16	\$102.80	\$20.26
	Pulley (Sheave 1.125")				\$125.60	
	Bushing 1"		2		\$32.66	
	Bushing 1.125"				\$16.35	
5	Measurement Tools and Misc Hardware	500	-	\$500.00	\$557.32	
	Strain gauge, Epoxy kit, wire				\$50.00	
	Bolts, Washers, and Nuts				\$79.60	
	Data Acquisition System				School	
	RPM sensor				\$100.00	\$25.00
	Motor wiring + Power Cord				\$71.00	
	Paint				\$10.00	
	Solder and shrink fit				\$10.00	
	End Mills, Taps				\$166.72	
	Aluminum Jig				\$30.00	
6	Testing Material			N/A	\$477.69	
	Fluorosint 500				\$184.80	\$21.20
	Fluorosint 207				\$221.75	\$21.20
	Aluminum 6061				\$28.74	
Total				\$3,523.86		\$4,922.17

CHAPTER 5: Product Realization

Manufacturing Processes

Welding

The Frame was made out of 2 inch square tube with a 1/8 inch wall thickness. The tubes were cut to length using a horizontal band saw and then welded together with a Miller MIG welder. The frame was lined up with a series of jigs to make sure it went together as straight as possible. The next thing to be welded was the collection bucket and the safety shield. These two items were both made out of 1/8 inch steel plate and cut using a plasma cutter. Then they were welded together with the Miller MIG welder. Figure 24A and 24B shows a photo of the welding process for the frame, collection bucket, and safety shield



(A)



(B)

Figure 24: A) and B) Photos showing the welding process

Lathe and Mill

The Motesa Lathe was used to machine the dummy shaft that connected the linear actuator to the material mount. The dummy shaft was made out of 6061 aluminum turned down using a carbide insert cutting tool. This tool gave for a more accurate and smoother cut.

The rest of the parts that needed machining were made with a Mill. Most of the Milling processes were done on the Bridgeport using a series of end mills. The material mount was made out of a piece of 3/4 inch plate aluminum 2 inches square. The holes in the plate were then drilled and tapped in the drill press. For accuracy the holes in the linear actuator mount were drilled in the mill. Because of inaccurate welding there were two shims that had to be made in the mill to accommodate for the frame not being straight. Both of the jigs that were used in the manufacturing of the rotor also were machined in the mill and lathe. To allow for proper clearance for the ACME screw to be able to pivot in the motor mount the through hole in the mount was milled to a length of 1.5 inches.

Drilling

All of the holes in the frame had to be drilled using a hand drill because the frame was too large to fit in any of the mills or drill presses in the machine shop. The larger holes that were used to mount the linear actuator and the rotor assembly were sealed with crush sleeves to give added strength to the frame.

The 20 balancing holes and the 3 center holes on the rotor were drilled out on the drill press which was used to keep the taps straight in tapping the 20 balancing holes.

Rotor Build

The rotor is one of the most important parts of this test rig. The more accurate the rotor is the better the test results from the material tests will be. It would be too expensive and take too long to send the rotor out to a machine shop to be machined. The rotor ended up being machined in house at the "Cal Poly Hanger" machine shop. The material of the rotor was made out of was 15-5 PH Stainless Steel with a 12.5" square plate $\frac{3}{4}$ " thick.

The first step in fabrication was to machine the square plate into a disk. To do this the HAAS VF2 CNC mill was used. The CNC ran a "roughing end mill" around the plate cutting the plate into a 12.5 inch diameter disk. The final process involving the mill was to drill the pilot holes for the 20 balancing holes and the 3 center holes that mount the bushing to the rotor. The rest of the machining was performed on a Motesa Lathe.

A jig had to be made to mount the rotor in the Motesa lathe, this Jig (1) was made out of a 3 inch diameter piece of 6061 aluminum. The rotor was then mounted in the lathe with jig (1) and bored the center hole tapered at 1.5 degrees to fit the bushing between the rotor and the shaft. The big end bore diameter is 1.8 inches. Another jig or Jig (2) had to be made to make the key way in the rotor. Jig(2) had to take into account the placement of the key in the rotor so it would be lined up with the 3 center bolt holes that bolt to the bushing. Using a broaching kit and a hydraulic press, a 3/8 inch key way was broached into the rotor.

The rotor was then mounted on the shaft and this assembly (rotor assembly) was placed in the Motesa Lathe to machine the labyrinth tooth. This is the most important machining process for the rotor in order to minimize the run out. A dial indicator was used to line up the rotor in the lathe then the labyrinth tooth was machined using the cross-feed on the lathe to get the right angle needed.

Once the labyrinth tooth was machined the rotor needed to be faced in order to take out the surface impurities of the plate. When the turning and facing of the rotor was finished the last process was to tap the 20 balancing holes to 1/4 -28 for Solar Turbines to balance the rotor for spinning at 5000 rpm. Figure 25 shows the lathing process.



Figure 25: Lathing process for the stainless steel rotor

Changes made in Construction

During the construction of the test rig few things were changed from the initial design. The main design change was the way the rotor was mounted to the shaft. Instead of using a heat shrink, a bushing that is commonly used to mount pulleys to shafts was used to mount the rotor to the shaft. This made the rotor removable if necessary. The motor mount also had to be changed because a 4 belt tensioning pulley could not be found. A tensioning system had to be designed into the motor mount making the motor able to pivot and move vertically tensioning the four v-belts. The dimensions of the dummy shaft were changed by decreasing the shaft diameter to increase sensitivity. The material of the shaft was changed from steel to aluminum for the same reason. The weak link in the dummy shaft was also taken out for fear that it would add too much error in the testing.

Recommendations for Future Manufacturing

The test rig worked well for a first model, but like any prototype it can always be improved upon. With a runout of 0.007 inches the rotor should be re-machined to have less run out. This can be done using a more accurate lathe. For the safety shield a better hinge that will reduce the amount of slack should be used. The linear actuator mount on the frame should be reattached with a better jig so it will be in line with the rotor more accurately. A new concept should be designed to accurately measure the axial load applied on the rotor by the linear actuator. This is because our current prototype doesn't read the proper axial strain generated during the abrasion process.

CHAPTER 6: Design Verification and Testing

Test Descriptions

The main goal of the test design for this project was to replicate the conditions that each sample underwent during testing so the material properties would be the only variable changing when switching between samples. A program was written in LabView that would move the test sample to the edge of the rotor and then would move the material into the rotor 0.01 in, pause for 5 seconds, and then move the material in another 0.01in before backing out (Please refer to Appendix G – Labview Programming). To find the edge initially before any abrading takes place the thickness of the sample is subtracted from the know air gap distance between the material mount and the rotor tooth. The initial distance between the material mount and the rotor tooth was found using a caliper. The motor was run at 56 HZ of the available 60 HZ which was the frequency that the Hall Effect sensor read 5000 rpm. The final step was to run the DAQ system to collect the bending strain which was converted to force and torque applied on the rotor. A full explanation of the testing procedure that was conducted is presented in Appendix G – Testing Procedure.

Fluorosint 207 Testing

Six samples of the Fluorosint 207 were tested following the procedure above, please note that all graphs can be seen in Appendix K – Testing Data. The average strain recorded for the Fluorosint 207 reached around 640 micro strain which equates to a force of 8.95 lbs acting at the end of the test sample and 53.7 lb-in of torque on the rotor. The peak strain occurred right at the first initial abrasion which then decreased as the material abraded away causing less rub. The second abrasion occurring 5 seconds after the first was on average a bit less than the first. Qualitatively analyzing the test sample the abrasion was very clean with no sign of burning of the material and had very fine particulate matter for the residue that abraded away. The material test logs, graphs, and the raw data recorded for each of the six test runs for the Fluorosint 207 can be seen in Appendix J– Testing Data.

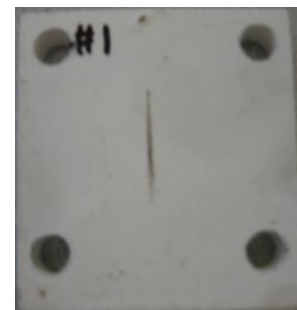
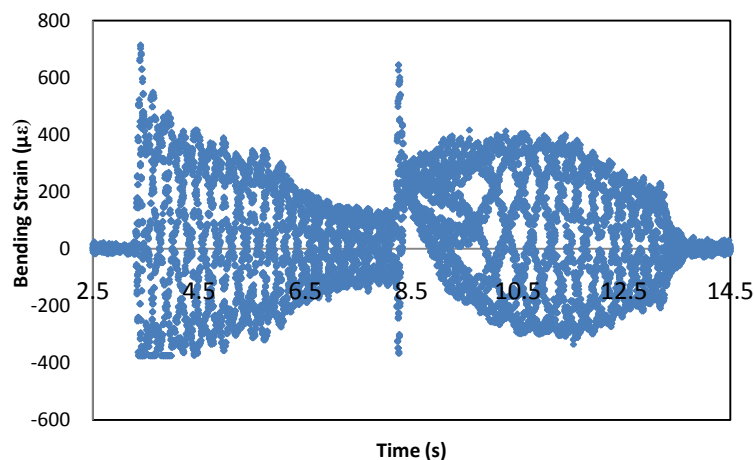


Figure 26: This graph shows the bending stain of the dummy shaft with respect to time for test 1 of the Fluorosint 207. A picture of the actual test sample is shown on the right.

Fluorosint 500 Testing

Due to error in the P3 box setup the strain was capped too low so we were only able to test 3 of the 6 samples of the Fluorosint 500 accurately. All graphs including the ones that were not reported may be seen in Appendix K- Testing Data. The average strain for the Fluorosint 500 tests was around 705 microstrain correlating to a force of 9.79 lb and a torque on the rotor of 58.74 lb-in (Figure 27). The Fluorosint 500 abraded similarly to the Fluorosint 207 with the largest strain being generated during the first abrasion. When qualitatively accessing the samples of Fluorosint 500 the material appeared to burn leaving black residue on the abrasion raising concerns about its ability to handle heat due to friction Figure 27. The material test logs, graphs, and the raw data recorded for each of the three test runs for the Fluorosint 500 can be seen in Appendix J - Data Collection.

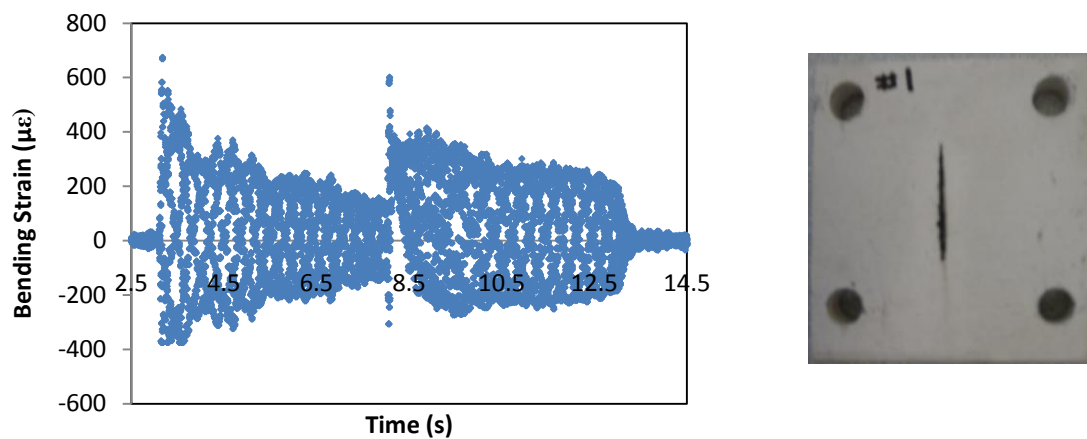


Figure 27: This graph shows the relationship between the bending strain of the dummy shaft with respect to for test 1 of the Fluorosint 500. An image of the actual test sample is show on the right.

Lead Babbitt Testing

To test the Lead Babbitt material a full ring of Lead Babbitt with steel backing had to be machined into the 2 inch by 2 inch square piece to attach to the material mount. Only one sample was fully tested due to time restrictions, however both test graphs done with the Lead Babbitt may be seen in Appendix K – Testing Data. The Lead Babbitt yielded a max strain of $357\ \mu\epsilon$ generating a force of 5 lb and a torque of 30 lb-in on the rotor. Qualitatively the lead Babbitt was a clean abrasion with no burning. Figure 28 shows the test data recorded by the DAQ system and the test sample associated with it. No leftover residue was collected during the abrasion of the Lead Babbitt material. The summary of the test results can be seen in Table 7. The material test logs, graphs, and the raw data recorded for each of the two test runs for the Lead Babbitt can be seen in Appendix J – Data Collection.

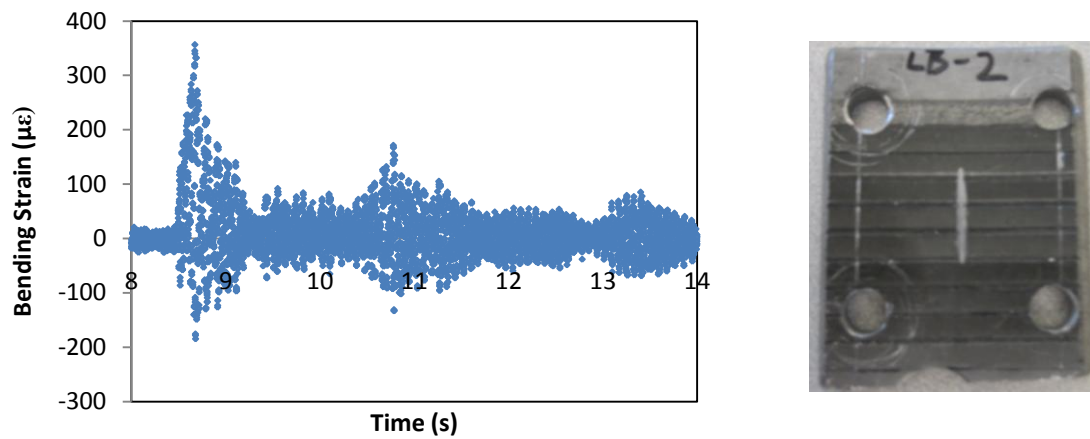


Figure 28: This graph shows the relationship between the bending strain on the dummy shaft with respect to time for test 2 of the Lead Babbitt. An image of the actual test sample is shown on the right.

Table 7: Summary of the Test Results

	Max Bending Strain ($\mu\epsilon$)	Force Acting on Test Sample (lb)	Torque Acting on Rotor (lb-in)
Fluorosint 270	640	8.95	53.7
Fluoroint 500	705	9.79	58.74
Lead Babbitt	357	5.0	30

Verification Check List

To protect the linear actuator our Linear Actuator assembly included two linear bearings and a dummy shaft that shield the linear actuator from transverse forces generate from the interaction between the rotor and the test samples. This design was verified when the linear actuator ran the test material into the rotor at a distance more than allowed. As a result the dummy shaft yielded to the torque that was applied to the test sample. Although the dummy shaft is permanently deformed it verified that the two linear bearings will protect the linear actuator from transverse loads.

In order to achieve a rotational speed of 5000 rpm a pulley system with a pulley ratio of 1.47 was implemented. The motor that drives the system spins at 3430 rpm and pulley system spins the rotor assembly to 5000 rpm. To verify that the rotor is spinning at the correct speed a Hall Effect sensor is used to monitor the frequency of the shaft assembly. Figure 29 shows the frequency of the Hall Effect sensor vs. the reading from the variable frequency drive. The slope of the plot gives the ratio of what the rotor is spinning at to the rotational speed of the motor. Theoretically this number should match the pulley ratio that was used. With a slope of 1.448 and a pulley ratio of 1.47 we are certain that the rotor assembly is spinning at the correct speed.

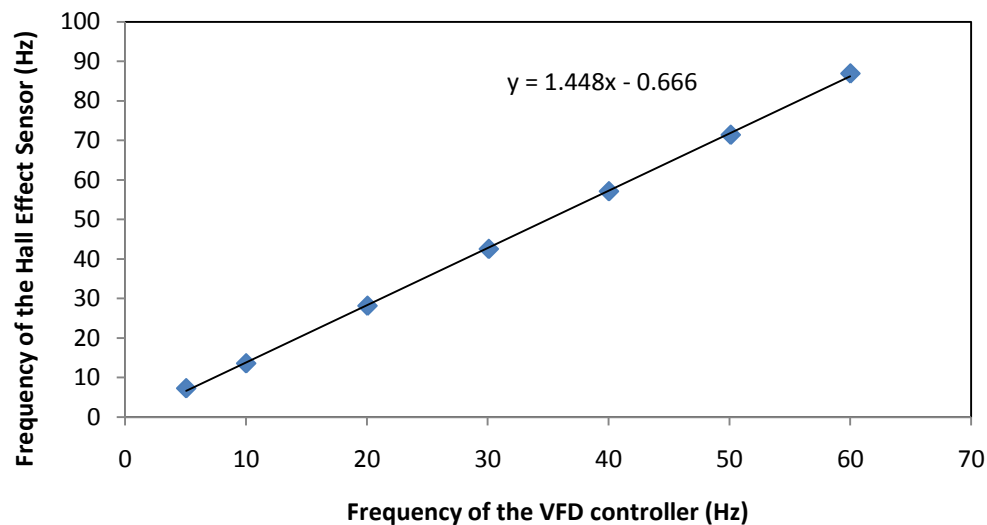


Figure 29: Frequency comparison of the Hall Effect sensor vs. VFD controller

CHAPTER 7: Conclusion and Recommendations

Conclusion

All the initial goals for this project have been fulfilled. By researching the ideal material properties for abradable seals we found that a good starting range for hardness is between 3 to 100 Vickers. Service temperature was another important aspect where anything above 100°F is worth testing. We also found that a yield strength and young's modulus ranging from 2 to 35ksi and 10Msi and below (respectively) are good candidates for testing. We found materials that met these criteria and procured the following materials: Fluorosint 207, Fluorosint 500, Aluminum 6061 T6511, and a Lead Babbitt material supplied by Solar.

The next goal was to design a test rig that would measure the force required to abrade into each test sample. Our test rig produced accurate and repeatable results for each test sample. The material that was easiest to abrade producing the least amount of force acting on the rotor was found to be the Lead Babbitt Material currently used by Solar. However according to CES the Fluorosint materials have a higher service temperature than the Lead Babbitt and could allow Solar to raise the operating temperature of their compressors. It was determined that the Fluorosint 207 was easier to abrade than the Fluorosint 500 and from visual inspection the Fluorosint 500 burned slightly leaving Black Residue on the sample. To increase the operating temperature of Solar's Compressors we recommend further testing be done on the Fluorosint 207 which we feel was the best material in terms of abrading with the highest service temperature.

Recommendations for the Future

While designing our prototype a lot of insight was gained in determining what is best for an abradable seal test rig. For designing a future test rig we feel that being able to test a full ring will be a crucial for increasing the accuracy of the simulation for a few reasons. First, a better estimate of the forces required to abrade a whole ring can be analyzed and second the material abraded away stays in the labyrinth longer helping to determine if damage occurs after the initial abrasion. It is also recommended that if a test rig that involves a linear actuator is used, a linear position sensor should be used to increase the accuracy of the design. Since the data acquisition system is not included when the project is handed over to Solar, we recommend a DAQ system that is more accurate and compact. The P3 boxes worked well but took up a lot of space on the test rig. For our project we were unable to collect any leftover residue, it is recommended to redesign the collection bucket and safety shield in order to analyze the material that was abraded. At operating speed the vibration of the test rig caused about 20 microstrain of noise which was equivalent to the amount of axial strain expected. To ensure that only axial force is measured, a load cell should be placed at the connection of the dummy shaft and linear actuator. It is important to note that the location is behind the two linear bearings which absorb the traverse loads leaving only the axial load onto the load cell. In the future it is also recommended that the prototype be designed to dampen the vibration.

Appendix A: Bibliography

H.I. Faraoun. "Modelling Route for Abradable Coatings." ScienceDirect 200 (June 2006): 6578-6582.

Phillip Dowson. "Development of abradable and rub-tolerant seal materials for application in centrifugal compressors and steam turbines." Science Direct 2004 (December 2004): 5-10.

Xiao Ma. "Evaluation of abradable seal coating mechanical properties." Science Direct 267 (September 2009): 1501-1510.

Yi Maozhong, Huang Baiyun , He Jiawen. "Erosion wear behavior and model of abradable seal coating." ScienceDirect 252 (January 2002): 9-15.

Y. N. Liang. "Effect of fiber orientation on a graphite fiber composite in single pendulum scratching." Science Direct 198 (October 1996): 122-128.

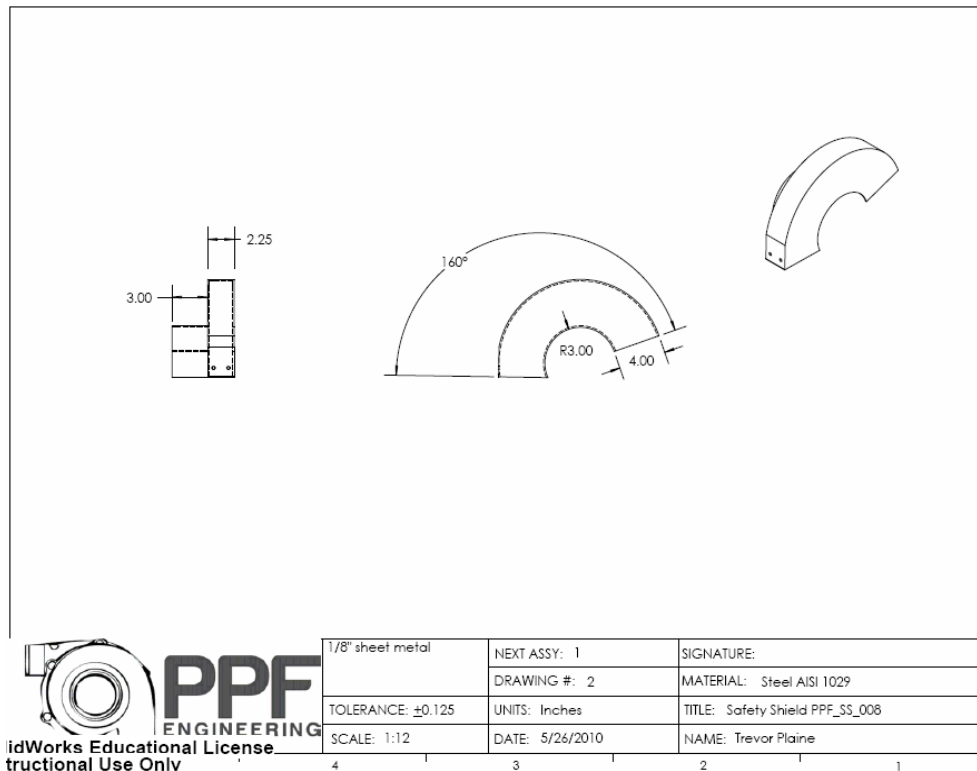
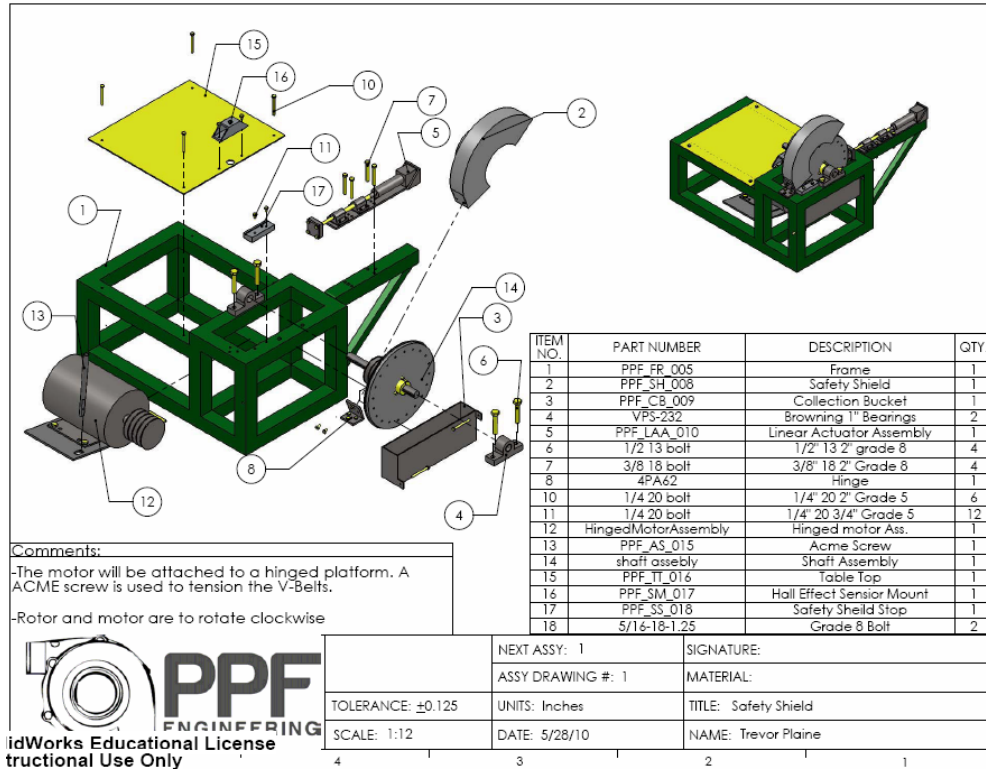
Jennifer V. Matthews, Thomas T. Hamrick. "Labyrinth Seal." Patent 3,701,536. 31 Oct 1972.

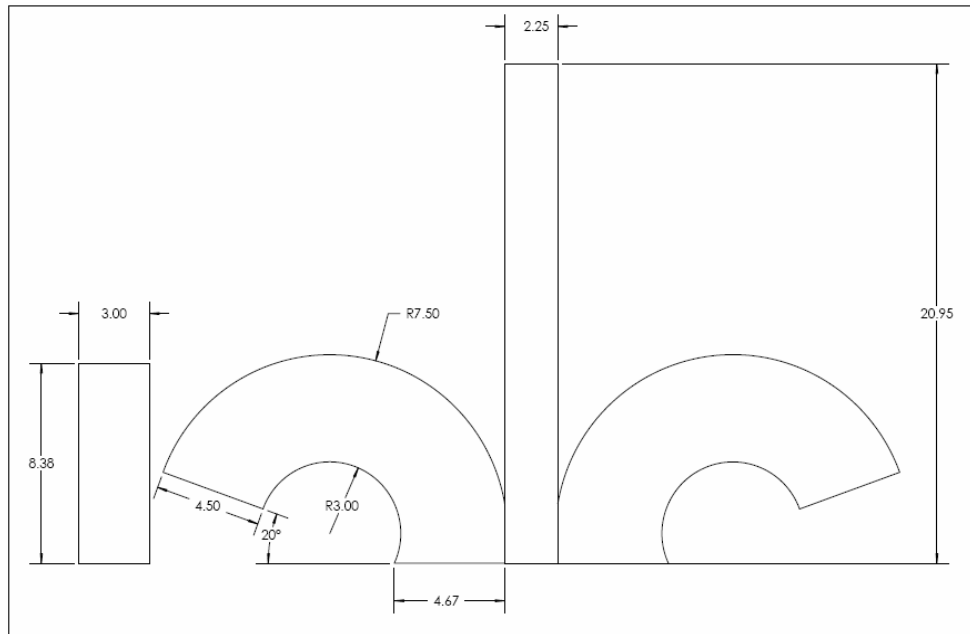
John E. Daunt, Max F. Grandey. "Abradable Material." Patent 3,053,694. 11 Sept, 1962


Raymond J. Elbert, Ernest G. Farrier. "Reinforced Porous Metal Structure and Manufacture." 27 Aug. 1974

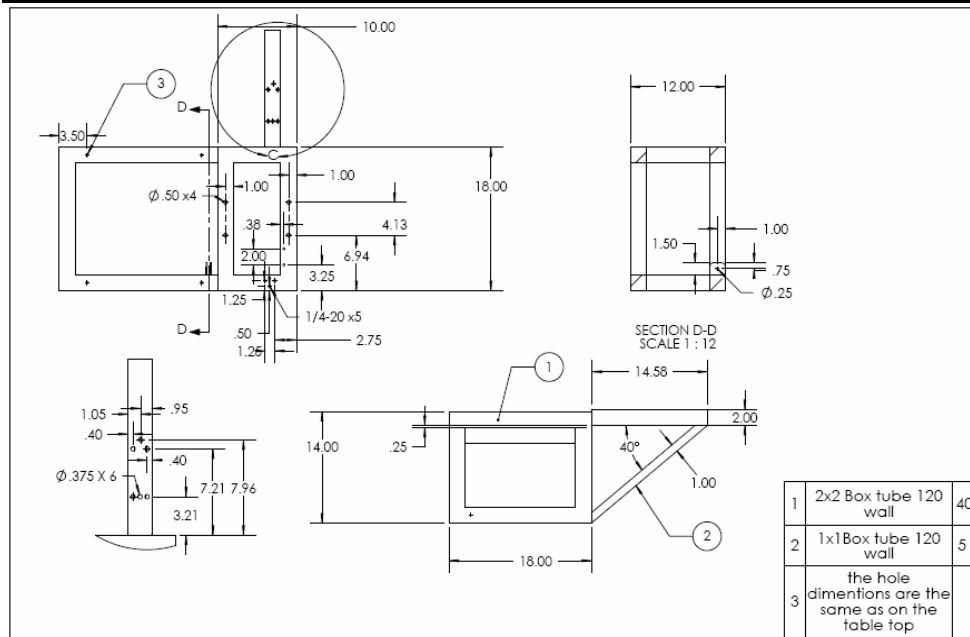
Dally, James W., William F. Riley, and Kenneth G. McConnell. *Instrumentation for Engineering Measurements*. New York [etc.: John Wiley & Sons, 1993. Print.


Appendix B: Final Drawings (Assemblies with Bill of materials)

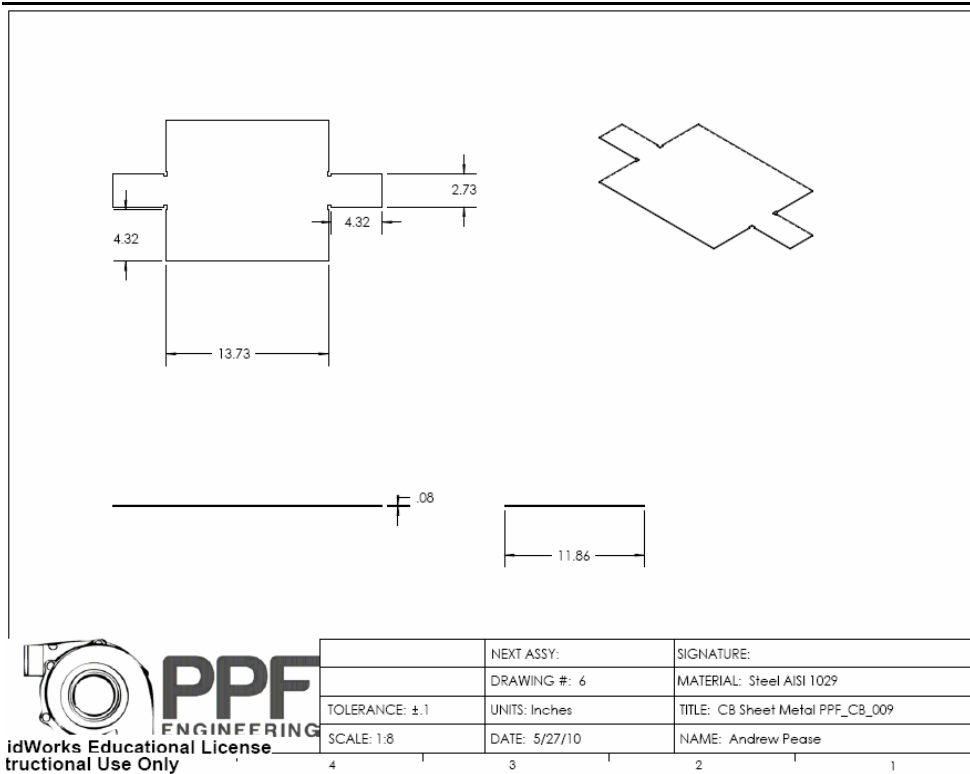
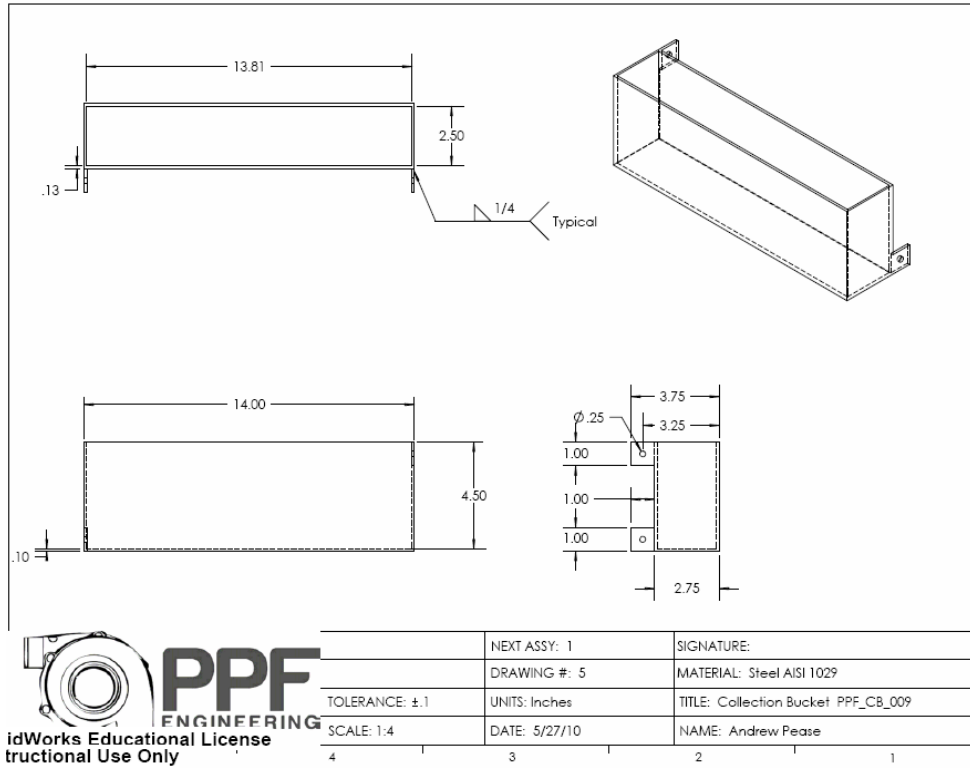


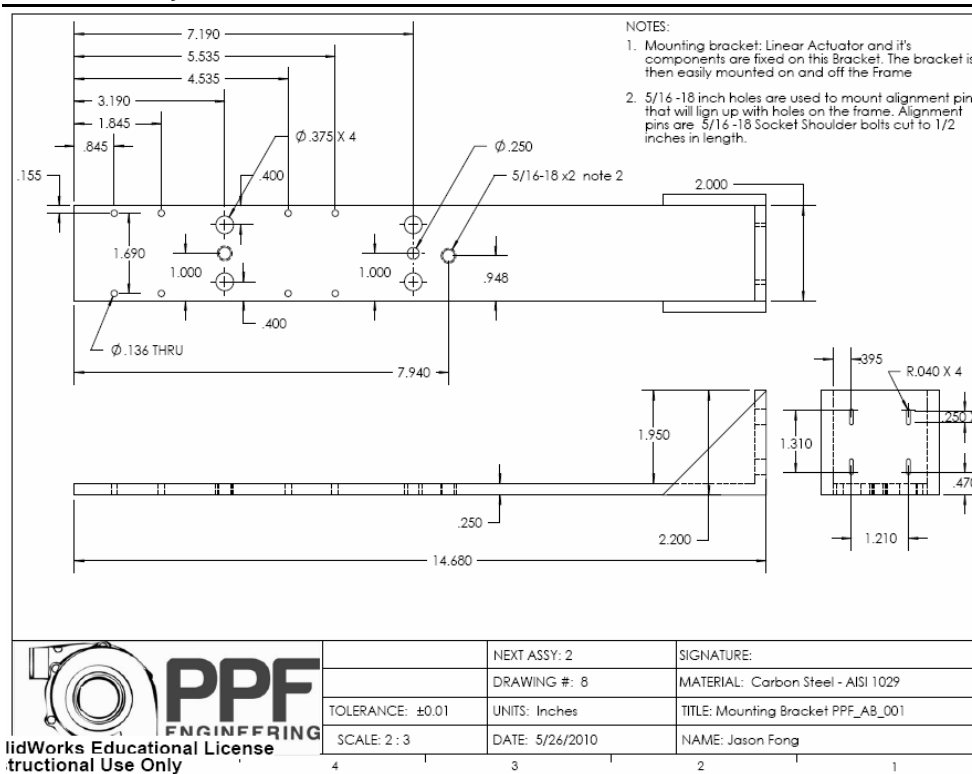
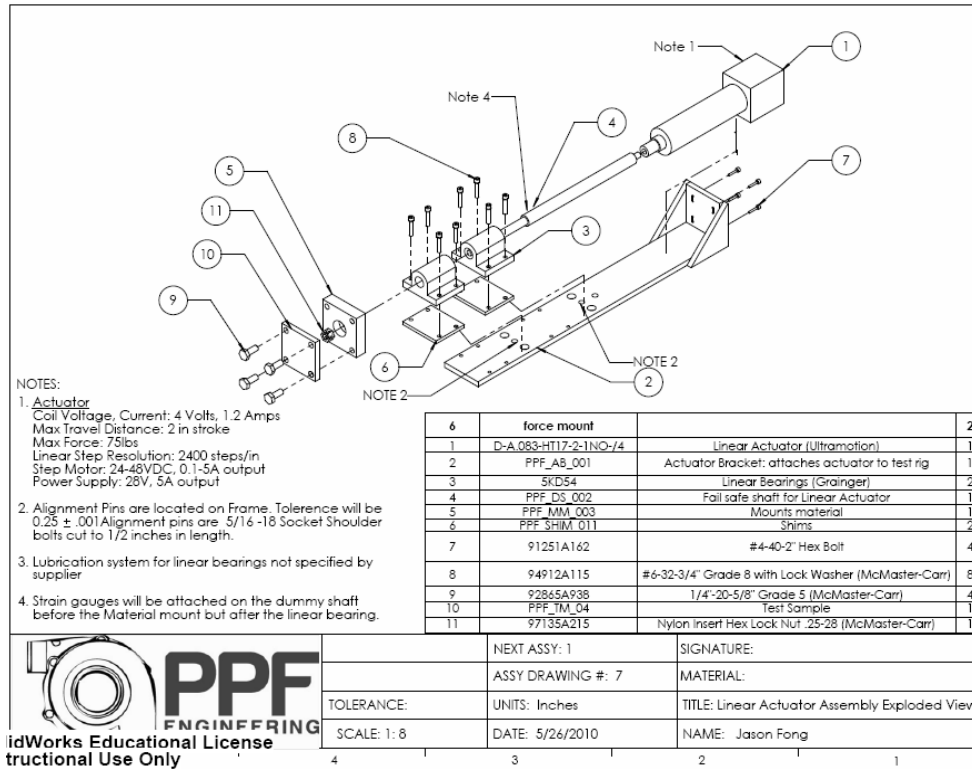


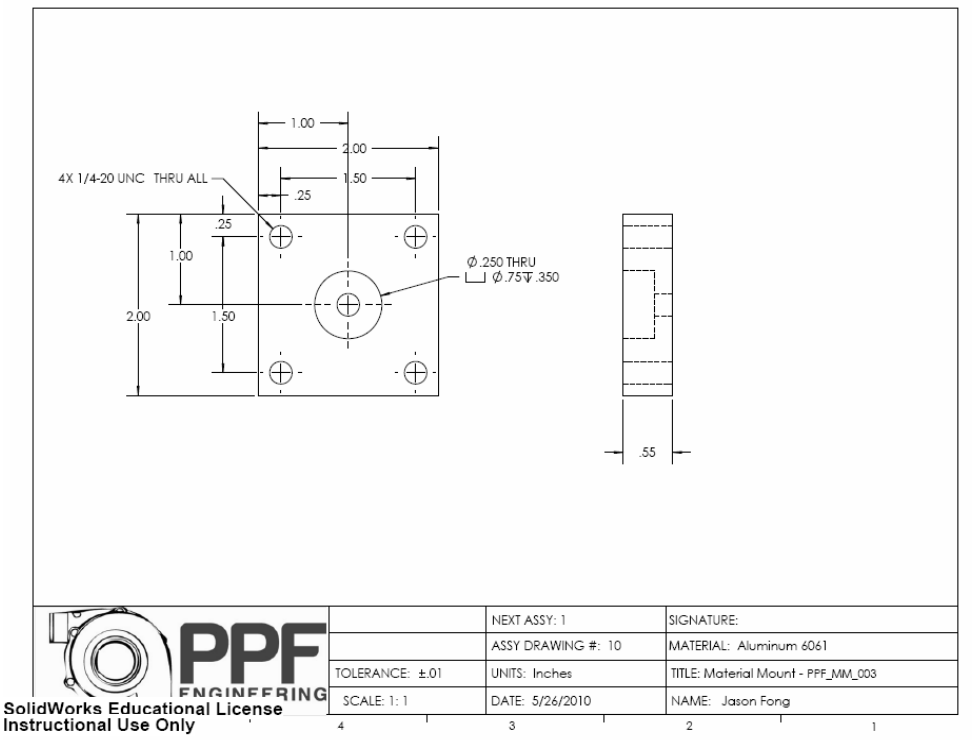
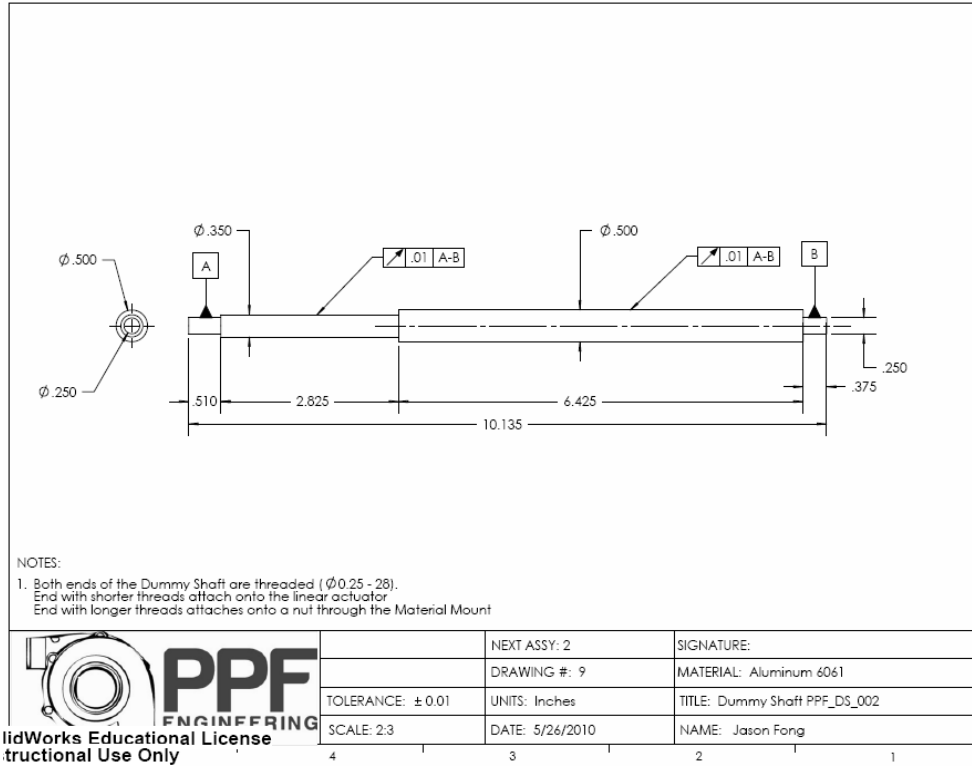
 idWorks Educational License structional Use Only	NEXT ASSY:		SIGNATURE:
	DRAWING #: 3		MATERIAL: Steel AISI 1029
	TOLERANCE: ± 0.1		TITLE: Shield Sheet Metal PPF_SS_008
	SCALE: 1:4		NAME: Andrew Pease

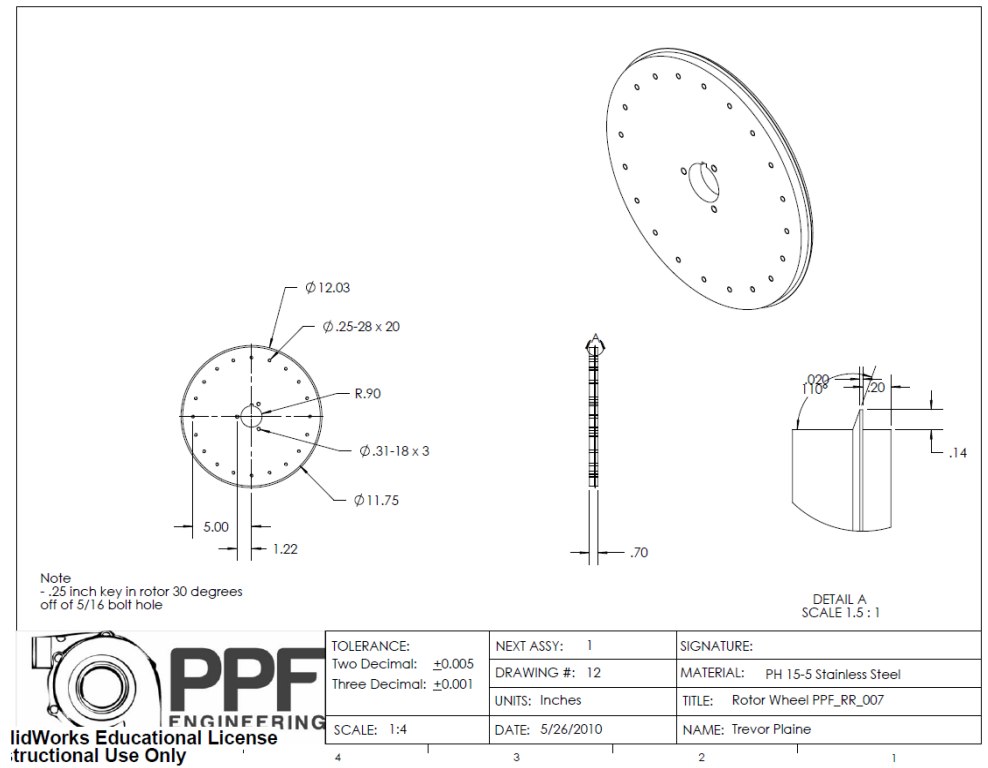
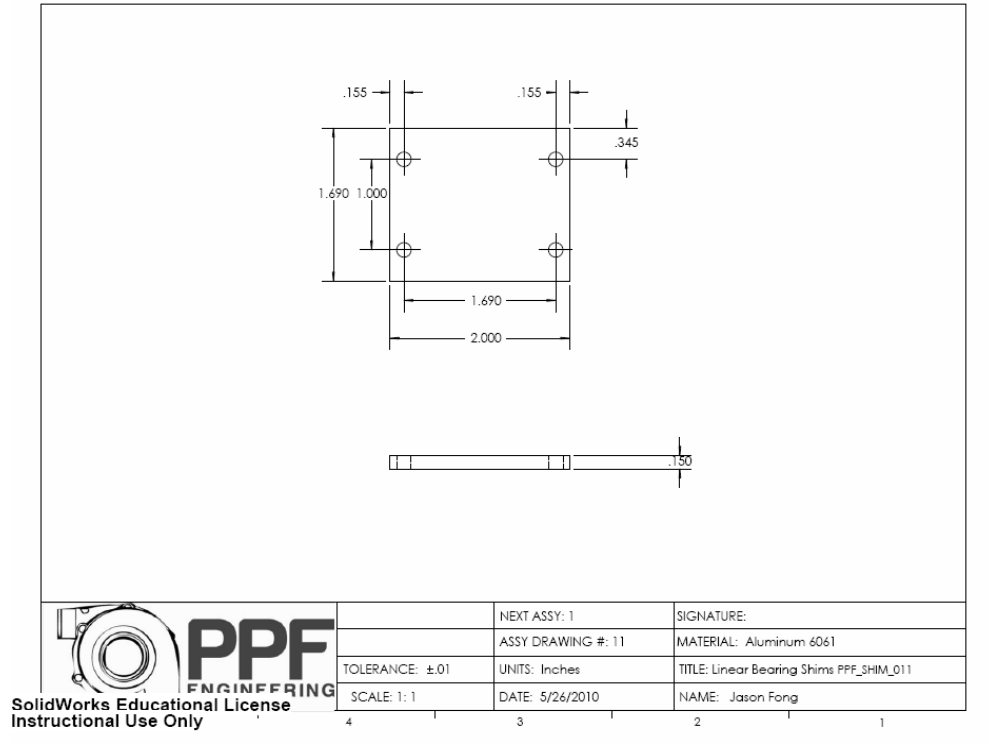


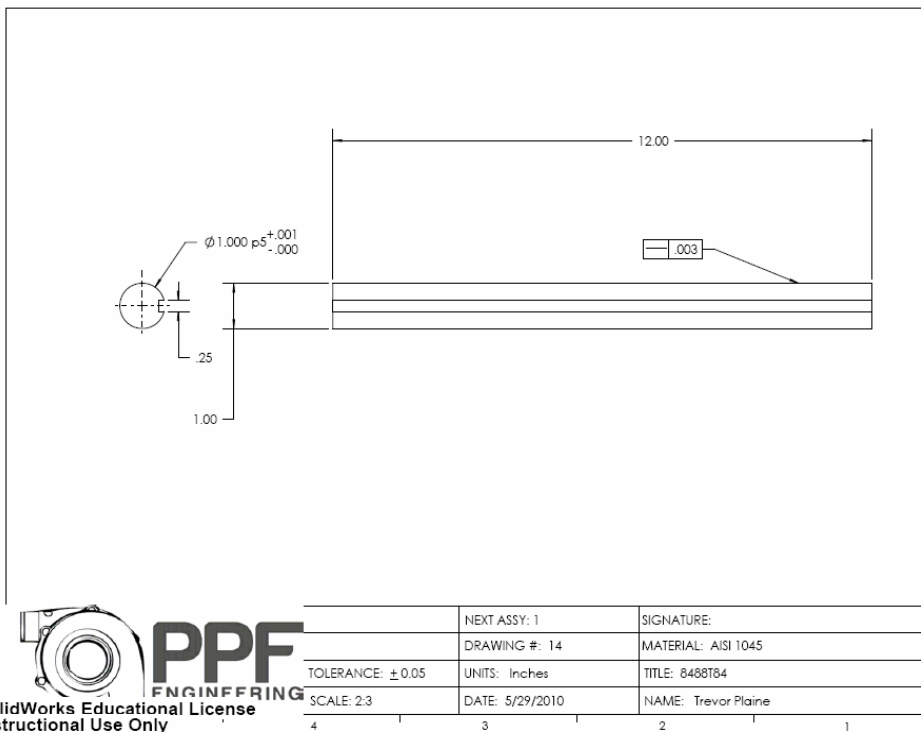
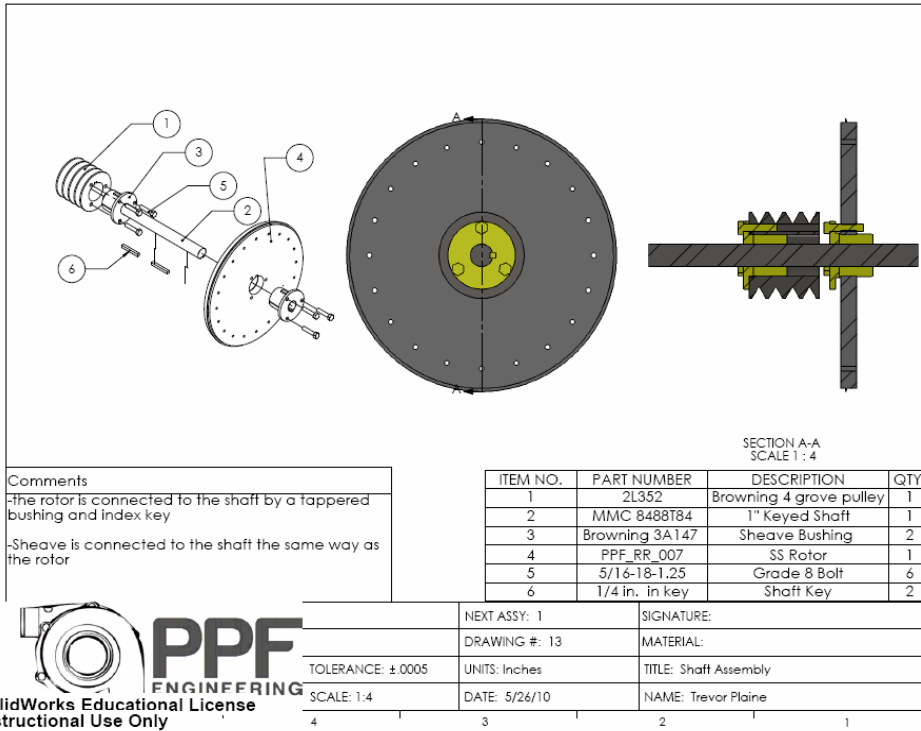
 idWorks Educational License structional Use Only	COMMENTS: All beams are 2" square 1/8" thick wall tubing unless otherwise specified. All beams connected by 1/8" welds. All holes will be closed with crush sleeves		NEXT ASSY: 1	SIGNATURE:
	TOLERANCE: ± 0.01		DRAWING #: 4	MATERIAL: Steel - AISI 1029
	SCALE: 1:12		UNITS: inches	TITLE: Frame PPF_FR_005
			DATE: 5/26/2010	NAME: Trevor Plaine

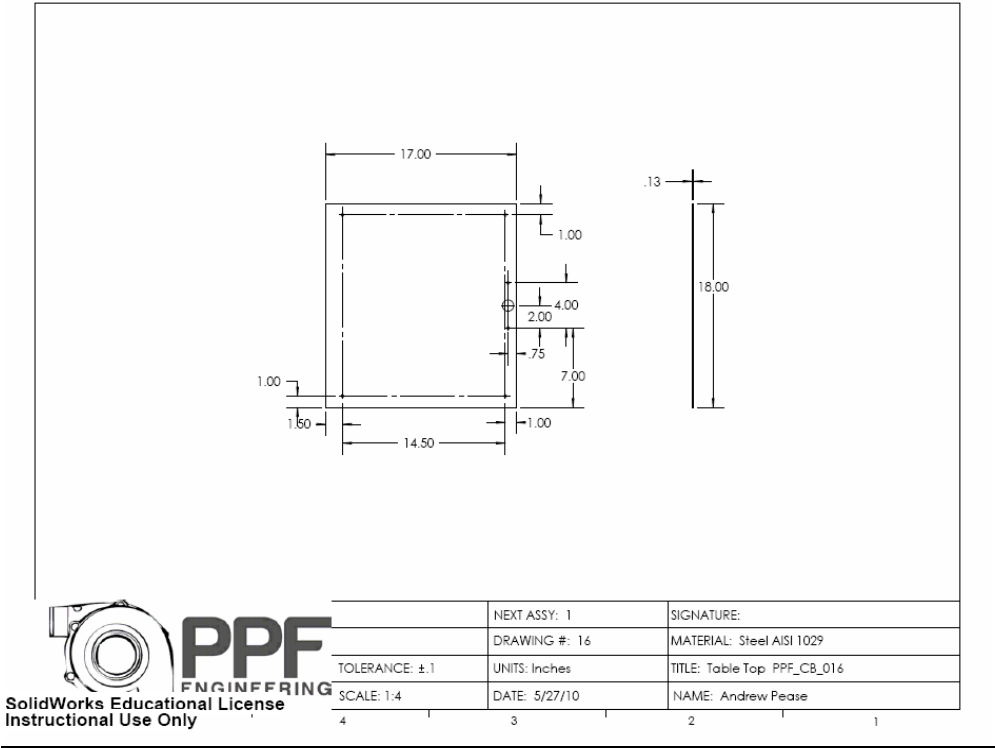
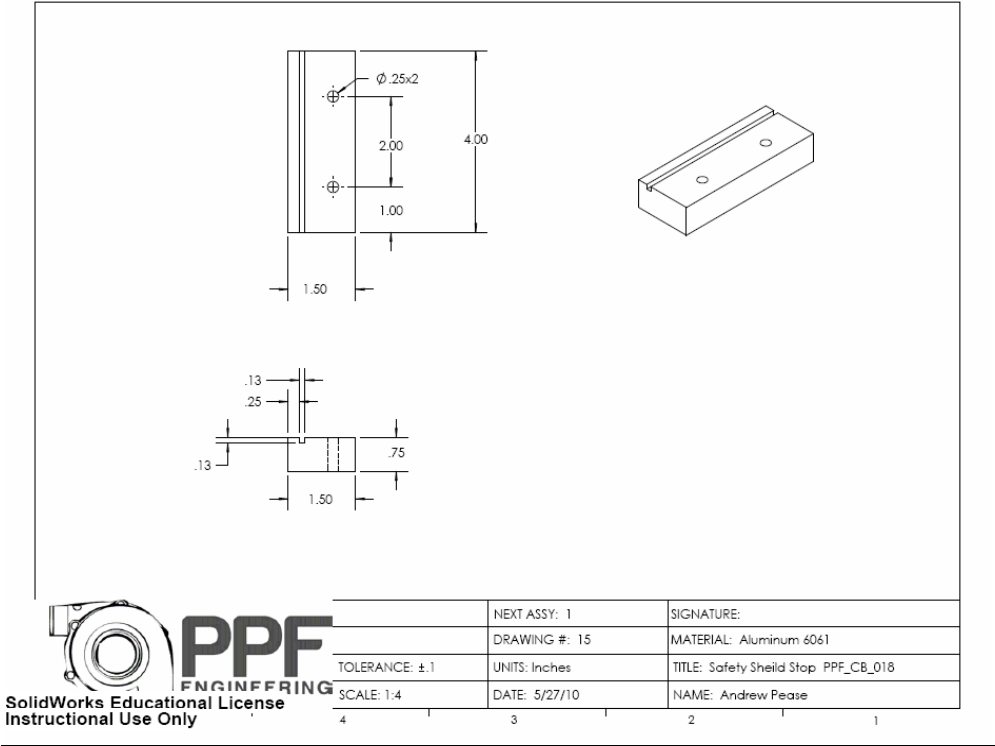


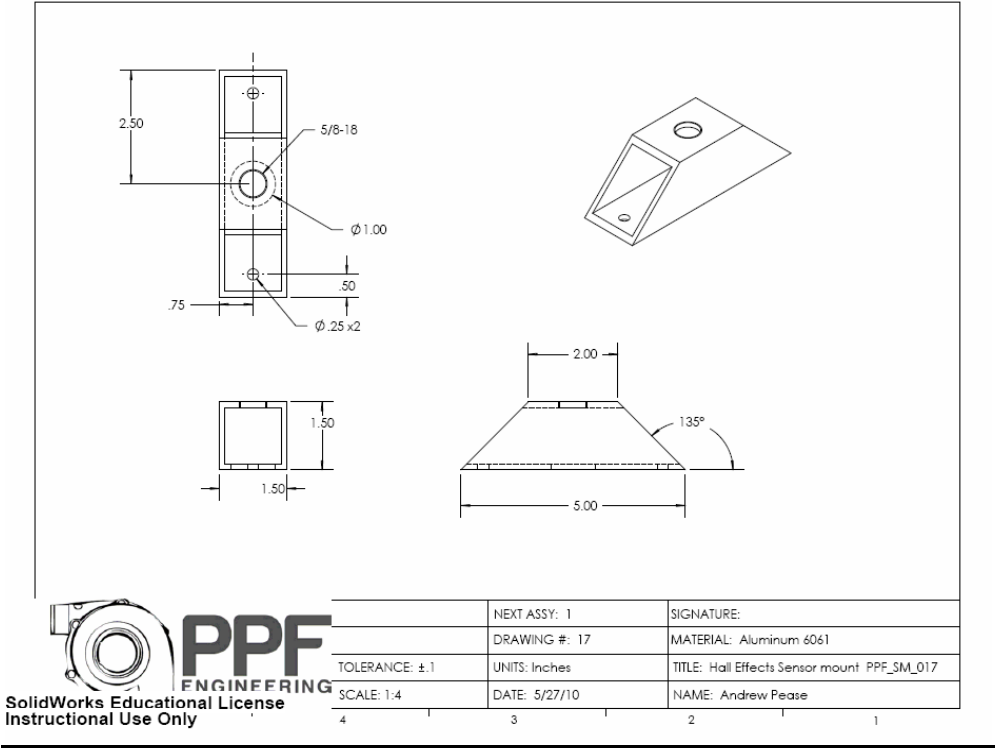












Appendix C: List of Vendors

Grainger: <http://www.grainger.com/>

Home Depot

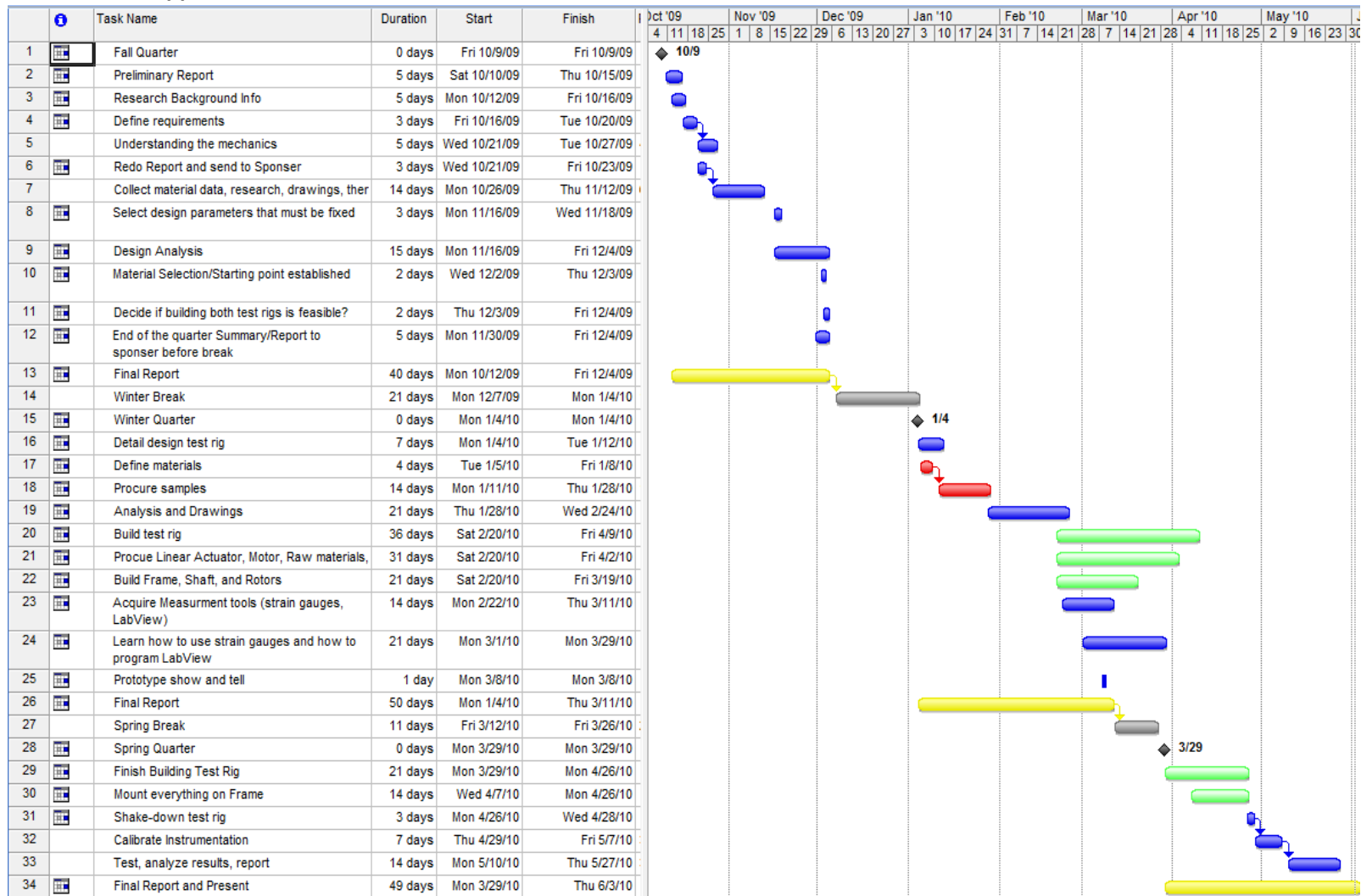
McCarthy Steel

McMaster-Carr: <http://www.mcmaster.com/>

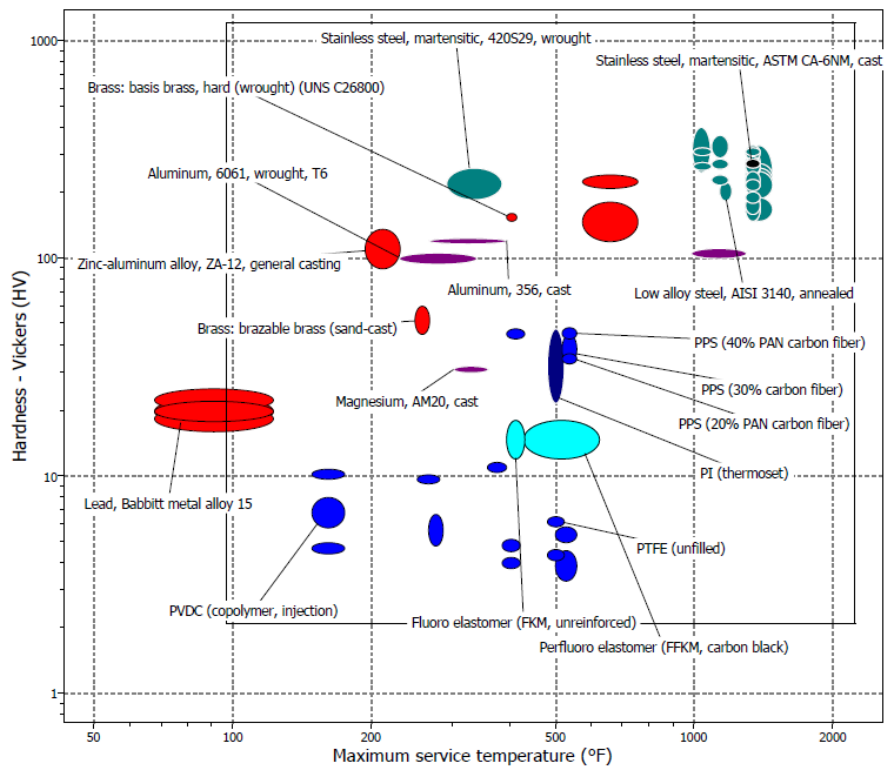
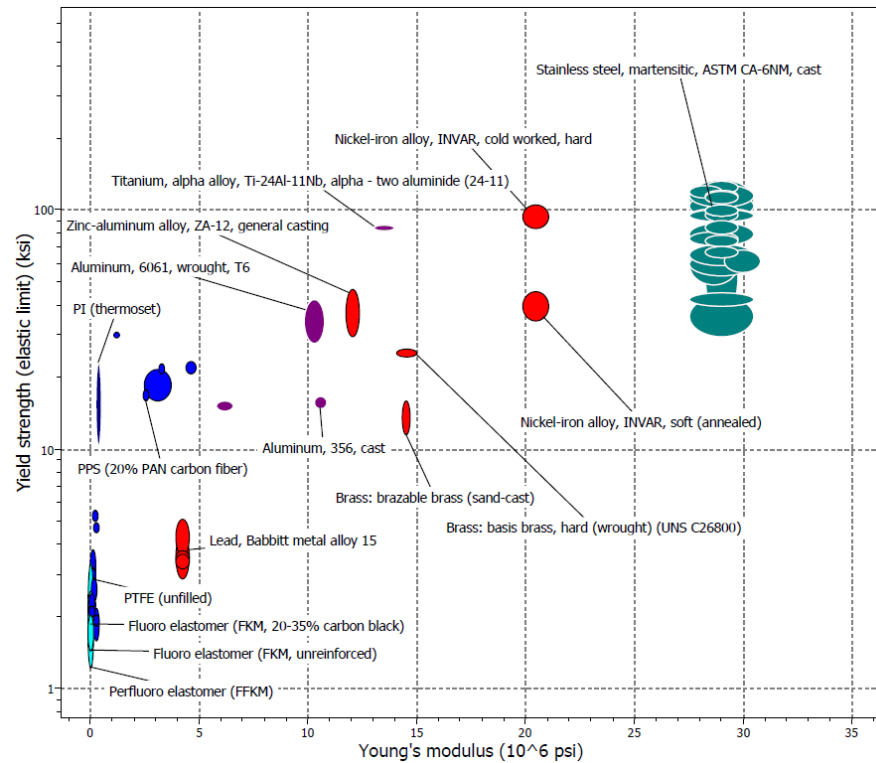
Milligan-Spika: <http://www.milliganspika.com/>

Ultra Motion Linear Actuators: <http://www.ultramotion.com/>

Appendix D: Gantt chart

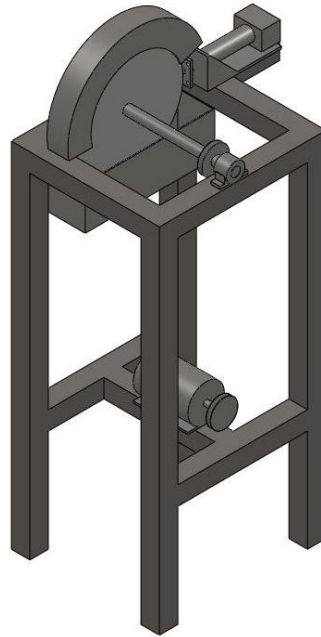


Appendix E: CES Material Chart



Name

Aluminum, 356, cast
 Aluminum, 6061, wrought, T6
 Brass: basis brass, hard (wrought) (UNS C26800)
 Brass: brazable brass (sand-cast)
 ECTFE (unfilled)
 FEP (20% milled glass fiber)
 FEP (unfilled)
 Fluoro elastomer (FKM, 20-35% carbon black)
 Fluoro elastomer (FKM, unreinforced)
 Lead, Babbitt metal alloy 13
 Lead, Babbitt metal alloy 15
 Lead, Babbitt metal alloy 7
 Lead, Babbitt metal alloy 8
 Low alloy steel, AISI 3140, annealed
 Magnesium, AM20, cast
 Nickel-iron alloy, INVAR, cold worked, hard
 Nickel-iron alloy, INVAR, soft (annealed)
 PAI (30% carbon fiber)
 PCTFE (unfilled)
 PFA (unfilled)
 PI (thermoset)
 PPS (20% PAN carbon fiber)
 PPS (30% carbon fiber)
 PPS (40% PAN carbon fiber)
 PTFE (15% glass fiber)
 PTFE (25% glass fiber)
 PTFE (unfilled)
 PVDC (copolymer, barrier film resin, plasticized)
 PVDC (copolymer, barrier film resin, unplasticized)
 PVDC (copolymer, injection)
 Perfluoro elastomer (FFKM)
 Perfluoro elastomer (FFKM, carbon black)
 SRP (extrusion & compression molding)
 Stainless steel, ferritic, AISI 403, wrought, annealed
 Stainless steel, ferritic, AISI 403, wrought, hard temper
 Stainless steel, ferritic, AISI 403, wrought, intermediate temper
 Stainless steel, martensitic, 416S41, wrought
 Stainless steel, martensitic, 420S29, wrought
 Stainless steel, martensitic, AISI 410, wrought, annealed
 Stainless steel, martensitic, AISI 410, wrought, intermediate temper
 Stainless steel, martensitic, AISI 410S, wrought, annealed
 Stainless steel, martensitic, AISI 414, wrought, intermediate temper
 Stainless steel, martensitic, AISI 414L, wrought, annealed
 Stainless steel, martensitic, AISI 418, wrought, tempered at 649°C
 Stainless steel, martensitic, AISI 431, wrought, annealed, wire
 Stainless steel, martensitic, AISI 431, wrought, tempered at 593°C
 Stainless steel, martensitic, AISI 440A, wrought, annealed
 Stainless steel, martensitic, AISI 440B, wrought, annealed
 Stainless steel, martensitic, AISI 440C, wrought, annealed
 Stainless steel, martensitic, ASTM CA-15, cast, tempered at 595°C
 Stainless steel, martensitic, ASTM CA-15, cast, tempered at 650°C
 Stainless steel, martensitic, ASTM CA-15, cast, tempered at 790°C
 Stainless steel, martensitic, ASTM CA-40, cast, tempered at 595°C
 Stainless steel, martensitic, ASTM CA-40, cast, tempered at 650°C
 Stainless steel, martensitic, ASTM CA-40, cast, tempered at 760°C
 Stainless steel, martensitic, ASTM CA-6NM, cast
 Stainless steel, martensitic, ASTM CB-7Cu, cast, aged at 620°C
 Titanium, alpha alloy, Ti-24Al-11Nb, alpha - two aluminide (24-11)
 Zinc-aluminum alloy, ZA-12, general casting

Appendix F: Original Horizontal Test Rig Modification

The Horizontal Plate Test Rig was originally designed to be a standalone unit. After much discussion, we decided that it was more practical and stable to develop a test rig that mounted on a table. Most of the calculations were performed on the original test rig, since the final design is just a modified design based on the original test rig, all that was changed were the layout and dimensions.

Appendix G - Operation Procedure

- I. Turn on computer (DAQ system)
 - a. Power on P3 Boxes, and Linear actuator
 - i. *Please note that stepper motor controller resets every time when power is disconnected*
 - ii. The following commands may need to be changed but the
 1. "DL" – Define Limit = 3 (No sensors enabled) default values are as follows:
 2. "VE" – Velocity = .25 (rev/s)
 3. "AC" – Acceleration = 10 (re/s/s)
 - b. Open VI's called "Temperature, Strain, RPM indicator" and "Position"
- II. In "Position" VI do the following
 - a. On the drop down menu select "Enable Sensor".
 - i. This switches DL3 to DL1 *Enables sensor for CCW limit*
 - b. Change "Velocity", "Acceleration", "Deceleration", and "Current" to desired values other than default.
- III. Measure test sample thickness
 - a. Input sample thickness in "Test sample thickness" in "Temperature, Strain, RPM indicator" VI.
- IV. The distance between the Material Mount and Rotor edge is fixed at 0.381 inches
 - a. Calculate required distance to move the test sample at the edge of the rotor.
(i.e. $0.381 - \text{"test sample thickness"} = \text{distance to move test sample to the rotor.}$)
- V. Bolt the test sample to the Material Mount using 4 quarter inch hex bolts.
 - a. Check the test rig for any loose bolts or connections
- VI. Place safety shield in place.
- VII. Turn on the Motor
 - a. Move material according to thickness to meet with the edge of the rotor.
- VIII. Start recording data for temperature and strain.
- IX. On the drop down menu select Case 1, hit run and the following actions will occur Case I:
 1. Actuator moves 0.01"
 2. Wait 5 seconds
 3. Actuator moves 0.01"
 4. Wait 5 seconds
 5. Feeds linear actuator back initial position.

Once the rotor has completely stopped, unbolt the test material and fill out the Material Test Log.

Appendix H: Vendor supplied Component Specifications and Data Sheets

Appendix H - F58S Hall Effect Cut Sheet



IN CHARGE OF SPEED

OPERATING INSTRUCTIONS
F58S REV. 1

Hall Effect Zero Speed Sensor F58S

GREEN LINE
INDUSTRIAL SPEED SENSORS

Product ID

Type #	Product #	Drawing #
F58S	385Z-05332	113.626 Rev.2

General

Function	The F58S series Hall effect speed sensors are suitable, in conjunction with a ferrous pole wheel, for generating square wave signals proportional to rotary speeds. They exhibit a static function, whereby pulse generation down to 0 Hz is guaranteed. The sensor function is independent of rotational mounting angle.
----------	---

Technical data

Supply voltage	8...25 VDC
Current consumption	Max. 12 mA (without load)
Signal output	Square wave signal from NPN output transistor with internal 2.7 kOhm pull-up resistor, DC-coupled to supply (negative pole = reference Voltage). <ul style="list-style-type: none"> • Sink current: max. 25 mA • Output voltage: <ul style="list-style-type: none"> • $U_{NPN} \sim$ supply voltage • $U_{CE} < 0.5$ V at $I = 25$ mA
Frequency range	0 Hz...15 kHz
Housing	5/8"-18 UNF-2A, tightening torque: max. 35 Nm
Connection	Cable with open leads: 3-wire, 3 x 0.34 mm ² (AWG22), stranded wires, elastomer isolation, green casing, fire retardant, low smoke, RoHS conform and halogen free, max. outer Ø = 4.8 mm, min. bending radius = 25 mm (static) and 50 mm (dynamic), cable length according to dimensional drawing
Protection	Sensor head: IP68 Cable outlet: IP67
Insulation	Housing and electronics galvanically isolated (Test: 500 V, 50 Hz for 1 minute)
Pole wheel	Prerequisite: Toothed wheel of a ferrous material (e.g. Steel 1.0036). Optimal performance with <ul style="list-style-type: none"> • Involute gear • Tooth width > 10 mm • Side offset < 0.2 mm • Eccentricity < 0.2 mm
Air gap between sensor and pole wheel	<ul style="list-style-type: none"> • Module 1.0 (DP 25.4): 0.3...0.5 mm • Module 2.0 (DP 12.7): 0.3...1.5 mm
Electromagnetic compatibility (EMC)	Please contact Jaquet for further details.
Vibration & shock immunity	Jaquet Greenline sensors are approved for rough environments. Please contact Jaquet for further details.
Operating temperature	-40°C...125°C

Further Information

Safety	All mechanical installations must be carried out by an expert. General safety requirements have to be met.
Installation	<p>The sensor has to be aligned to the pole wheel according to the sensor drawing independent of its rotational orientation. Deviations in positioning may affect the performance and decrease the noise immunity of the sensor. During installation, the smallest possible pole wheel to sensor gap should be set. The gap should however be set to prevent the face of the sensor ever touching the pole wheel. Within the air gap specified the amplitude of the output signal is not influenced by the air gap.</p> <p>A sensor should be mounted with the middle of the face side over the middle of the pole wheel. Dependent upon the wheel width, a certain degree of axial movement is permissible. However, the middle of the sensor must be at minimum in a distance of 3 mm from the edge of the pole wheel under all operating conditions.</p> <p>A solid and vibration free mounting of the sensor is important. Eventual sensor vibration relative to the pole wheel can induce additional output pulses. The sensors are insensitive to oil, grease etc. and can be installed in arduous conditions.</p>
Maintenance	Product cannot be repaired.
Transport	Product must be handled with care to prevent damage of the front face.
Storage	Product must be stored in dry conditions. The storage temperature corresponds to the operation temperature.
Disposal	Product must be disposed of properly, it must not be disposed as domestic waste.

Appendix H - SCB-68 (Manual for Connect Block)

SCB-68 User Guide

68-Pin Shielded Desktop Connector Block

This guide describes how to connect and use the NI SCB-68 with 68-pin or 100-pin data acquisition (DAQ) devices and other NI products with a 68-pin SCSI or VHDCI I/O connector. For a complete list of supported devices and available SCB-68 features, refer to the KnowledgeBase document, *Compatible Devices and Cabling for the NI SCB-68 Terminal Block*. To access this document, go to ni.com/info and enter the info code `scb68dev`.

Figure 1 shows the SCB-68 connector block.

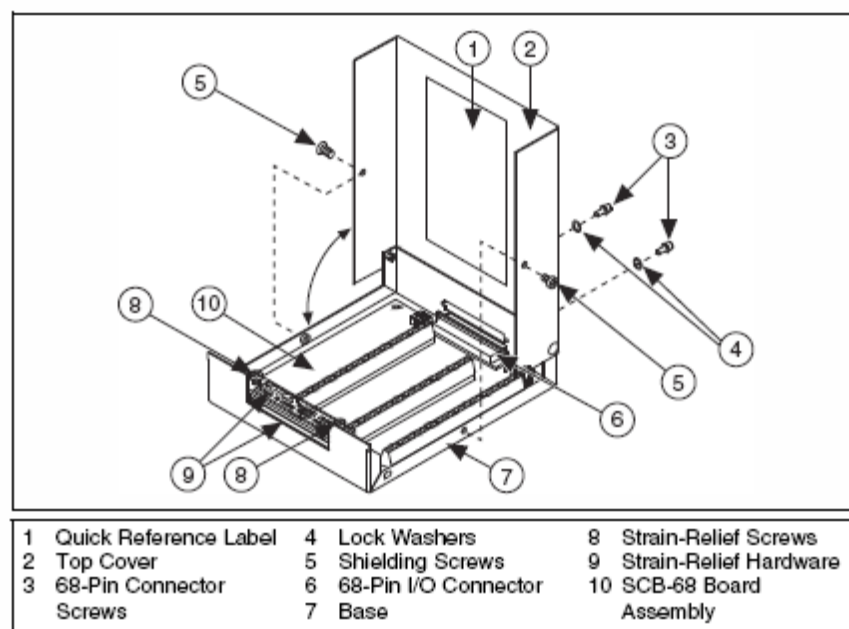


Figure 1. SCB-68 Parts Locator Diagram



Note To use the SCB-68 with devices without analog input functionality, you *must* change the default switch setting. Refer to the [Using the SCB-68 in Direct Feedthrough Mode](#) section for more information.



What You Need to Get Started

To set up and use your SCB-68, you need the following:

- ☐ SCB-68 68-pin shielded connector block kit(s)¹, containing the SCB-68, SCB-68 quick reference label, and *SCB-68 User Guide*
- ☐ Compatible 68-pin or 100-pin DAQ device, and device documentation
- ☐ The correct cable(s) for your device, as listed in the KnowledgeBase document, *Compatible Devices and Cabling for the NI SCB-68 Terminal Block*. To access this document, go to ni.com/info and enter the info code `scb68dev`.
- ☐ Phillips #1 and #2 screwdrivers
- ☐ 0.125 in. flathead screwdriver
- ☐ 14–30 AWG wire
- ☐ Wire cutters
- ☐ Wire insulation stripper

Getting Started with the SCB-68

The following cautions contain important safety information concerning hazardous voltages and connector blocks.



Cautions To avoid electrical shock, do *not* remove equipment covers or shields unless you are qualified to do so. Before removing the cover, disconnect any live circuit from the connector block.

The chassis ground terminals on your SCB-68 are for grounding high-impedance sources, such as a floating source (1 mA maximum). Do *not* use these terminals as safety earth grounds.

Do *not* connect hazardous voltages ($\geq 42 \text{ V}_{\text{pk}}/60 \text{ VDC}$).

¹ You can use up to two SCB-68 accessories with AO/M Series devices with two connectors and E Series 100-pin devices.

You can use up to four SCB-68 accessories with R Series devices with four connectors, and up to three SCB-68 accessories with R Series devices with three connectors.

Figure 2 shows the SCB-68 board parts locator diagram.

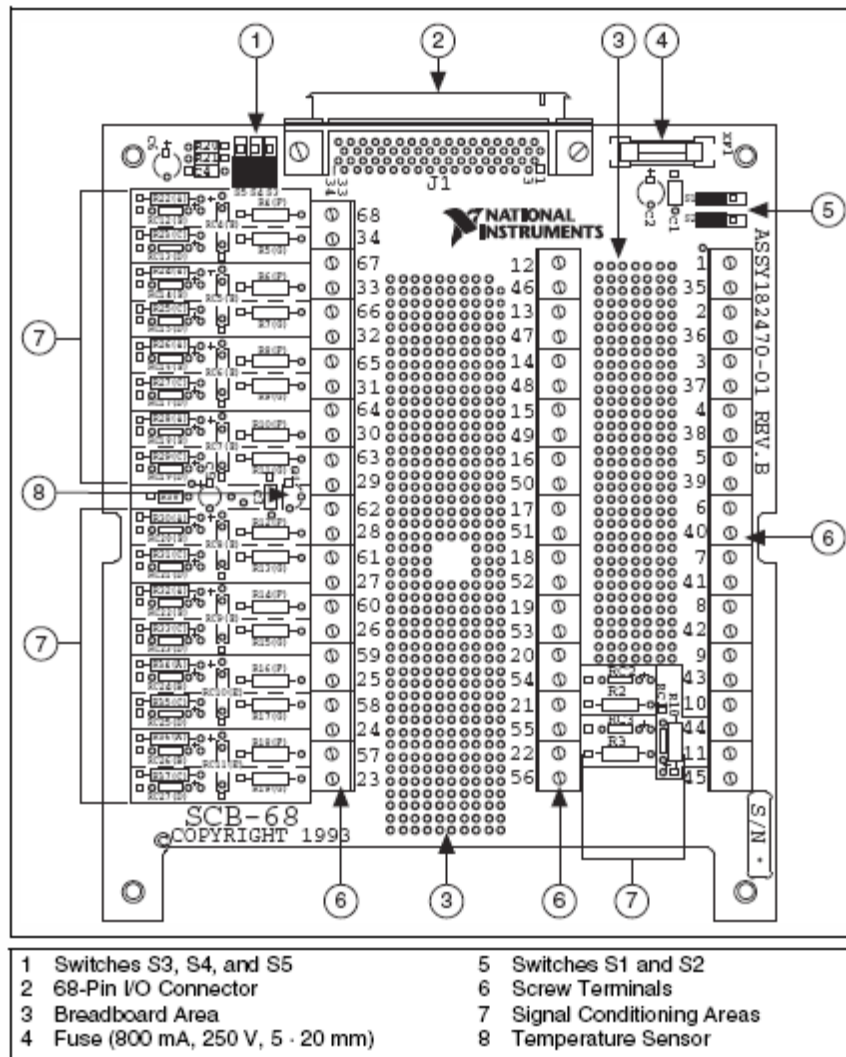



Figure 2. SCB-68 Printed Circuit Board Diagram

To get started with the SCB-68, complete the following steps while referring to Figures 1 and 2. If you have not already installed your DAQ device, refer to the *DAQ Getting Started Guide* for instructions.

1. Disconnect the cable from the SCB-68, remove the shielding screws with a Phillips #1 screwdriver, and open the top cover.
2. Attach the quick reference label to the inside of the top cover as shown in Figure 1. For quick reference label PDFs for most compatible devices, refer to the KnowledgeBase document, *Where Can I Find*

- SCB-68/SCB-100 Quick Reference Labels?*. To access this KnowledgeBase, go to ni.com/info and enter the info code `rdwpdf`.
3. Configure switches for the signal types you are using, as explained in the [Using the SCB-68 in Direct Feedthrough Mode](#) section or the [Using the SCB-68 with MIO DAQ Devices](#) section.
 4. Adjust the strain-relief hardware by loosening the strain-relief screws with a Phillips #2 screwdriver and sliding the signal wires through the front panel strain-relief opening. If you are connecting multiple signals, remove the top strain-relief bar and add insulation or padding if necessary.
 5. Connect the wires to the screw terminals by stripping 6.35 mm (0.25 in.) of insulation, inserting the wires into the screw terminals, and securely tightening the screws with the flathead screwdriver to a torque of 0.5–0.6 N · m (4.43–5.31 lb · in.).
 6. Reinstall the strain-relief (if removed) and tighten the strain-relief screws.
 7. Close the top cover and reinsert the shielding screws to ensure proper shielding.
-  **Caution** Do *not* connect input voltages $\geq 42.4 V_{pk}/60$ VDC to the SCB-68. The SCB-68 is not designed for any input voltages $\geq 42.4 V_{pk}/60$ VDC, even if a user-installed voltage divider reduces the voltage to within the input range of the DAQ device. Input voltages $\geq 42.4 V_{pk}/60$ VDC can damage the SCB-68, all devices connected to it, and the host computer.
8. Connect the SCB-68(s) to the DAQ device using the appropriate cable(s) for your device. For a complete list of cabling options for supported devices, refer to the KnowledgeBase document, *Compatible Devices and Cabling for the NI SCB-68 Terminal Block*. To access this document, go to ni.com/info and enter the info code `scb68dev`.
 9. Launch Measurement & Automation Explorer (MAX), confirm that your DAQ device is recognized, and configure your device settings. Refer to the *DAQ Getting Started Guide* for more information.
 10. (Optional) If you are going to take measurements with an MIO DAQ device, configure the SCB-68 as an accessory for a DAQ device using MAX by completing the following steps.
 - a. Navigate to MAX by selecting **Start»Programs»National Instruments»Measurement & Automation**.
 - b. In the left pane of MAX, expand **Devices and Interfaces**, then right-click on your DAQ device and select **Properties** from the pull-down menu.
 - c. Select the **Accessory** tab from the dialog box, select **SCB-68** from the pull-down menu, then select **Configure**.

For more information about configuring the SCB-68 for a DAQ device, refer to the *Measurement & Automation Explorer Help for NI-DAQmx*.

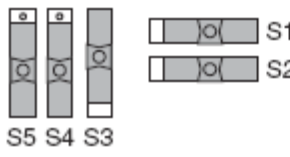
11. Test specific device functionality. Refer to the *DAQ Getting Started Guide* for detailed information about running test panels in MAX.

When you have finished using the SCB-68, power off any external signals connected to the SCB-68 before you power off your computer.

Using the SCB-68 in Direct Feedthrough Mode

High-Speed Digital I/O (DIO), NI Switch, R Series, AO Series, and TIO Series devices, and devices without analog input functionality *must* use direct feedthrough mode. Move the switches to the direct feedthrough mode switch setting shown in Table 1.

Table 1. Direct Feedthrough Switch Setting

Switch Setting	Description
 <p>S5 S4 S3</p>	<p>Direct feedthrough mode—Move switches S1, S2, S3, S4, and S5 to the positions shown at left. In this mode:</p> <ul style="list-style-type: none"> All 68 signals from the device connect directly to screw terminals. <p>Refer to Figure 3 for a detailed diagram.</p>

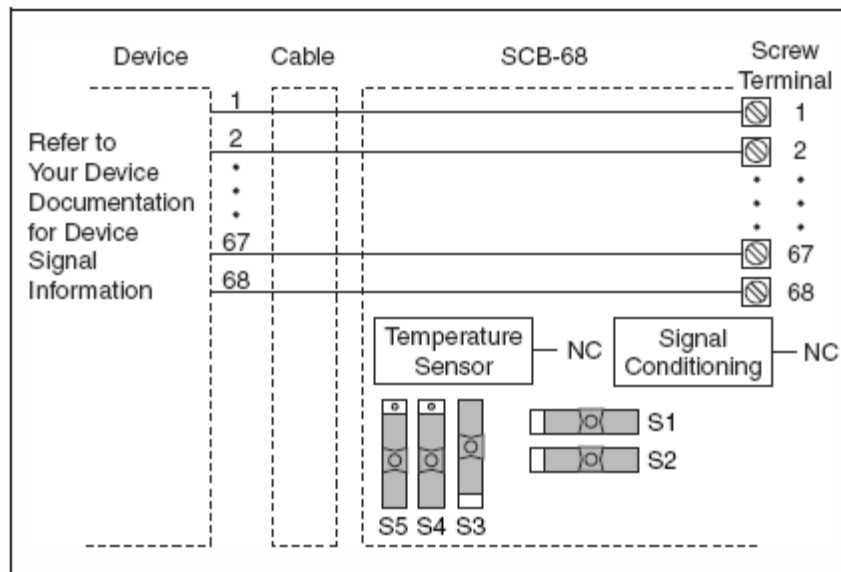


Figure 3. Direct Feedthrough Mode Switch Setting

Using the SCB-68 with MIO DAQ Devices

You can take measurements with the SCB-68 and multifunction I/O (MIO) DAQ devices, such as E/M/S Series devices, in a number of ways. Switches S1 and S2 provide power to the signal conditioning area of the accessory. The SCB-68 has a temperature sensor for cold-junction compensation (CJC) to accommodate thermocouples; switches S3, S4, and S5 configure the temperature sensor for different analog input settings. Table 2 shows the different switch settings for MIO DAQ devices.

Table 2. MIO DAQ Device Switch Settings

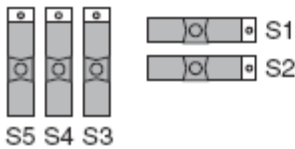
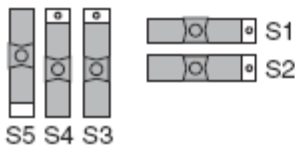
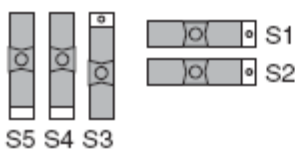
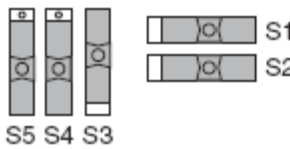
Switch Setting	Description
 <p>S5 S4 S3</p> <p>S1 S2</p>	<p>MIO with disabled temperature sensor mode (default configuration)*—Move switches S1, S2, S3, S4, and S5 to the positions shown at left. In this mode:</p> <ul style="list-style-type: none"> • The temperature sensor is not used. • AI 0 and AI 8 are available on screw terminals. • +5 V power provided to signal conditioning area of the accessory. <p>Refer to Figure 4 for a detailed diagram.</p>
 <p>S5 S4 S3</p> <p>S1 S2</p>	<p>MIO with single-ended temperature sensor mode*†—Move switches S1, S2, S3, S4, and S5 to the positions shown at left. In this mode:</p> <ul style="list-style-type: none"> • The temperature sensor can be read using AI 0 in referenced single-ended (RSE) mode. • AI 8 is available on a screw terminal. • +5 V power provided to signal conditioning area of the accessory. <p>Refer to Figure 4 for a detailed diagram.</p>
 <p>S5 S4 S3</p> <p>S1 S2</p>	<p>MIO with differential temperature sensor mode*—Move switches S1, S2, S3, S4, and S5 to the positions shown at left. In this mode:</p> <ul style="list-style-type: none"> • The temperature sensor can be read using AI 0 and AI 8 in differential mode. • +5 V power provided to signal conditioning area of the accessory. <p>Refer to Figure 4 for a detailed diagram.</p>

Table 2. MIO DAQ Device Switch Settings (Continued)

Switch Setting	Description
 S5 S4 S3 S1 S2	Direct feedthrough mode —Move switches S1, S2, S3, S4, and S5 to the positions shown at left. In this mode: <ul style="list-style-type: none">All 68 signals from the device connect directly to screw terminals. Refer to Figure 3 for a detailed diagram.
* Not available on Connector 1 of NI 6225/6255 devices. † Not available on S Series devices.	

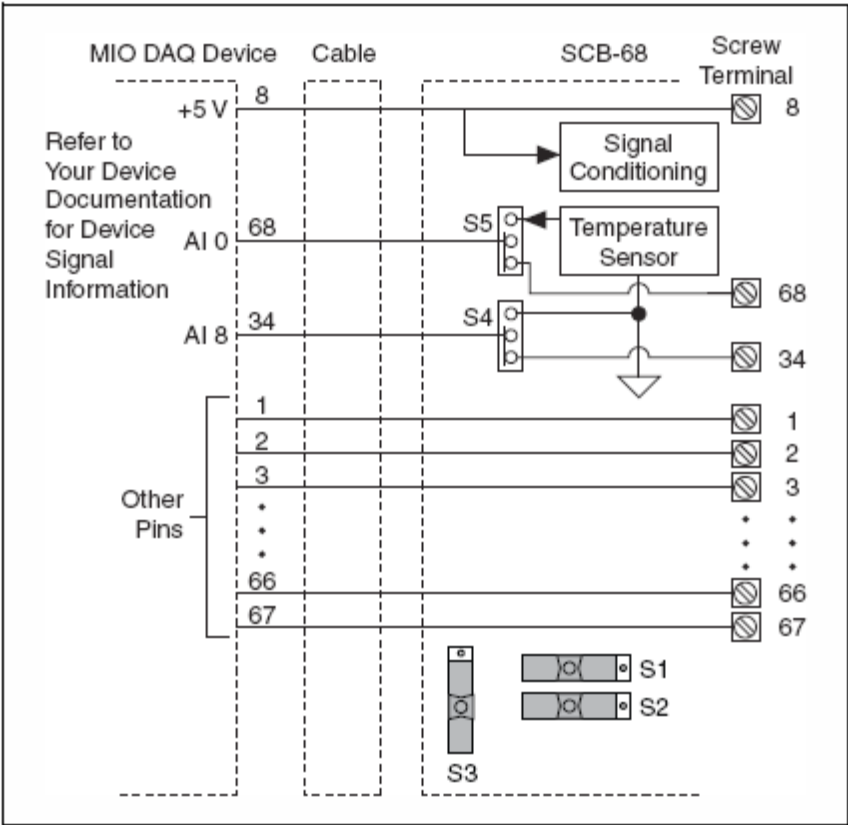


Figure 4. MIO DAQ Device Modes Switch Settings

Connecting Signal Sources to Analog Inputs

For detailed information about connections from floating or ground-referenced signal sources to analog inputs, refer to your device documentation.

Refer to the *SCB-68 User Manual for Advanced Functions* for more information about using the temperature sensor, taking thermocouple measurements, and adding bias resistors and signal conditioning components to the SCB-68.

Fuse and Power Information

Some DAQ devices provide +5 V power on pin 8 and pin 14. Pin 8 from the DAQ device is protected by an 800 mA, 250 V, 5 × 20 mm fuse on the SCB-68, shown in Figure 2. Shorting pin 8 to ground blows the fuse on the SCB-68. Pin 14 is *not* fuse-protected on the SCB-68. Shorting pin 14 will cause the fuse on the DAQ device to open.

If the SCB-68 does not work when you power on the DAQ device, check the switch settings, then check the fuse on the SCB-68, shown in Figure 2, and the output fuse (if any) on the DAQ device. Littelfuse part number 235.800 (www.littelfuse.com) is a suitable replacement fuse. Before replacing any fuses, check for short circuits from power to ground.

Refer to the *SCB-68 User Manual for Advanced Functions* for information about filtering the power on the SCB-68.

Where to Go from Here

Refer to the *SCB-68 User Manual for Advanced Functions*, available from ni.com/manuals, for information about the temperature sensor, thermocouple measurements, bias resistors, soldering components on the SCB-68, filtering, current input measurements, and accessory specifications.

National Instruments, NI, ni.com, and LabVIEW are trademarks of National Instruments Corporation. Refer to the *Terms of Use* section on ni.com/legal for more information about National Instruments trademarks. Other product and company names mentioned herein are trademarks or trade names of their respective companies. For patents covering National Instruments products/technology, refer to the appropriate location: Help>Patents in your software, the `patents.txt` file on your media, or the *National Instruments Patent Notice* at ni.com/patents.

© 1994–2009 National Instruments Corp. All rights reserved.

371745C-01

Mar09

Appendix H - Strain Gauges selection

Gage Series - Stress Analysis Gages

Vishay Micro-Measurements



Technical Data

GAGE SERIES

All Vishay Micro-Measurements strain gages incorporate precision foil grids mounted on organic backing materials. The strain-sensing alloys and backing materials cannot be arbitrarily combined in specifying a gage type. Instead, a selection must be made from among the available gage systems, or series, where each series generally incorporates special design or construction features, as well as a specific combination of alloy and backing material.

Descriptions of all standard gage series are given on the following pages, along with performance specifications and application notes. The information includes, in each case, the alloy and backing combination employed, as well as the principal construction features common to the series. The allowable strain range is specified, and operating temperature ranges are recommended for different types of applications.

The plots of cyclic strain level versus number of cycles shown for each series represent general guidelines for the nominal fatigue characteristics. This data is a function of gage size with the upper curve indicative of larger gage patterns, and the lower curve of smaller gage patterns. Since the fatigue life of a strain gage is subject to special interpretation, reference should be made to Vishay Micro-

Measurements Tech Note TN-508, Fatigue Characteristics of Vishay Micro-Measurements Strain Gages, for a full understanding of the plotted data.

The fatigue curves on the following pages correspond to fully reversed strain levels. They can also be applied, approximately, to unidirectional strains and to combinations of mean and variable strains by derating the peak-to-peak amplitude by 10%. As an example, a fully reversed strain range of $\pm 1500\mu\epsilon$ is approximately equivalent in gage fatigue damage to strain levels of:

0 to $+2700\mu\epsilon$

0 to $-2700\mu\epsilon$

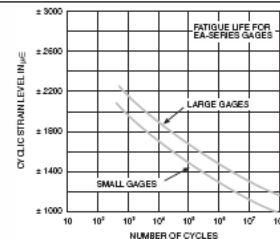
-200 to $+2500\mu\epsilon$

However, a mean strain which increases in the tensile direction during cycling will lead to much earlier failure.

It must be noted that all performance specifications for strain gages are nominal, since the behavior of a particular gage may be modified by installation or application circumstances. Moreover, the specifications apply primarily to gages of 0.125 in [3 mm] gage length and larger, and without optional features, unless otherwise indicated.

EA Series

EA-Series constantan gages are widely used in general-purpose experimental stress analysis applications. The basic gage is of open-faced construction on a 0.001 in [0.025 mm] tough, flexible cast polyimide backing. The strength and heat resistance of this backing provide excellent handling and performance qualities. This series is available in the widest range of patterns and will usually be the lowest in cost for a particular pattern design. A large number of options may be obtained for EA-Series gages, covering various forms of lead attachment and protective encapsulation. The backing is treated for strong bond formation with all standard strain gage adhesives. Strain limits are approximately $\pm 5\%$ for gages of 1/8 in [3 mm] or greater gage length and $\pm 3\%$ for smaller sizes.



Appendix I – Detailed Supporting Analysis

Please note that all major calculations were done with Engineering Equation Solver

Strain Gauge Analysis

File:D:\Senior Project\Bending and Axial Strain Calculations.EES

6/3/2010 10:31:59 AM Page 1

EES Ver. 8.400: #552: For use by Mech. Engin. Students and Faculty at Cal Poly

Strain Estimation

Constants

$$c = 0.175$$

$$D = 0.35$$

$$I_x = \frac{\pi \cdot D^4}{64}$$

$$L = 3.5$$

$$A = \pi \cdot \left[\frac{D}{2} \right]^2$$

$$E = 10.3 \cdot 10^6$$

Equations Used

$$M = \text{Force} \cdot L$$

$$\sigma_B = \frac{M \cdot c}{I_x}$$

$$\sigma_A = \frac{\text{Force}}{A}$$

$$\text{Bending}_{\text{strain}} = \frac{\sigma_B}{E} \cdot 1000000$$

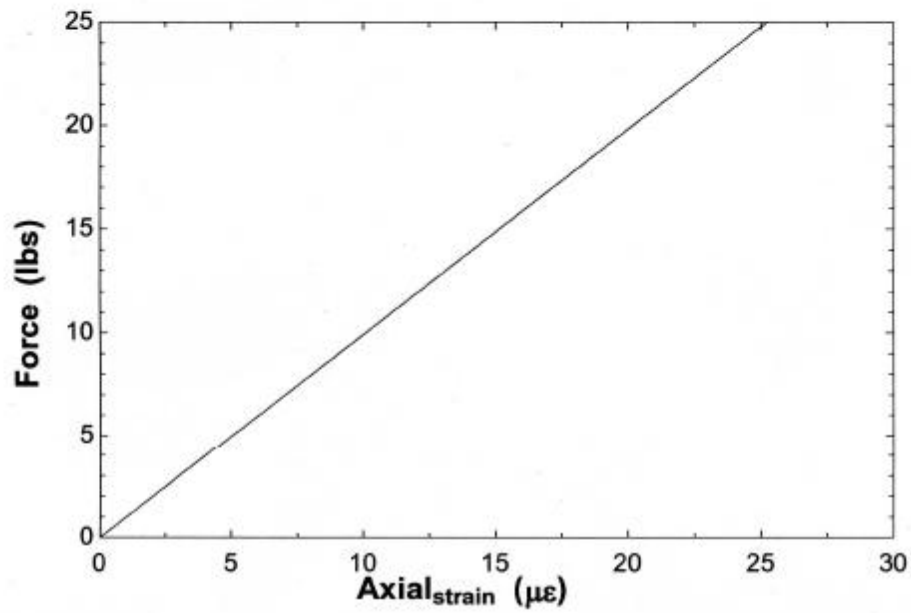
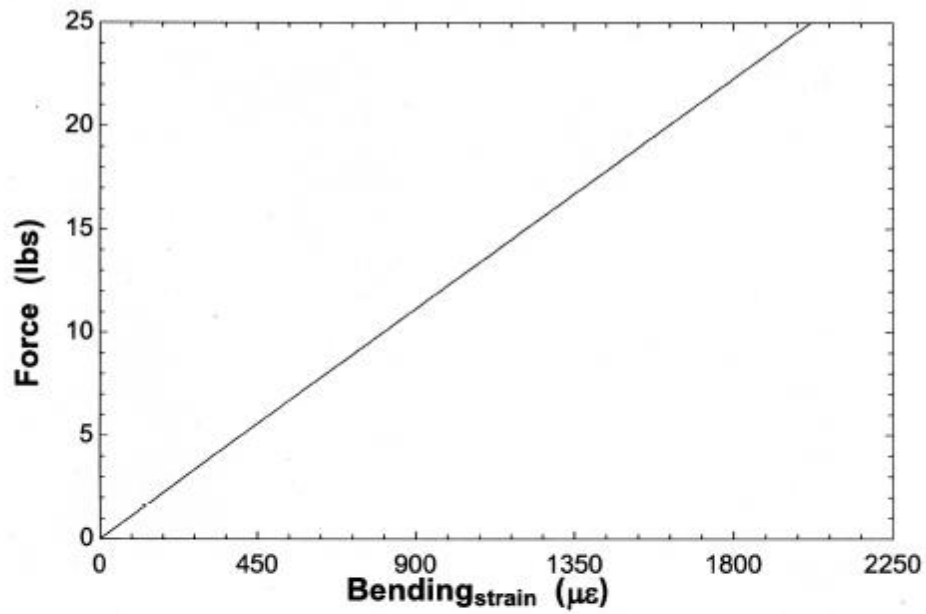
$$\text{Axial}_{\text{strain}} = \frac{\sigma_A}{E} \cdot 1000000$$

Parametric Table: Table 1

	Force [lbs]	Axial _{strain} [microstrain]	Bending _{strain} [microstrain]	σ_A [psi]	σ_B [psi]
Run 1	0	0.0	0.0	3.009E-36	0
Run 2	1	1.0	80.7	10.39	831.5
Run 3	2	2.0	161.5	20.79	1663
Run 4	3	3.0	242.2	31.18	2495
Run 5	4	4.0	322.9	41.58	3326
Run 6	5	5.0	403.6	51.97	4158
Run 7	6	6.1	484.4	62.36	4989
Run 8	7	7.1	565.1	72.76	5821
Run 9	8	8.1	645.8	83.15	6652
Run 10	9	9.1	726.6	93.54	7484
Run 11	10	10.1	807.3	103.9	8315
Run 12	11	11.1	888.0	114.3	9147

Parametric Table: Table 1

	Force	Axial _{strain}	Bending _{strain}	σ_A	σ_B
	[lbs]	[microstrain]	[microstrain]	[psi]	[psi]
Run 13	12	12.1	968.7	124.7	9978
Run 14	13	13.1	1049.5	135.1	10810
Run 15	14	14.1	1130.2	145.5	11641
Run 16	15	15.1	1210.9	155.9	12473
Run 17	16	16.1	1291.7	166.3	13304
Run 18	17	17.2	1372.4	176.7	14136
Run 19	18	18.2	1453.1	187.1	14967
Run 20	19	19.2	1533.8	197.5	15799
Run 21	20	20.2	1614.6	207.9	16630
Run 22	21	21.2	1695.3	218.3	17462
Run 23	22	22.2	1776.0	228.7	18293
Run 24	23	23.2	1856.8	239.1	19125
Run 25	24	24.2	1937.5	249.5	19956
Run 26	25	25.2	2018.2	259.8	20788
Run 27	26	26.2	2098.9	270.2	21619
Run 28	27	27.2	2179.7	280.6	22451
Run 29	28	28.3	2260.4	291	23282
Run 30	29	29.3	2341.1	301.4	24114
Run 31	30	30.3	2421.9	311.8	24945
Run 32	31	31.3	2502.6	322.2	25777
Run 33	32	32.3	2583.3	332.6	26608
Run 34	33	33.3	2664.0	343	27440
Run 35	34	34.3	2744.8	353.4	28271
Run 36	35	35.3	2825.5	363.8	29103
Run 37	36	36.3	2906.2	374.2	29934
Run 38	37	37.3	2987.0	384.6	30766
Run 39	38	38.3	3067.7	395	31597
Run 40	39	39.4	3148.4	405.4	32429
Run 41	40	40.4	3229.1	415.8	33260
Run 42	41	41.4	3309.9	426.1	34092
Run 43	42	42.4	3390.6	436.5	34923
Run 44	43	43.4	3471.3	446.9	35755
Run 45	44	44.4	3552.1	457.3	36586
Run 46	46	46.4	3713.5	478.1	38249



Belt Design

File:F:\senior project\belt\design.EES

6/3/2010 10:34:03 AM Page 1

EES Ver. 8.400: #552: For use by Mech. Engin. Students and Faculty at Cal Poly

V=Belt design $w_1 = 3430$ motor speed $w_2 = 5000$ shaft speed $d_2 = 3$ sheave diameter on shaft (in)*Law of Gears*

$$\frac{w_1}{w_2} = \frac{d_2}{D_1}$$

Belt Speed

$$W = w_1 \cdot 2 \cdot \pi \cdot \frac{1}{60}$$

$$v_{\text{belt}} = \frac{D_1}{2} \cdot W \cdot \frac{1}{12} \cdot 60$$

Pitch Length $c = 9$ in

$$L_p = 2 \cdot c + \frac{\pi}{2} \cdot [D_1 + d_2] + \frac{[D_1 - d_2]^2}{4 \cdot c} \text{ in}$$

Corrected Horse Power $P_r = 2.96$ look up in shigley's (HP)

$$F = \frac{D_1 - d_2}{c}$$

 $k_1 = 0.76$ look up in shigley's $k_2 = 0.85$ look up in shigley's

$$P_{rc} = k_1 \cdot k_2 \cdot P_r$$

Design Horse Power $k_s = 1.4$ service factor $P = 5$ HP in drive

$$P_d = k_s \cdot P$$

Number of Belts

$$N = \frac{P_d}{P_{rc}}$$

Forces of Belt

File:F:\senior project\motor.EES

6/3/2010 10:37:39 AM Page 1

EES Ver. 8.400: #552: For use by Mech. Engin. Students and Faculty at Cal Poly

"Dynamic Analysis for the Motor" $I_{zz}=427$ [lb/in²] $w_0=0$ [rad/s] $w_1=524$ [rad/s] $\alpha=w_1/\text{time}$ $T=I_{zz}*\alpha*(1/144)*(1/32)$ $P=T*w_1$ $HP=P*(.0018181818)$ *Dynamic Analysis for the Motor* $I_{zz} = 427$ [lb/in²] $w_0 = 0$ [rad/s] $w_1 = 524$ [rad/s] $\alpha = \frac{w_1}{\text{time}}$ $T = I_{zz} \cdot \alpha \cdot \frac{1}{144} \cdot \frac{1}{32}$ $P = T \cdot w_1$ $HP = P \cdot 0.0018181818$

Shaft Analysis

File:D:\solar turbines SP\shaft.EES

EES Ver. 8.400: #552: For use by Mech. Engin. Students and Faculty at Cal Poly

6/3/2010 10:4

L1 = 2

L2 = 9

L3 = 2

D = 0.5

P = 10

R1 = 6

R2 = 2

RPM = 5000

$Mp = P \cdot \frac{R1}{R2}$

$Hp = Mp \cdot \frac{R2}{12} \cdot \frac{RPM}{60} \cdot 2 \cdot \frac{\pi}{550}$

$Rb = \frac{-P \cdot L1 + Mp \cdot [L2 - L3]}{L2}$

$Ra = -P - Rb + Mp$

$M1 = L3 \cdot Rb$

$I = \pi \cdot \frac{D^4}{64}$

$stress1 = M1 \cdot \frac{D}{2 \cdot I}$

SOLUTION

Unit Settings: [F]/[psia]/[lbm]/[degrees]

D = 0.5	Hp = 4.76	I = 0.003068	L1 = 2
L2 = 9	L3 = 2	M1 = 42.22	Mp = 30
P = 10	R1 = 6	R2 = 2	Ra = -1.111
Rb = 21.11	RPM = 5000	stress1 = 3441	

No unit problems were detected.

File:D:\solar turbines SP\shaft deflection.EES

6/3/2010 10:46:49 AM Page 1

EES Ver. 8.400: #552: For use by Mech. Engin. Students and Faculty at Cal Poly

$$T = 194.2 \text{ [lb}_f\text{] tension}$$

$$F = 0.2 \cdot T \text{ Forces on wheel}$$

$$L_1 = 2 \text{ [in] length from bearings}$$

$$L_3 = 9 \text{ [in] overall length}$$

$$L_2 = L_3 - L_1$$

$$E = 3 \times 10^7 \text{ [psia] modulus of elasticity}$$

$$D = 1 \text{ [in] diameter of shaft}$$

$$I = \pi \cdot \frac{D^4}{64} \text{ moment of inertia}$$

$$\delta_B = \frac{T \cdot L_1 \cdot L_2}{6 \cdot E \cdot I \cdot L_3} \cdot [2 \cdot L_1^2 - 2 \cdot L_3 \cdot L_1] - \frac{F \cdot L_2^2}{6 \cdot E \cdot I \cdot L_3} \cdot [L_1^2 + L_2^2 - 2 \cdot L_3 \cdot L_1] \text{ displacement at pulley}$$

$$\delta_C = \frac{T \cdot L_1^2}{6 \cdot E \cdot I \cdot L_3} \cdot [L_2^2 + L_1^2 - 2 \cdot L_3 \cdot L_2] - \frac{F \cdot L_2 \cdot L_1}{6 \cdot E \cdot I \cdot L_3} \cdot [2 \cdot L_2^2 - 2 \cdot L_3 \cdot L_2] \text{ displacement at rotor}$$

SOLUTION**Unit Settings: [F]/[psia]/[lbm]/[degrees]**

$$D = 1 \text{ [in]} \quad \delta_B = -0.001364 \text{ [in]}$$

$$\delta_C = -0.0005216 \text{ [in]}$$

$$E = 3.000\text{E}+07 \text{ [psia]}$$

$$F = 38.84 \text{ [lb}_f\text{]}$$

$$I = 0.04909 \text{ [in}^4\text{]}$$

$$L_1 = 2 \text{ [in]}$$

$$L_2 = 7 \text{ [in]}$$

$$L_3 = 9 \text{ [in]}$$

$$T = 194.2 \text{ [lb}_f\text{]}$$

No unit problems were detected.

$$T = 300 \text{ [lb]}_f$$

$$F = 0.2 \cdot T$$

$$L_1 = 2 \text{ [in]}$$

$$L_3 = 9 \text{ [in]}$$

$$L_2 = L_3 - L_1$$

$$R_D = \frac{F \cdot L_2 - T \cdot L_1}{L_3} \text{ reaction forces}$$

$$R_A = T + R_D - F$$

$$D = 1 \text{ [in]}$$

$$M_B = L_1 \cdot R_A \text{ max bending moment}$$

$$V = R_A \text{ max shear force}$$

$$Tor = 52.1 \text{ [in-lb]}_f$$

$$I = \pi \cdot \frac{D^4}{64}$$

$$J = \pi \cdot \frac{D^4}{32}$$

$$A = \pi \cdot \frac{D^2}{4}$$

$$c = \frac{D}{2}$$

$$\sigma = M_B \cdot \frac{c}{I}$$

$$\tau = Tor \cdot \frac{c}{J} + \frac{V}{A}$$

$$\sigma_{max} = [\sigma^2 + \tau^2]^{0.5}$$

$$S_y = 94000 \text{ [psia]}$$

$$S_e = \frac{S_y}{2}$$

$$N = \frac{S_e}{\sigma_{max}}$$

SOLUTION

Unit Settings: [kJ]/[C]/[kPa]/[kg]/[degrees]

A = 0.7854 [in ²]	c = 0.5 [in]	D = 1 [in]
F = 60 [lb _f]	I = 0.04909 [in ⁴]	J = 0.09817 [in ⁴]
L ₁ = 2 [in]	L ₂ = 7 [in]	L ₃ = 9 [in]
M _B = 440 [in·lb _f]	N = 10.41	R _A = 220 [lb _f]
R _D = -20 [lb _f]	σ = 4482 [psia]	σ _{max} = 4515 [psia]
S _e = 47000 [psia]	S _y = 94000 [psia]	T = 300 [lb _f]
τ = 545.5 [psia]	Tor = 52.1 [in·lb _f]	V = 220 [lb _f]

No unit problems were detected.

Bearing Analysis

File: D:\solar turbines SP\bearing life.EES 6/3/2010 10:48
 EES Ver. 8.400: #552: For use by Mech. Engin. Students and Faculty at Cal Poly

$n = 5000$
 $c = 2801$
 $p = 200$
 $a_1 = 0.62$
 $a_2 = 1$
 $a_3 = 0.456$
 $L_{10} = \left[\frac{c}{p} \right]^3 \cdot \frac{16667}{n}$
 $L_n = a_1 \cdot a_2 \cdot a_3 \cdot L_{10}$
 $t = \frac{L_n}{8 \cdot 5 \cdot 52}$

SOLUTION
 Unit Settings: [kJ]/[C]/[kPa]/[kg]/[degrees]
 $a_1 = 0.62$ $a_2 = 1$ $a_3 = 0.456$ $c = 2801$
 $L_{10} = 9157$ $L_n = 2589$ $n = 5000$ $p = 200$
 $t = 1.245$

No unit problems were detected.

Strain Gauge Calibration

Channel Calibration Report

5/31/2010

Channel Name : Axial Strain

Calibration Date : 5/21/2010

Expiration Date : 5/21/2011

Calibration Enabled? : Yes

If the calibration is expired, apply calibration and return warning.

Sample Size : 100

Sample Rate : 1000 Hz

Additional Information :

Reference	Uncalibrated	Calibrated	Reference - Calibrated
-1.060000E+2	-1.107262E+2		
-9.000000E+1	-9.17506E+1		
-5.700000E+1	-5.68501E+1		
-4.500000E+1	-4.50652E+1		
0.00000E+0	-8.8827E-2		
7.500000E+1	7.50000E+1		

Units: microstrain

History :

5/21/2010 Jason : Calibrated

Channel Calibration Report

5/31/2010

Channel Name : Bending Strain

Calibration Date : 5/21/2010

Expiration Date : 5/21/2011

Calibration Enabled? : Yes

If the calibration is expired, apply calibration and return warning.

Sample Size : 100

Sample Rate : 1000 Hz

Additional Information :

Reference	Uncalibrated	Calibrated	Reference - Calibrated
-1.5000000E+3	-1.5000000E+3		
0.0000E+0	5.8480E-1		
4.180000E+2	4.272818E+2		
8.380000E+2	8.512837E+2		
1.2230000E+3	1.2471228E+3		
1.4750000E+3	1.5114918E+3		
3.5220000E+3	3.1891411E+3		

Units: Microstrain

History :

5/28/2010 Jason : Calibration values edited

5/21/2010 Jason : Calibrated

Appendix J: Material Test Logs

Lead Babbitt Alloy:

Lab Seal Material Test Log							
Test Engineer(s):							
Date:	5/28/2010						
Material:	Lead Babbitt-1	Lead Babbitt-2					
Manufacturer:							
Computer Program:							
Room Temperature (°F):	70						
Sample Number:	1	2					
Clearance:	0.381	0.381					
Material Thickness (inches):	0.25	0.25					
Distance from test sample to rotor edge:	0.11	0.115					
Sample Temp - Start (°F):							
Sample Temp - Max (°F):							
Rotor Speed (RPM):	4826.4	4871.4					
Max Bending Strain	106	356					
Incurion (Bending) Load - Max(lbf):	1.49	5					
Incurion rate (in/s):	0.0833	0.1666					
Travel distance (in):	0.005 x 2	0.01 x 2					
Max (Shear Force) Torque (in-lbf):							
Shavings:	None	None					
Shaving Tupe: (Ribbon, Chip, or Clump)	None	None					
Material Edge Raised (Yes or No):							
Material Smearing (Yes or No):							
Emissions (Smoke) (Yes or No):							
Discoloration (Yes or No):	No	No					
Material Adherence to Tooth (Yes or No):	No	No					
Observations:							

Fluorosint 500:

Lab Seal Material Test Log							
Test Engineer(s):							
Date:	5/28/2010						
Material:	F500-1	F500-2	F500-3	F500-4	F500-5	F500-6	
Manufacturer:							
Computer Program:							
Room Temperature (°F):	70						
Sample Number:	1	2	3	4	5	6	7
Clearance:	0.381	0.381	0.381	0.381	0.381	0.381	
Material Thickness (inches):	0.304	0.304	0.3	0.3	0.303	0.303	
Distance from test sample to rotor edge:	0.077	0.077	0.081	0.081	0.078	0.078	
Sample Temp - Start (°F):							
Sample Temp - Max (°F):							
Rotor Speed (RPM):				4842	4862.4	4868.4	
Max Bending Strain	NA	NA	NA	674	703	740	
Incurion (Bending) Load - Max(lbf):	NA	NA	NA	9.36	9.75	10.25	
Incurion rate (in/s):	0.1666	0.1666	0.1666	0.1666	0.1666	0.1666	
Travel distance (in):	0.01 x 2	0.01 x 2	0.01 x 2	0.01 x 2	0.01 x 2	0.01 x 2	
Max (Shear Force) Torque (in-lbf):							
Shavings:	Fine Strands	Fine Strands	Fine Strands	Fine Strands	Fine Strands	Fine Strands	
Shaving Tupe: (Ribbon, Chip, or Clump)							
Material Edge Raised (Yes or No):							
Material Smearing (Yes or No):							
Emissions (Smoke) (Yes or No):							
Discoloration (Yes or No):	yes	yes	yes	yes	yes	yes	
Material Adherence to Tooth (Yes or No):							
Observations:	Black Residue left of the abrasion						

Fluorosint 207:

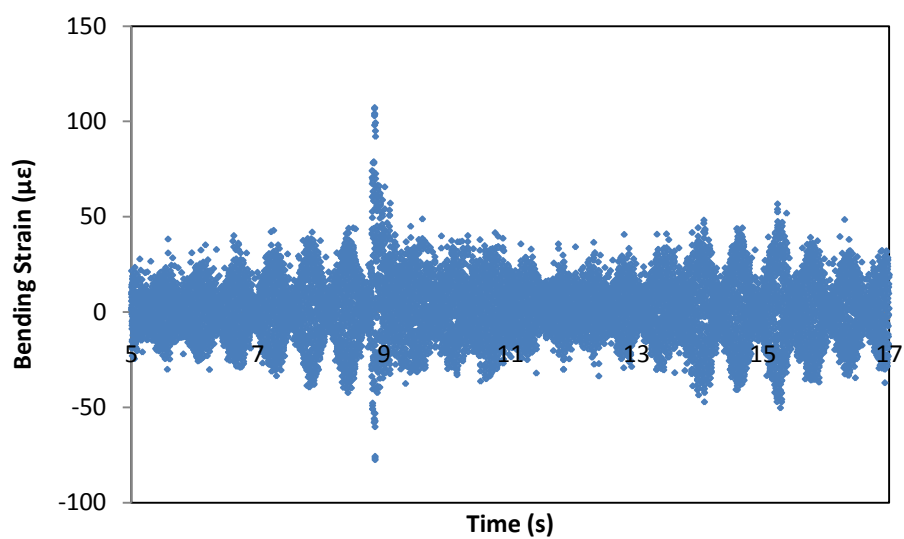
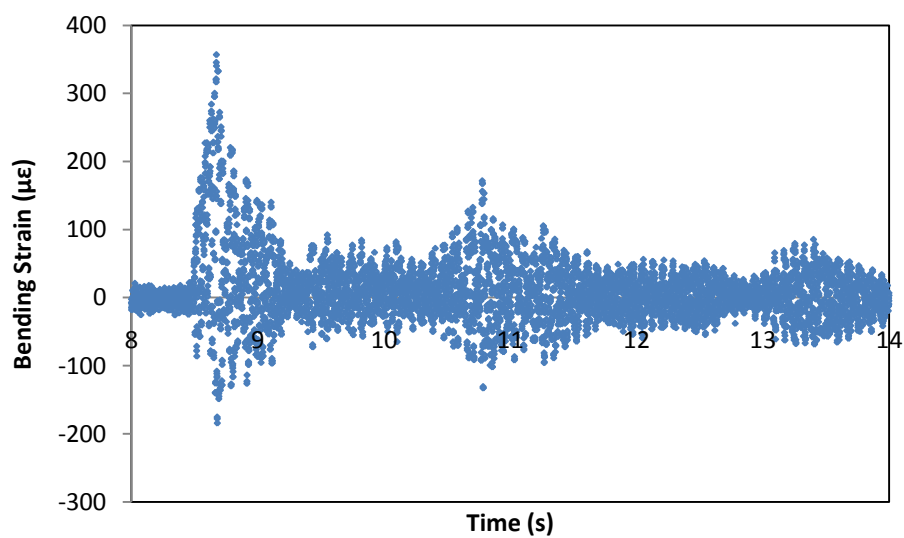
Lab Seal Material Test Log							
Test Engineer(s):							
Date:	5/28/2010						
Material:	F207-1	F207-2	F207-3	F207-4	F207-5	F207-6	
Manufacturer:							
Computer Program:							
Room Temperature (°F):	70						
Sample Number:	1	2	3	4	5	6	7
Clearance:	0.381	0.381	0.381	0.381	0.381	0.381	
Material Thickness (inches):	0.325	0.325	0.325	0.325	0.326	0.326	
Distance from test sample to rotor edge:	0.056	0.056	0.056	0.056	0.055	0.055	
Sample Temp - Start (°F):							
Sample Temp - Max (°F):							
Rotor Speed (RPM):	4860	4898.4	4830	4871.4	4832.4	4872.6	
Max Bending Strain	714	627	595	635	616	647	
Incursion (Bending) Load - Max(lbf):							
Incursion rate (in/s):	0.1666	0.1666	0.1666	0.1666	0.1666	0.1666	
Travel distance (in):	0.01 x 2	0.01 x 2	0.01 x 2	0.01 x 2	0.055	0.01 x 2	
Max (Shear Force) Torque (in-lbf):							
Shavings:	Fine Strands	Fine Strands	Fine Strands	Fine Strands	Fine Strands	Fine Strands	
Shaving Tupe: (Ribbon, Chip, or Clump)							
Material Edge Raised (Yes or No):							
Material Smearing (Yes or No):							
Emissions (Smoke) (Yes or No):							
Discoloration (Yes or No):	no	no	no	no	no	no	
Material Adherence to Tooth (Yes or No):							
Observations:	Clean Cut	Clean Cut	Clean Cut	Clean Cut	Clean Cut	Clean Cut	

Aluminum 6061:

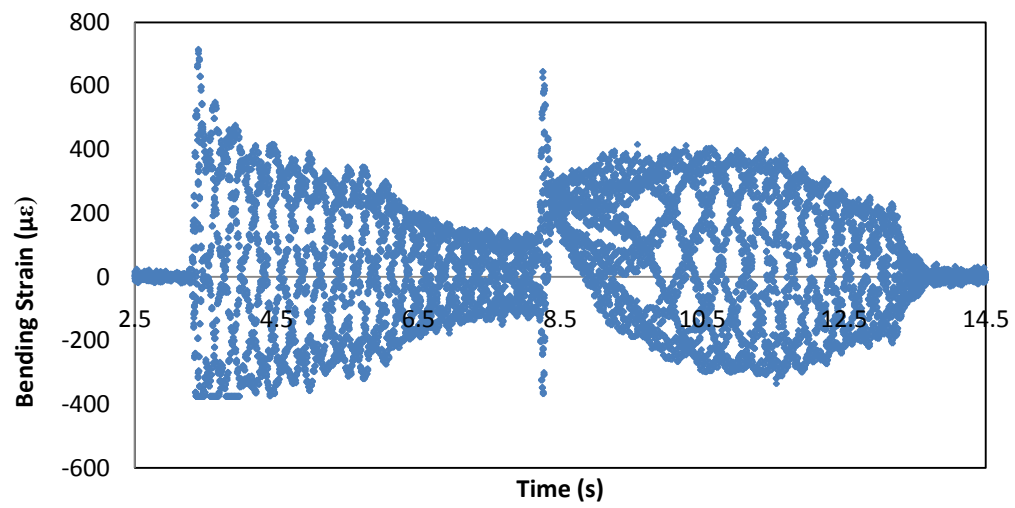
Lab Seal Material Test Log							
Test Engineer(s):							
Date:	5/28/2010						
Material:	AL6061-1						
Manufacturer:							
Computer Program:							
Room Temperature (°F):							
Sample Number:	1	2	3	4	5	6	7
Clearance:	0.381						
Material Thickness (inches):	0.125						
Distance from test sample to rotor edge:	0.256						
Sample Temp - Start (°F):							
Sample Temp - Max (°F):							
Rotor Speed (RPM):							
Max Bending Strain							
Incursion (Bending) Load - Max(lbf):							
Incursion rate (in/s):	0.1666						
Travel distance (in):	0.256 x 2						
Max (Shear Force) Torque (in-lbf):							
Shavings:							
Shaving Tupe: (Ribbon, Chip, or Clump)	Aluminum Clumps						
Material Edge Raised (Yes or No):	Yes						
Material Smearing (Yes or No):	Yes						
Emissions (Smoke) (Yes or No):							
Discoloration (Yes or No):							
Material Adherence to Tooth (Yes or No):	Yes						
Observations:	Forcing the material into the rotor more than allowed gummed up the rotor and bent the aluminum shaft						

Lead Babbitt Test 1:

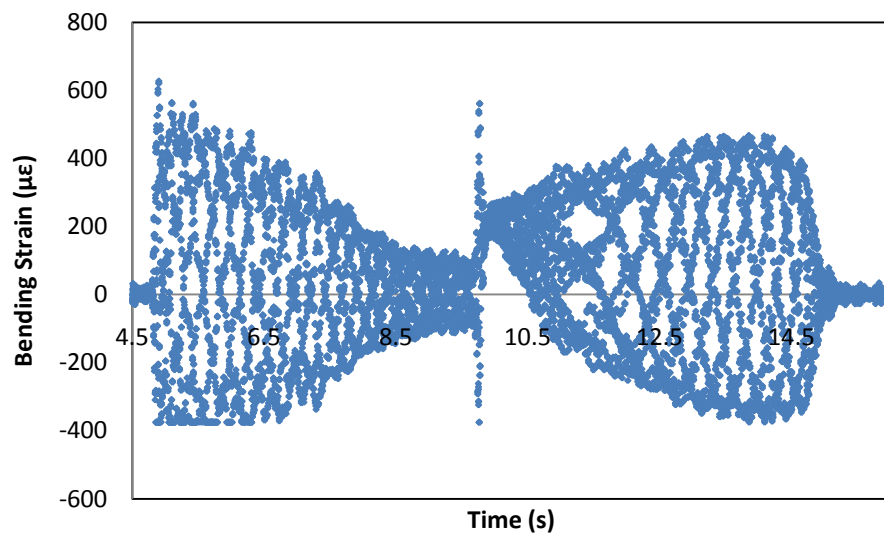
*Data was not used in comparison to other materials due to different abrasion depth and speed

**Lead Babbitt Test 2:**

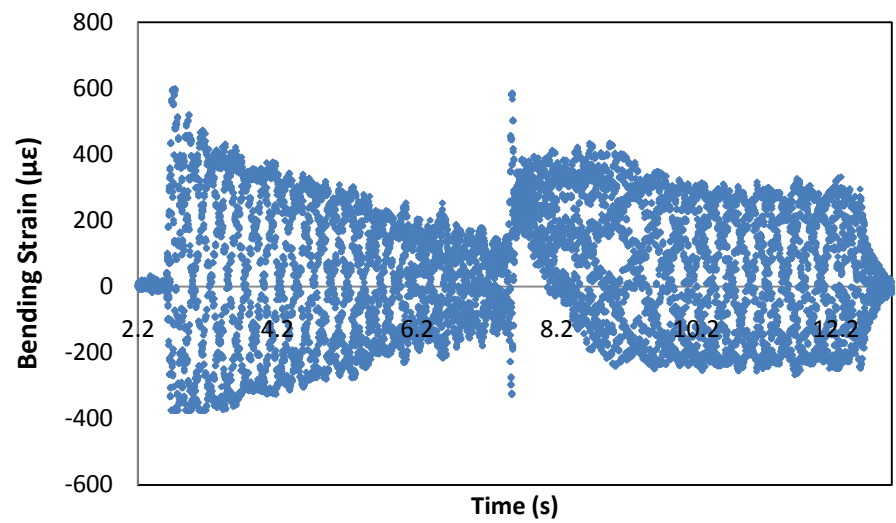
Fluorosint 207 Test 1:



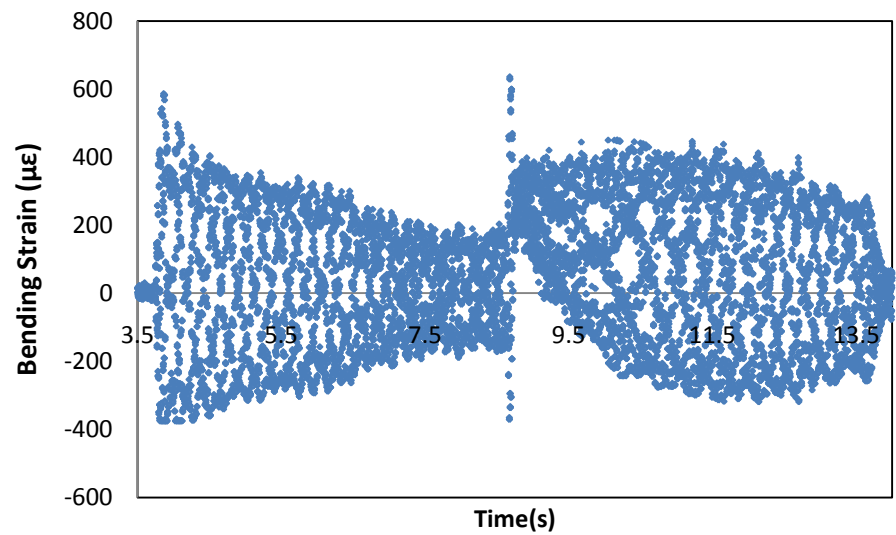
Fluorosint 207 Test 2:

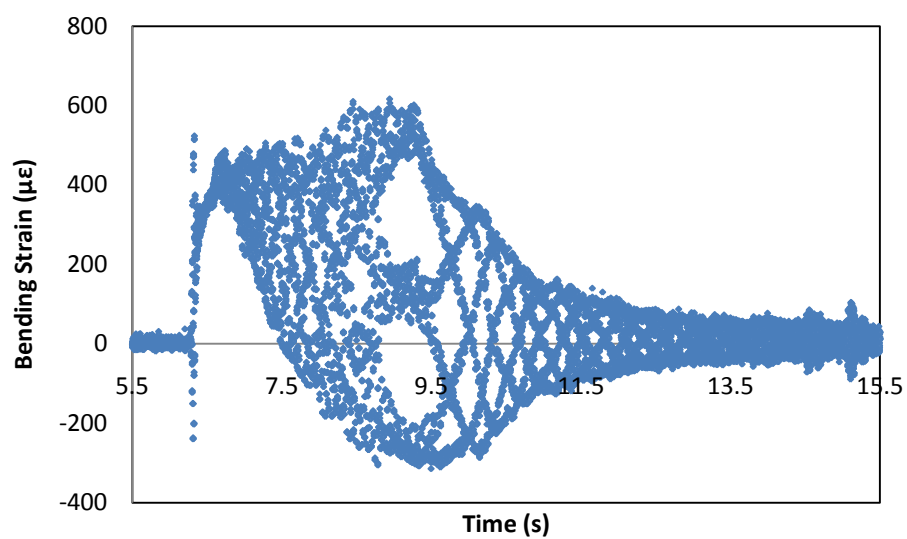
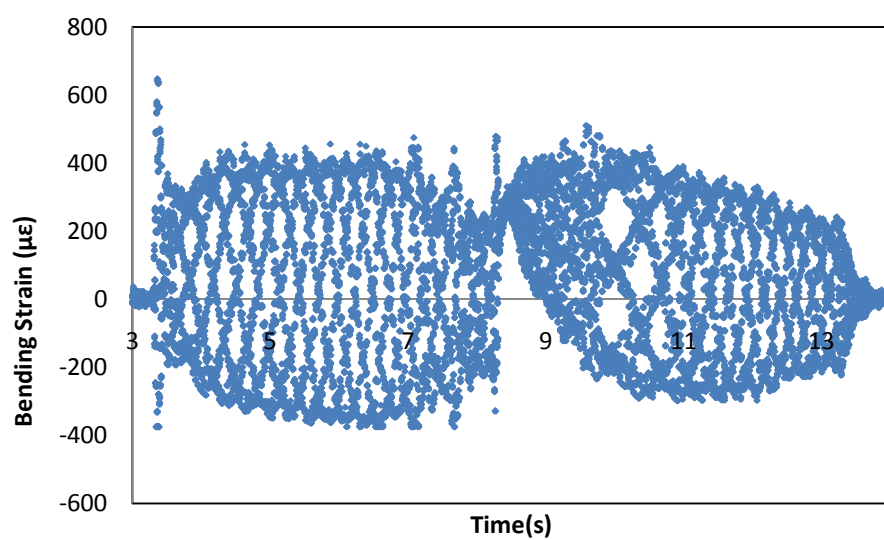


Fluorosint 207 Test 3:



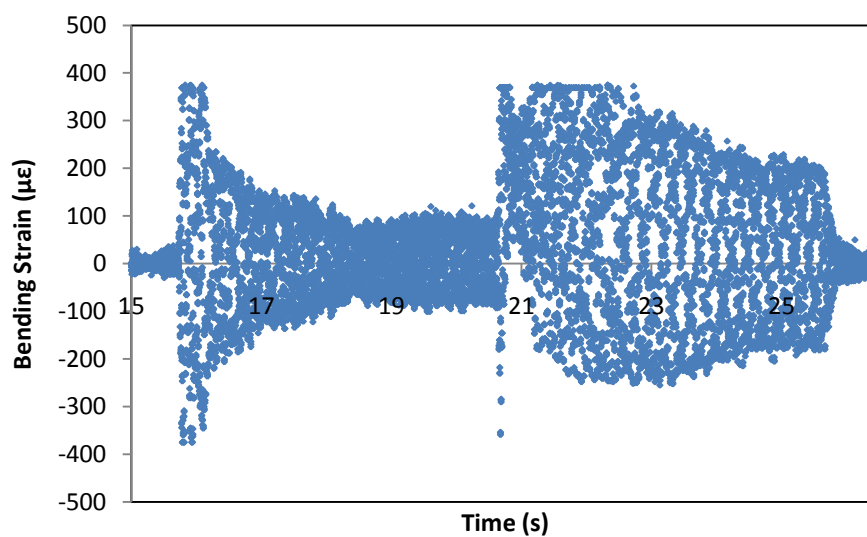
Fluorosint 207 Test 4:



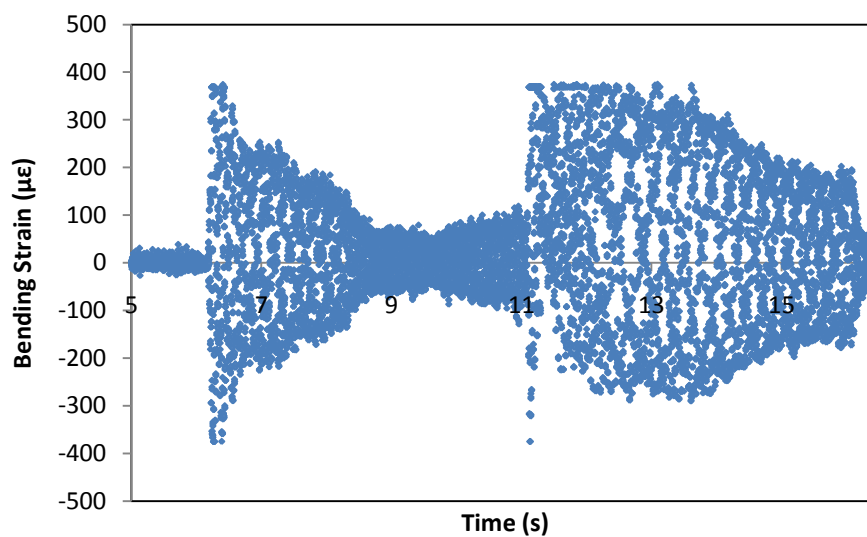
Fluorosint 207 Test 5:**Fluorosint 207 Test 6:**

Fluorosint 500 Test 1:

*Data was not used in comparison to other materials due to equipment limit

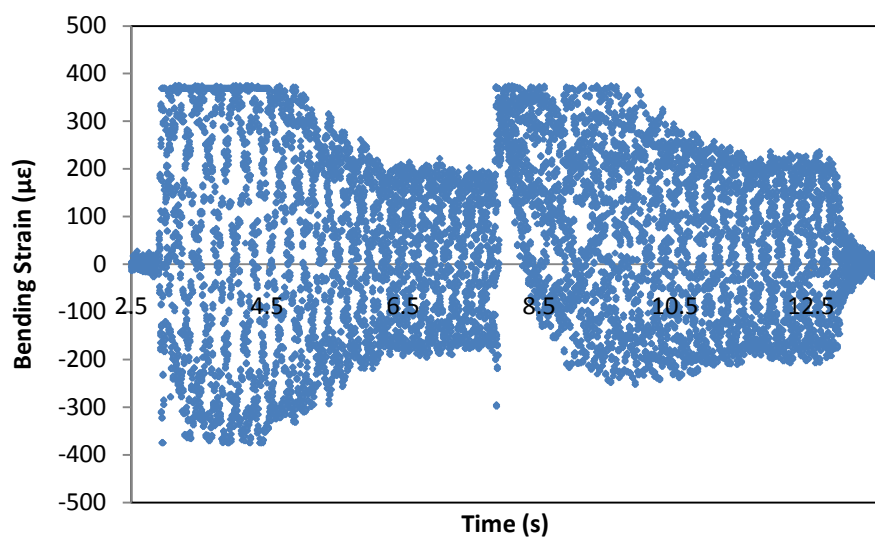
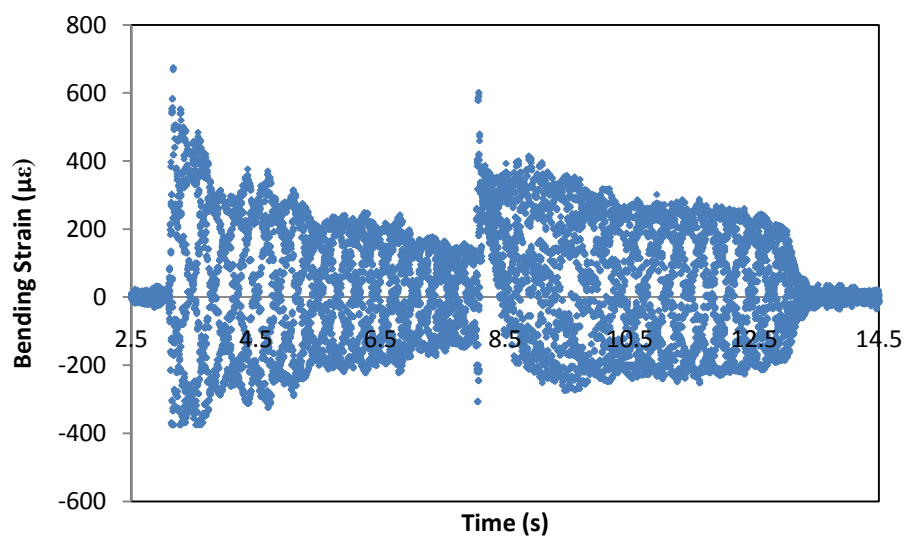
**Fluorosint 500 Test 2:**

*Data was not used in comparison to other materials due to equipment limit

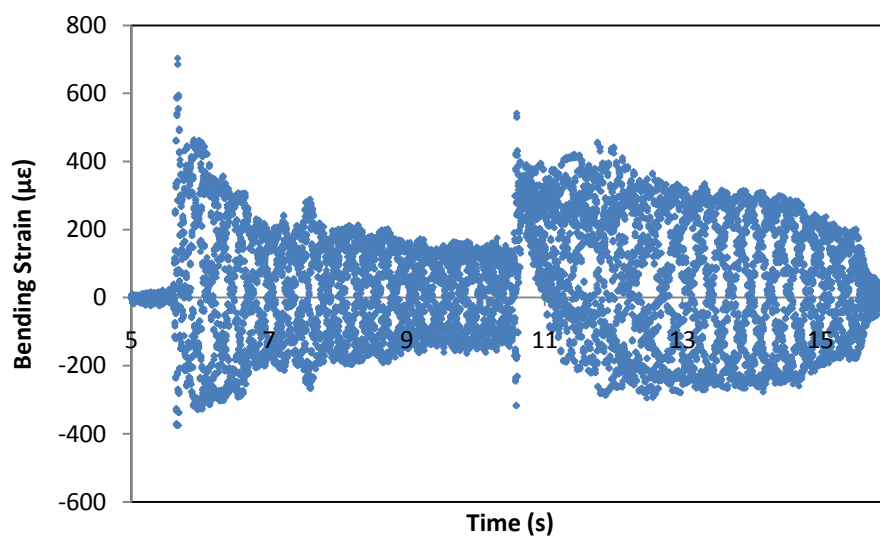


Fluorosint 500 Test 3:

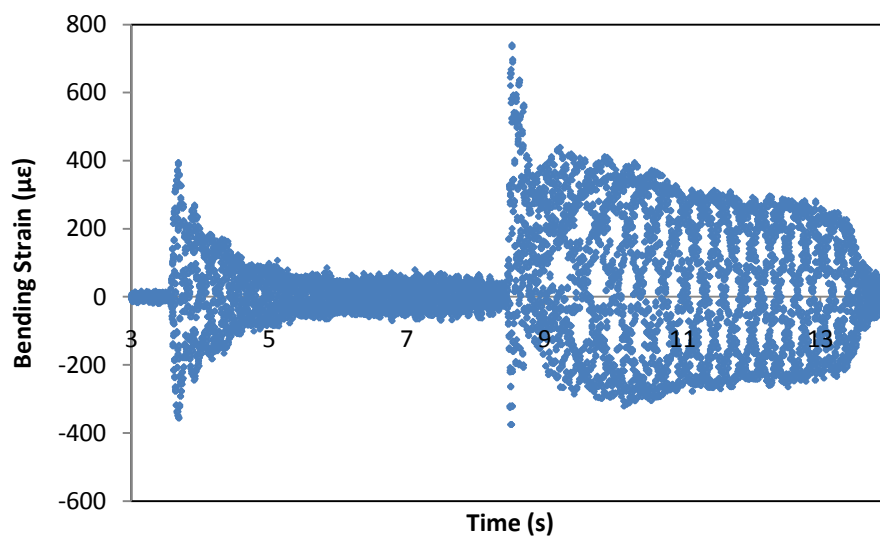
*Data was not used in comparison to other materials due to equipment limit

**Fluorosint 500 Test 4:**

Fluorosint 500 Test 5:

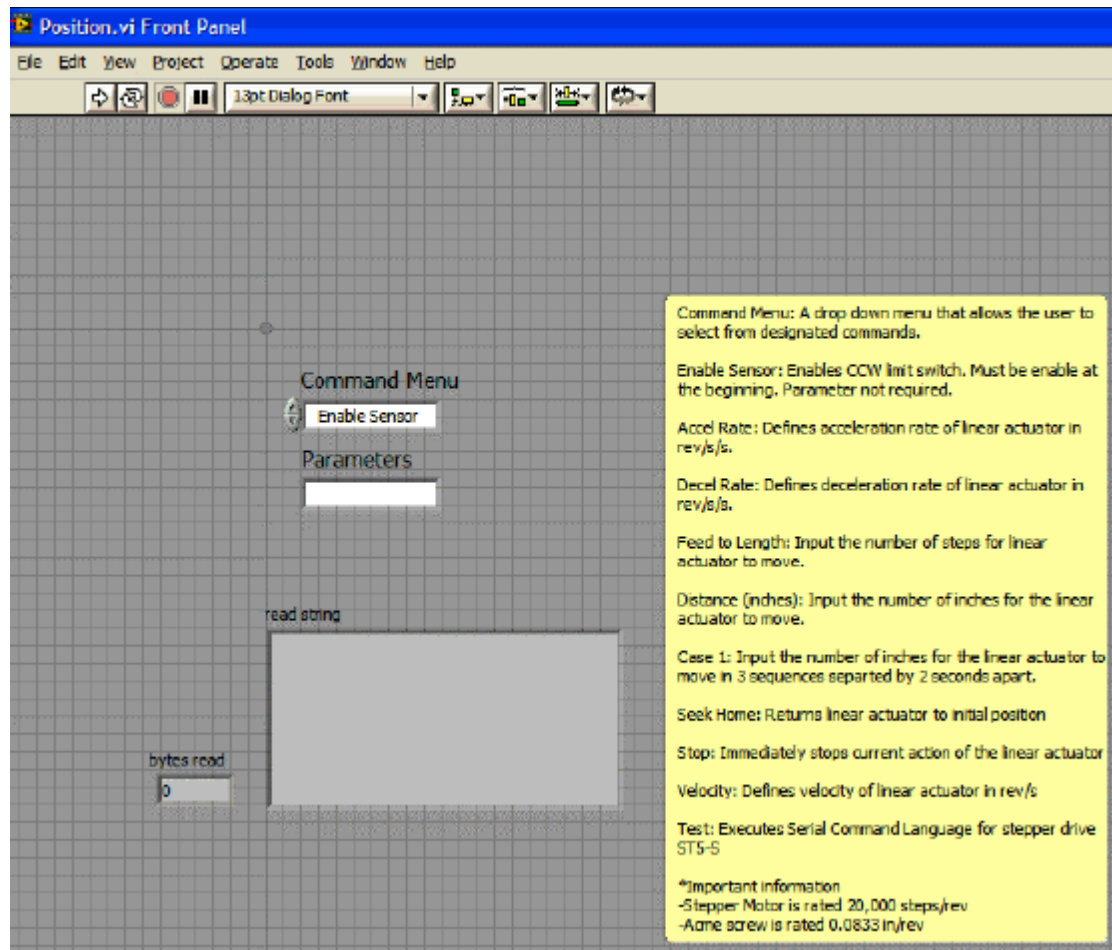


Fluorosint 500 Test 6:

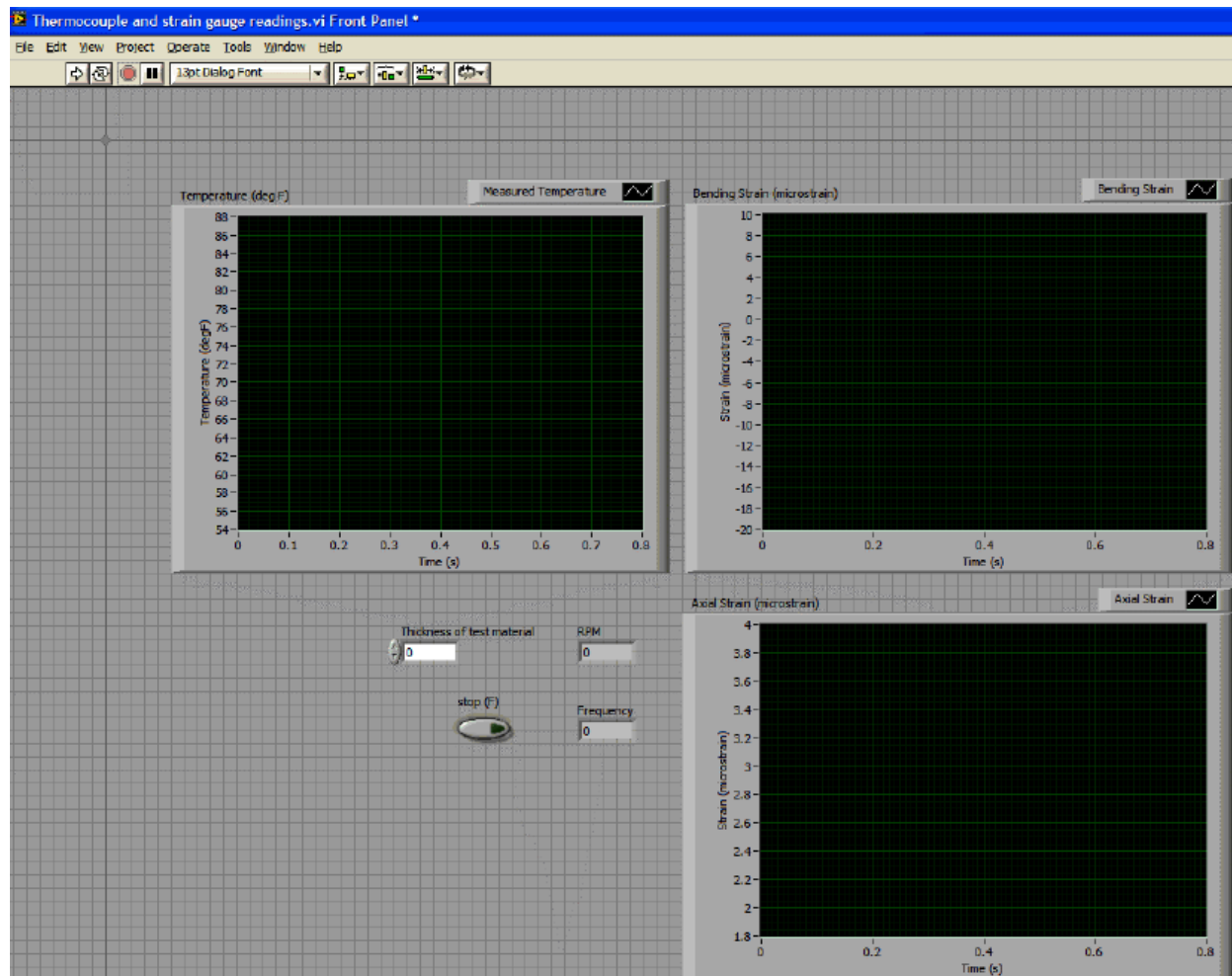


Appendix K – LabView Program

“Positioning VI” – This VI allows the user to control the movement of the linear actuator.



“Temperature and Strain Monitor VI” – This VI conditioned all the analog signals (Temperature, Strain, and RPM) and outputs the data into a text file.



Appendix L – Fluorosint 500 MSDS**MATERIAL SAFETY DATA SHEET****MSDS# 1401****SECTION 1**

QUADRANT EPP
 2120 FAIRMONT AVENUE
 P.O. BOX 14235
 READING, PA. 19612-4235

TELEPHONE NUMBERS:
 PRODUCT INFORMATION(Quadrant EPP) -
 610-320-6600
 TRANSPORTATION EMERGENCY (CHEMTREC) -
 800-424-9300

MATERIAL IDENTIFICATION

PRODUCT NAME: FLUROSINT 500 (FFM-500), FLUROSINT 590 (FFM-590) and FLUROSINT 620 (FF-620) and MT-01

CHEMICAL NAME: POLYTETRAFLUOROETHYLENE (PTFE) PLUS
 FLUOROPHLOGOPITE (SYNTHETIC MICA)

CAS NO.: 9002-84-0 (PTFE)
 12001-26-2 (MICA-GROUP MINERALS)

PRODUCT USE: MOLDED AND FABRICATED PARTS.

TSCA INVENTORY STATUS: ALL REPORTABLE INGREDIENTS ARE LISTED
 IN THE TSCA CHEMICAL SUBSTANCE INVENTORY.

SECTION 2**HAZARDOUS INGREDIENTS (ADDITIVES NOT HAZARDOUS BY 29 CFR 1910.1200)**

IDENTITY	CAS#	ACGIH TVL
POLYTETRAFLUOROETHYLENE	9002-84-0	NO EXPOSURE LIMIT ESTABLISHED
*Carbon Fiber	7440-44-0	2 MG/M ³

SECTION 3**HEALTH HAZARD DATA**

ACUTE OR IMMEDIATE EFFECTS: ROUTES OF ENTRY AND SYSTEMS.

INGESTION: NOT A PROBABLE ROUTE OF EXPOSURE FOR SHAPES. POWDER
 MAY BE HARMFUL IF SWALLOWED, MATERIAL DOES NOT DISSOLVE.

SKIN: POWDER MAY CAUSE SKIN IRRITATION.

EYE: MECHANICAL IRRITATION ONLY.

INHALATION: SHAPES NOT RESPIRABLE.

MSDS# 1401

Quadrant EPP

Page 2

SECTION 4

EMERGENCY FIRST AID

- If exposed to fumes from overheating, move to fresh air.
Consult a physician if symptoms persist.
- Wash skin with soap and plenty of water.
- Flush eyes with water. Consult a physician if symptoms persist.

CHRONIC EFFECTS: NONE KNOWN.

MEDICAL CONDITIONS GENERALLY AGGRAVATED BY THIS MATERIAL: NONE KNOWN.

SECTION 5FIRE AND EXPLOSION HAZARD DATA

FLASH IGNITION TEMPERATURE: WILL NOT FLASH.

UNUSUAL FIRE, EXPLOSION HAZARDS: NONE KNOWN.

HAZARDOUS DECOMBUSTION PRODUCTS: HEATING ABOVE THE MELTING POINT, OR PROLONGED HEATING ABOVE 260 C./500 F., MAY CAUSE THERMAL DEGRADATION OF POLYTETRAFLUORETHYLENE WHICH LEADS TO THE FORMATION OF OXIDIZED PRODUCTS CONTAINING CARBON, FLUORINE AND OXYGEN.

SPECIAL FIRE FIGHTING INSTRUCTIONS: FIRE FIGHTERS AND OTHERS EXPOSED TO PRODUCTS OF COMBUSTION SHOULD WEAR FULL PROTECTIVE CLOTHING INCLUDING SELF-CONTAINED BREATHING APPARATUS. FIRE FIGHTING EQUIPMENT SHOULD BE THOROUGHLY DECONTAMINATED AFTER USE.

EXTINGUISHING MEDIA: WATER SPRAY OR ANY CLASS A EXTINGUISHING AGENT.

>= Physical health Hazards:

DUST MAY FORM EXPLOSIVE MIXTURES WITH AIR. AVOID DUST FORMATION AND CONTROL IGNITION SOURCES. ALL PLASTIC DUST PARTICLES SUSPENDED IN AIR ARE COMBUSTIBLE AND MAY BE EXPLOSIVE. KEEP AWAY FROM HEAT, SPARKS, FLAME, AND OTHER IGNITION SOURCES. PREVENT DUST ACCUMULATIONS AND DUST CLOUDS. EMPLOY GROUNDING, VENTING, AND EXPLOSIVE RELIEF PROVISIONS IN ACCORDANCE WITH ACCEPTED ENGINEERING PRACTICES AND NFPA PROVISIONS IN ANY PROCESS CAPABLE OF GENERATING DUST AND/OR STATIC ELECTRICITY. EXPLOSION HAZARDS APPLY ONLY TO DUSTS, NOT GRANULAR FORMS OF THIS PRODUCT. SEE ALSO SPECIAL PRECAUTIONS SECTION BELOW.

MSDS# 1401

Quadrant EPP

Page 3

SECTION 6

ACCIDENTAL RELEASES

SPILL OR RELEASE: CLEAN UP BY VACUUMING OR SWEEPING TO PREVENT FALLS.

SECTION 7

STORAGE CONDITIONS

Dry storage. Keep containers closed to prevent contamination.

SECTION 8

PROTECTION INFORMATION

EYE: Safety glasses are recommended to prevent particulate matter from entering eyes while grinding or machining.

SKIN: This product is not likely to be hazardous by skin contact, but cleansing the skin after use is advisable.

VENTILATION: Local exhaust at processing equipment to keep particulates below 15 mg/m³, the OSHA limit for nuisance dusts. Grinding and machining of parts should be reviewed to assure that particulate levels are kept at recommended levels.

OTHER: Avoid contamination of cigarettes or tobacco with Fluorosint dust.

RESPIRATOR: None under normal processing, if ventilation is adequate.

MSDS# 1401

Quadrant EPP

Page 4

SECTION 9

PHYSICAL/CHEMICAL DATAODOR: **ESSENTIALLY ODORLESS.**MELTING POINT: **342 C./ 648 F.**SOLUBILITY IN WATER: **INSOLUBLE.**VOLATILE CONTENT %: **<1%**SPECIFIC GRAVITY: **2.25-2.35**

>= Precautions For Repair & Maintenance Of Contaminated Equipment: Eliminate ignition sources:

TRANSFER FROM STORAGE WITH A MINIMUM AMOUNT OF DUSTING. GROUND ALL TRANSFER, BLENDING, AND DUST COLLECTING EQUIPMENT TO PREVENT STATIC SPARKS IN ACCORDANCE WITH NFPA 70 "NATIONAL ELECTRIC CODE". REVIEW AND COMPLY WITH ALL RELEVANT NFPA PROVISIONS, INCLUDING BUT NOT LIMITED TO NFPA 484 AND NFPA 654 RELATED TO COMBUSTIBLE DUST HAZARDS. REMOVE ALL IGNITION SOURCES FROM MATERIAL HANDLING, TRANSFER, AND PROCESSING AREAS WHERE DUST MAY BE PRESENT. LOCAL EXHAUST VENTILATION SHOULD BE PROVIDED IN WORK AREA.

SECTION 10

HAZARDOUS REACTIVITYSTABILITY AT ROOM TEMPERATURE: **STABLE.**MATERIALS TO AVOID: **NONE KNOWN.**CONDITIONS TO AVOID: **HEATING ABOVE 400 C./750 F.**

MSDS# 1401

Quadrant EPP

Page 5

SECTION 11

TOXICOLOGICAL INFORMATION

CHRONIC TOXICITY: SPECIFIC TOXICITY TESTS HAVE NOT BEEN CONDUCTED ON THIS PRODUCT. THE HAZARD EVALUATION IS BASED ON INFORMATION FROM SIMILAR PRODUCTS, THE INGREDIENTS, TECHNICAL LITERATURE, AND/OR PROFESSIONAL EXPERIENCE FROM THE RESIN MANUFACTURER.

THIS PRODUCT CONTAINS POLYTETRAFLUOROETHYLENE (PTFE). VAPORS WHICH CAN CAUSE FLU-LIKE SYMPTOMS ARE LIBERATED FROM PTFE AT TEMPERATURES ABOVE 250 C./480 F. OR IF CIGARETTES OR OTHER SMOKING MATERIALS ARE CONTAMINATED WITH FLUOROSINT DUST OR MACHINE WASTE.

CARCINOGENICITY: NO COMPONENT OF THIS PRODUCT PRESENT AT LEVELS GREATER THAN 0.1% IS IDENTIFIED AS A CARCINOGEN BY NTP, IARC OR OSHA.

SECTION 12

ECOLOGICAL INFORMATION

AQUATIC TOXICITY: Toxicity is expected to be low based on insolubility of product in water.

SECTION 13

DISPOSAL

SPILL OR RELEASE: Clean up by vacuuming or wet sweeping to minimize dust exposure.

WASTE DISPOSAL: Recycling is encouraged, Landfill or incineration in compliance with Federal, State, and Local regulations.

SECTION 14

TRANSPORT INFORMATION

DOT HAZARD CLASS: **NA**
SHIPPING NAME: **NA**

MSDS# 1401

Quadrant EPP

Page 6

**SECTION 15A
REGULATORY INFORMATION**

SECTION 313 SUPPLIER NOTIFICATION:
SARA TITLE III-TOXIC CHEMICALS LIST)

This product contains no known toxic chemicals subject to the reporting requirements of section 313 of the Emergency Planning and Community Right-To-Know Act of 1986 and 40 CFR 372.

STATE RIGHT TO KNOW LAWS

No substances on the state hazardous list, for the states indicated below, are used in the manufacture of products on this Material Safety Data Sheet, with the exceptions indicated. While we do not specifically analyze these products, or the raw materials used in their manufacture, for substances on various state hazardous substances lists, to the best of our knowledge the products on this Material Safety Data Sheet contain no such substances except for those specifically listed below:

PENNSYLVANIA:

SUBSTANCES ON THE PENNSYLVANIA HAZARDOUS SUBSTANCES LIST PRESENT AT A CONCENTRATION OF 1% OR MORE: **NONE KNOWN.**

SUBSTANCES ON THE PENNSYLVANIA SPECIAL HAZARDOUS SUBSTANCES LIST PRESENT AT A CONCENTRATION OF 0.01% OR MORE: **NONE KNOWN.**

CALIFORNIA PROPOSITION 65:

SUBSTANCES KNOWN TO THE STATE OF CALIFORNIA TO CAUSE CANCER: **NONE KNOWN.**

SUBSTANCES KNOWN TO THE STATE OF CALIFORNIA TO CAUSE BIRTH DEFECTS OR OTHER REPRODUCTIVE HARM: **NONE KNOWN.**

**SECTION 15B
LABELING INFORMATION**

Health	0
Flammability	1
Reactivity	0
PPE	A
#Acute *Chronic	

MSDS# 1401

Quadrant EPP

Page 7

SECTION 16

MISCELLANEOUS INFORMATION

Issued by: Richard Frey, SHE Manager, NA

Issued: January 8, 2009

Supersedes: October 29, 2008

The information set forth herein has been gathered from standard reference materials and/or supplier test data and is, to the best knowledge and belief of Quadrant EPP, accurate and reliable. Such information is offered solely for your consideration, investigation and verification, and it is not suggested or guaranteed that the hazard precautions or procedures mentioned are the only ones which exist. Quadrant EPP makes no warranties, expressed or implied, with respect to the use of such information or the use of the specific material identified herein in combination with any other material or process, and assumes no responsibility therefor.

* = Ingredient for MT-01 material

NA = Not applicable

NE = Not established.

>= New or revised information in this section when " > " appears in the left margin.

END OF MSDS

Appendix L – Fluorosint 207 MSDS**MATERIAL SAFETY DATA SHEET****MSDS# 1400****SECTION 1**

QUADRANT EPP
 2120 FAIRMONT AVENUE
 P.O. BOX 14235
 READING, PA. 19612-4235

TELEPHONE NUMBERS:
 PRODUCT INFORMATION(Quadrant EPP) -
 610-320-6600
 TRANSPORTATION EMERGENCY (CHEMTREC) -
 800-424-9300

MATERIAL IDENTIFICATION

PRODUCT NAME: **FLUROSINT 207 (LF-207)**

CHEMICAL NAME: **POLYTETRAFLUOROETHYLENE (PTFE) PLUS
 FLUOROPHLOGOPITE (SYNTHETIC MICA)**

CAS NO.: **9002-84-0 (PTFE)
 12001-26-2 (MICA-GROUP MINERALS)**

PRODUCT USE: **MOLDED AND FABRICATED PARTS.**

TSCA INVENTORY STATUS: **ALL REPORTABLE INGREDIENTS ARE LISTED
 IN THE TSCA CHEMICAL SUBSTANCE INVENTORY.**

SECTION 2**HAZARDOUS INGREDIENTS (ADDITIVES NOT HAZARDOUS BY 29 CFR 1910.1200)**

IDENTITY	CAS#	ACGIH TVL
POLYTETRAFLUOROETHYLENE	9002-84-0	NO EXPOSURE LIMIT ESTABLISHED

SECTION 3**HEALTH HAZARD DATA**

ACUTE OR IMMEDIATE EFFECTS: ROUTES OF ENTRY AND SYSTEMS.

INGESTION: **NOT A PROBABLE ROUTE OF EXPOSURE FOR SHAPES. POWDER
 MAY BE HARMFUL IF SWALLOWED, MATERIAL DOES NOT DISSOLVE.**

SKIN: **POWDER MAY CAUSE SKIN IRRITATION.**

EYE: **MECHANICAL IRRITATION ONLY.**

INHALATION: **SHAPES NOT RESPIRABLE.**

MSDS #1400

Quadrant EPP

Page 2

SECTION 4

EMERGENCY FIRST AID

- If exposed to fumes from overheating, move to fresh air. Consult a physician if symptoms persist.
- Wash skin with soap and plenty of water.
- Flush eyes with water. Consult a physician if symptoms persist.

CHRONIC EFFECTS: NONE KNOWN.

MEDICAL CONDITIONS GENERALLY AGGRAVATED BY THIS MATERIAL: NONE KNOWN.

SECTION 5

FIRE AND EXPLOSION HAZARD DATA

FLASH IGNITION TEMPERATURE: WILL NOT FLASH.

UNUSUAL FIRE, EXPLOSION HAZARDS: NONE KNOWN.

HAZARDOUS DECOMBUSTION PRODUCTS: HEATING ABOVE THE MELTING POINT, OR PROLONGED HEATING ABOVE 260 C./500 F., MAY CAUSE THERMAL DEGRADATION OF POLYTETRAFLUORETHYLENE WHICH LEADS TO THE FORMATION OF OXIDIZED PRODUCTS CONTAINING CARBON, FLUORINE AND OXYGEN.

SPECIAL FIRE FIGHTING INSTRUCTIONS: FIRE FIGHTERS AND OTHERS EXPOSED TO PRODUCTS OF COMBUSTION SHOULD WEAR FULL PROTECTIVE CLOTHING INCLUDING SELF-CONTAINED BREATHING APPARATUS. FIRE FIGHTING EQUIPMENT SHOULD BE THOROUGHLY DECONTAMINATED AFTER USE.

EXTINGUISHING MEDIA: WATER SPRAY OR ANY CLASS A EXTINGUISHING AGENT.

>= Physical health Hazards:

DUST MAY FORM EXPLOSIVE MIXTURES WITH AIR. AVOID DUST FORMATION AND CONTROL IGNITION SOURCES. ALL PLASTIC DUST PARTICLES SUSPENDED IN AIR ARE COMBUSTIBLE AND MAY BE EXPLOSIVE. KEEP AWAY FROM HEAT, SPARKS, FLAME, AND OTHER IGNITION SOURCES. PREVENT DUST ACCUMULATIONS AND DUST CLOUDS. EMPLOY GROUNDING, VENTING, AND EXPLOSIVE RELIEF PROVISIONS IN ACCORDANCE WITH ACCEPTED ENGINEERING PRACTICES AND NFPA PROVISIONS IN ANY PROCESS CAPABLE OF GENERATING DUST AND/OR STATIC ELECTRICITY. EXPLOSION HAZARDS APPLY ONLY TO DUSTS, NOT GRANULAR FORMS OF THIS PRODUCT. SEE ALSO SPECIAL PRECAUTIONS SECTION BELOW.

MSDS #1400

Quadrant EPP

Page 3

SECTION 6

ACCIDENTAL RELEASES

SPILL OR RELEASE: Clean up by vacuuming or wet sweeping to minimize dust exposure.

SECTION 7

STORAGE CONDITIONS

Dry storage. Keep containers closed to prevent contamination.

SECTION 8

PROTECTION INFORMATION

EYE: Safety glasses are recommended to prevent particulate matter from entering eyes while grinding or machining.

SKIN: This product is not likely to be hazardous by skin contact, but cleansing the skin after use is advisable.

VENTILATION: Local exhaust at processing equipment to keep particulates below 15 mg/m³, the OSHA limit for nuisance dusts. Grinding and machining of parts should be reviewed to assure that particulate levels are kept at recommended levels.

OTHER: Avoid contamination of cigarettes or tobacco with Fluorosint dust.

RESPIRATOR: None under normal processing, if ventilation is adequate.

MSDS #1400

Quadrant EPP

Page 4

SECTION 9PHYSICAL/CHEMICAL DATAODOR: **ESSENTIALLY ODORLESS.**MELTING POINT: **342 C./ 648 F.**SOLUBILITY IN WATER: **INSOLUBLE.**VOLATILE CONTENT %: **<1%**SPECIFIC GRAVITY: **2.25-2.35**

>= Precautions For Repair & Maintenance Of Contaminated Equipment: Eliminate ignition sources:

TRANSFER FROM STORAGE WITH A MINIMUM AMOUNT OF DUSTING. GROUND ALL TRANSFER, BLENDING, AND DUST COLLECTING EQUIPMENT TO PREVENT STATIC SPARKS IN ACCORDANCE WITH NFPA 70 "NATIONAL ELECTRIC CODE". REVIEW AND COMPLY WITH ALL RELEVANT NFPA PROVISIONS, INCLUDING BUT NOT LIMITED TO NFPA 484 AND NFPA 654 RELATED TO COMBUSTIBLE DUST HAZARDS. REMOVE ALL IGNITION SOURCES FROM MATERIAL HANDLING, TRANSFER, AND PROCESSING AREAS WHERE DUST MAY BE PRESENT. LOCAL EXHAUST VENTILATION SHOULD BE PROVIDED IN WORK AREA.

SECTION 10HAZARDOUS REACTIVITYSTABILITY AT ROOM TEMPERATURE: **STABLE.**MATERIALS TO AVOID: **NONE KNOWN.**CONDITIONS TO AVOID: **HEATING ABOVE 400 C./750 F.**

MSDS #1400

Quadrant EPP

Page 5

SECTION 11

TOXICOLOGICAL INFORMATION

CHRONIC TOXICITY: SPECIFIC TOXICITY TESTS HAVE NOT BEEN CONDUCTED ON THIS PRODUCT. THE HAZARD EVALUATION IS BASED ON INFORMATION FROM SIMILAR PRODUCTS, THE INGREDIENTS, TECHNICAL LITERATURE, AND/OR PROFESSIONAL EXPERIENCE FROM THE RESIN MANUFACTURER.

THIS PRODUCT CONTAINS POLYTETRAFLUOROETHYLENE (PTFE). VAPORS WHICH CAN CAUSE FLU-LIKE SYMPTOMS ARE LIBERATED FROM PTFE AT TEMPERATURES ABOVE 250 C./480 F. OR IF CIGARETTES OR OTHER SMOKING MATERIALS ARE CONTAMINATED WITH FLUOROSINT DUST OR MACHINE WASTE.

CARCINOGENICITY: NO COMPONENT OF THIS PRODUCT PRESENT AT LEVELS GREATER THAN 0.1% IS IDENTIFIED AS A CARCINOGEN BY NTP, IARC OR OSHA.

SECTION 12ECOLOGICAL INFORMATION

AQUATIC TOXICITY: Toxicity is expected to be low based on insolubility of product in water.

SECTION 13DISPOSAL

WASTE DISPOSAL: Recycling is encouraged, Landfill or incineration in compliance with Federal, State, and Local regulations.

SECTION 14TRANSPORT INFORMATION

DOT HAZARD CLASS: **NA**
SHIPPING NAME: **NA**

MSDS #1400

Quadrant EPP

Page 6

**SECTION 15A
REGULATORY INFORMATION**

SECTION 313 SUPPLIER NOTIFICATION:
(SARA TITLE III-TOXIC CHEMICALS LIST)

This product contains no known toxic chemicals subject to the reporting requirements of section 313 of the Emergency Planning and Community Right-To-Know Act of 1986 and 40 CFR 372.

STATE RIGHT TO KNOW LAWS

No substances on the state hazardous list, for the states indicated below, are used in the manufacture of products on this Material Safety Data Sheet, with the exceptions indicated. While we do not specifically analyze these products, or the raw materials used in their manufacture, for substances on various state hazardous substances lists, to the best of our knowledge the products on this Material Safety Data Sheet contain no such substances except for those specifically listed below:

PENNSYLVANIA:

SUBSTANCES ON THE PENNSYLVANIA HAZARDOUS SUBSTANCES LIST PRESENT AT A CONCENTRATION OF 1% OR MORE: **NONE KNOWN.**

SUBSTANCES ON THE PENNSYLVANIA SPECIAL HAZARDOUS SUBSTANCES LIST PRESENT AT A CONCENTRATION OF 0.01% OR MORE: **NONE KNOWN.**

CALIFORNIA PROPOSITION 65:

SUBSTANCES KNOWN TO THE STATE OF CALIFORNIA TO CAUSE CANCER: **NONE KNOWN.**

SUBSTANCES KNOWN TO THE STATE OF CALIFORNIA TO CAUSE BIRTH DEFECTS OR OTHER REPRODUCTIVE HARM: **NONE KNOWN.**

**SECTION 15B
LABELING INFORMATION**

Health	0
Flammability□	1□
Reactivity□	0□
PPE□	A□
#Acute□*Chronic□	

MSDS #1400

Quadrant EPP

Page 7

SECTION 16

MISCELLANEOUS INFORMATION

Issued by: Richard Frey, SHE Manager, NA

Issued: January 8, 2009

Supersedes: October 29, 2008

The information set forth herein has been gathered from standard reference materials and/or supplier test data and is, to the best knowledge and belief of Quadrant EPP, accurate and reliable. Such information is offered solely for your consideration, investigation and verification, and it is not suggested or guaranteed that the hazard precautions or procedures mentioned are the only ones, which exist. Quadrant EPP makes no warranties, expressed or implied, with respect to the use of such information or the use of the specific material identified herein in combination with any other material or process, and assumes no responsibility therefor.

NA = Not applicable

NE = Not established.

> = New or revised information in this section when " > " appears in the left margin.

END OF MSDS